KUOPION YLIOPISTON JULKAISUJA D. LÄÄKETIEDE 473
KUOPIO UNIVERSITY PUBLICATIONS D. MEDICAL SCIENCES 473

PAULA BENDEL

Imaging of the Brain After Aneurysmal Subarachnoid Hemorrhage

One-year MRI Outcome of Surgical and Endovascular Treatment

Doctoral dissertation

To be presented by permission of the Faculty of Medicine of the University of Kuopio
for public examination in Auditorium, Kuopio University Hospital,
on Friday 15th January 2010, at 12 noon

Institute of Clinical Medicine
Department of Clinical Radiology,
Department of Neurosurgery
Kuopio University Hospital
University of Kuopio

KUOPION YLIOPISTO

KUOPIO 2009

Distributor: Kuopio University Library
P.O. Box 1627
FI-70211 KUOPIO
FINLAND
Tel. +358 40 355 3430
Fax +358 17 163 410
www.uku.fi/kirjasto/julkaisutoiminta/julkmyyn.shtml

Series Editors: Professor Raimo Sulkava, M.D., Ph.D.
School of Public Health and Clinical Nutrition

Professor Markku Tammi, M.D., Ph.D.
Institute of Biomedicine, Department of Anatomy

Author´s address: Department of Clinical Radiology
Kuopio University Hospital
P.O.Box 1777
FI-70211 KUOPIO
FINLAND
Tel. +358 17 173 907
Fax +358 17 173 342

Supervisors: Professor Ritva Vanninen, M.D., Ph.D.
Institute of Clinical Medicine
Department of Clinical Radiology
University of Kuopio

Docent Timo Koivisto, M.D., Ph.D.
Institute of Clinical Medicine
Department of Neurosurgery
University of Kuopio

Reviewers: Docent Veikko Kähärä, M.D., Ph.D.
Department of Radiology
Tampere University Hospital

Docent Ari Karttunen, M.D., Ph.D.
Department of Diagnostic Radiology
Oulu University Hospital

Opponent: Docent Leena Valanne, M.D., Ph.D.
Helsinki Medical Imaging Center
Helsinki University Hospital

ISBN 978-951-27-1373-8
ISBN 978-951-27-1390-5 (PDF)
ISSN 1235-0303

Kopijyvä
Kuopio 2009
Finland

Bendel, Paula. Imaging of the Brain after Aneurysmal Subarachnoid Hemorrhage-One-year MRI Outcome of Surgical and Endovascular Treatment. Kuopio University Publications D. Medical Sciences 473. 2009. 124p.

ISBN 978-951-27-1373-8
ISBN 978-951-27-1390-5 (PDF)
ISSN 1235-0303

ABSTRACT

Background: Aneurysmal subarachnoid hemorrhage (aSAH) is a devastating disease with an overall case-fatality of 40-50%. Most of the surviving patients are left with neurological deficits and cognitive impairments. Brain MRI could possibly provide valuable information on patients' recovery potential together with detailed neurological and neuropsychological examination after aSAH.

Patients and Methods: One-hundred and sixty-eight consecutive aSAH patients were randomly assigned to either endovascular (n=82) or surgical (n=86) treatment. Altogether 138 conventional and 77 volumetric MRI examinations were available one year after aSAH. T2PD and 3DT1-weighted images were analyzed in detail. Volumetric analyses focused to temporomesial structures; hippocampus (HC) and amygdala (AM), and gray matter (GM) volume loss in patients with ruptured anterior cerebral artery (ACA) aneurysm. The atrophic enlargement of the cerebrospinal fluid (CSF) volumes was quantified. MRI findings were correlated with neuropsychological test scores.

Results: Forty-four (31.9%) of 138 patients had no lesions associated with aSAH. According to intention to treat, lesions were more frequent after surgical treatment, predominating in frontal and temporal lobes. Ischemic lesions of the parental artery territory of the ruptured aneurysm were more frequent after surgery. Ischemic lesion volumes correlated with neuropsychological test scores. After aSAH, the HC and AM volumes were found to be smaller than in the matched control individuals. After treatment of an ACA aneurysm, GM atrophy was detected on frontobasal cortical areas and HC ipsilateral to the surgical approach. Enlarged ventricular and sulcal CSF volumes were detected after aSAH. Higher Fisher scores, preoperative hydrocephalus and older age were found to associate with ventricular and sulcal enlargement, both correlating with neuropsychological defects.

Conclusion: aSAH is frequently followed by brain parenchymal changes, especially in frontotemporal areas. Lesions seem to be more frequent after surgical than endovascular treatment. Temporomesial volume loss is a common finding after aSAH in general. GM atrophy, principally involving the frontobasal cortical areas and hippocampus ipsilateral to the surgical approach is detected after aSAH and treatment of the ruptured ACA aneurysm. Atrophic CSF-enlargement together with reduced GM volumes is a common sequela after aSAH. Both enlarged CSF-spaces and brain parenchymal lesion volumes correlate with neuropsychological test performance after aSAH.

National Library of Medicine Classification: WG 580, WL 355, WN 185

Medical Subject Headings: Amygdala; Aneurysm; Atrophy; Embolization, Therapeutic/methods; Follow-Up Studies; Hippocampus; Humans; Imaging, Three-Dimensional; Intracranial Aneurysm /surgery; Magnetic Resonance Imaging; Neuropsychological Tests; Randomized Controlled Trial; Rupture; Subarachnoid Hemorrhage; Treatment Outcome

ACKNOWLEDGEMENTS

This work was carried out in the Department of Clinical Radiology, University of Kuopio, in Collaboration with Departments of Neurosurgery and Neurology, Kuopio University Hospital during the years 2002-2009.

I owe my deepest feeling of gratitude to my principal supervisor Professor Ritva Vanninen, M.D., who kindly suggested this most interesting topic. It has been a true privilege to work in her excellent, enthusiastic, energetic, warm and professional guidance. This thesis would never have been finished without her encouragement. She has given her essential support in all phases of this study. Besides her excellent scientific and psychological skills, I also admire her expertise as a clinical neuroradiologist.

I owe my deepest gratitude to Docent Timo Koivisto, M.D., my other supervisor. He has originally collected the patients who were included in this study. It was a priority to deepen the radiological aspect of his originally unique, prospective, randomized Outcome Study of Aneurysmal Subarachnoid Hemorrhage. He has always found time to discuss this study with me. I have also enjoyed our friendship and the time we have spent together with our families.

I wish to express my warm gratitude to Head of The Department of Clinical Radiology, Professor Hannu Manninen, M.D. His favourable attitude towards research projects has provided excellent atmosphere and realistic possibilities to combine clinical work and research.

I am greatly indebted for the physicists Mervi Könönen, M.Sc. and Eini Niskanen M.Sc., who have been extremely essential persons to resolve all the technical and mathematical problems we have faced during this study. I highly appreciate their positive and constructive attitude and skills to communicate.

I want to express my gratitude to Professors and neurosurgeons Matti Vapalahti, M.D. and Juha Hernesniemi, M.D., who were essential persons to build up the original randomized study protocol and who have also performed most of the surgical operations during this study. I am also grateful for the possibility to begin my medical career on 1997 by working as a resident in the Department of Neurosurgery.

My warmest thanks belong to my co-workers; deceased neuropsychologist Heleena Hurskainen, M.Sc., who performed all the neuropsychological tests; Docent Tuomo

Hänninen, M.S.c. and Marja Äikiä, M.S.c., Ph.D. who have further interpreted the neuropsychological data and essentially helped with the neuropsychological aspects in the manuscripts; neurointerventionist Tapani Saari, M.D., who has performed all the embolization procedures together with Professor Ritva Vanninen. I want to specially thank my colleque Päivi Koskenkorva, M.D., for sharing the VBM-mysteries with me. I owe my warm thanks to Anni Kolehmainen, M. D., and Corina Pennanen, M.D, Ph.D for their help in the volumetric measurements.

I am most grateful to all my collegues in the Department of Neuroradiology; especially Teppo Mäkelä for always having “a minute”. I also warmly want to thank Aki Ikonen, Anna Sutela, Antti Lehtimäki, Juhana Hakumäki and Sanna Keränen for sharing their knowledge and expertise in Neuroradiology.

I thank the official referees of this study, Docent Veikko Kähärä, M.D., and Docent Ari Karttunen, M.D., for their time, effort and valuable comments.

I wish to warmly thank Docent David Laaksonen, M.D., and Juulia Vanninen, B. A. for linguistic editing of the manuscripts and thesis.

I owe my sincerest thanks to the skilful personnel of our department; especially people working on the MRI-unit on that time the imaging studies were performed. I also want to especially thank Jari Räisänen for essential help he had provided me with numerous technical problems.

I owe my sincere thanks to Tuula Bruun, Eija Hassinen and Taina Airola for their invaluable secretarial assistance.

The collaboration and positive attitude to work, sports and moments after work has been very special and important in the Department of Clinical Radiology and I want to thank all my collegues for providing the most positive atmosphere to work at.

I want to warmly thank my father- and mother-in law, Marja and Burghardt Bendel for their patience and support. I cordially want to thank my brothers; Kuku, Juhana and Janne together with their families for their help and stimulating company. I want to owe my sincerest gratitude to my cousin and friend Veera for everything.

There is (or hopefully will be) life beyond the work and research. I want to thank all my dear friends; especially Annika, Adrienn, Ulla, Petri, Mikko and Otto for sharing the most enjoyable moments and also sorrows of life.

I dedicate my dearest thanks to my parents Leena and Matti Puranen for their love and everlasting patience and unselfish, loving support with our children during and beyond this work. This thesis would not exist without your invaluable help and encouragement.

I want to thank all the seriously ill patients who participated in this study.

Finally, I want to express my deepest love to my family; to my dear, loving, patient, equal and practical husband Stepani and our dearest children Jaakko, Venla and the Baby One urging me to finish up with this thesis, for teaching and reminding me what is essential in this life.

This study was finally supported Kuopio University EVO funding (Grants 5063515 and 5063501), Natalia and Frederik Trube Foundation from the Finnish Cultural Foundation Pohjois-Savo Regional Fund, Instrumentarium Foundation, The Finnish Society of Radiology, Maire Taponen Foundation and The Finnish Medical Society Duodecim.

Kuopio, December 2009 Paula Bendel

ABBREVIATIONS

ACA	anterior cerebral artery
AComA	anterior communicating artery
ADC	apparent diffusion coefficient
AM	amygdala
aSAH	aneurysmal subarachnoid hemorrhage
BBB	blood brain barrier
CSF	cerebrospinal fluid
CBF	cerebral blood flow
CBV	cerebral blood volume
CI	cerebral infarct
CMI	cella media index
CT	computed tomography
CSF	cerebrospinal fluid
DIND	delayed ischemic neurological deficit
3DRA	3 dimensional rotational angiography
DSA	digital subtraction angiography
DWI	diffusion weighted imaging
FDR	false discovery rate
FWE	family-wise error
GCS	Glasgow Coma Scale
GM	gray matter
GOS	Glasgow outcome scale
HC	hippocampus
IA	intracranial aneurysm
ICA	internal carotid artery
ISUIA	International study on Unruptured Intracranial Aneurysms
ISAT	International Subarachnoid Aneurysm Trial
H&H	Hunt and Hess scale
MCA	middle cerebral artery
MDCTA	multidetector computed tomography angiography
MIA	multiple intracranial aneurysms
MNI	Montreal Neurological Institute

MPR	multiplanar reformat
MPRAGE	magnetization prepared rapid acquisition gradient echo
MRA	magnetic resonance angiography
MRI	magnetic resonance imaging
MTT	mean transit time
PCA	posterior cerebral artery
PComA	posterior communicating artery
PCT	perfusion computed tomography
PD	proton density
QOL	quality of life
ROI	region of interest
SAH	subarachnoid hemorrhage
SD	standard deviation
SI	signal intensity
SPET	single photon emission computed tomography
SPM	statistical parametrical mapping
TCD	transcranial Doppler
VBA	vertebrobasilar artery
VBM	voxel-based morphometry
WM	white matter
WMH	white matter hyperintensity

LIST OF ORIGINAL PUBLICATIONS

The thesis is based on the following original articles, which are referred to in the text by their Roman numerals:

I Bendel P, Koivisto T, Könönen M, Hänninen T, Hurskainen H, Saari T, Vapalahti M, Hernesniemi J, Vanninen R. MR imaging of the brain 1 year after aneurysmal subarachnoid hemorrhage: randomized study comparing surgical with endovascular treatment. Radiology. 2008 Feb; 246 (2):543-52.

II Bendel P, Koivisto T, Hänninen T, Kolehmainen A, Könönen M, Hurskainen H, Pennanen C, Vanninen R. Subarachnoid hemorrhage is followed by temporomesial volume loss: MRI volumetric study. Neurology. 2006 Aug 22; 67(4):575-82.

III Bendel P, Koivisto T, Niskanen E, Könönen M, Äikiä M, Hänninen T, Koskenkorva P, Vanninen R. Brain atrophy and neuropsychological outcome after treatment of ruptured anterior cerebral artery aneurysms: a voxel-based morphometric study. Neuroradiology. 2009 Nov; 51(11):711-22.

IV Bendel P, Koivisto T, Äikiä M, Niskanen E, Könönen M, Hänninen T, Vanninen R. Atrophic enlargement of CSF volume after Subarachnoid Hemorrhage; Correlation with Neuropsychological Outcome. AJNR Am J Neuroradiol. 2009 Nov 26; [Epub ahead of print].

CONTENTS

1. INTRODUCTION

Aneurysmal subarachnoidal hemorrhage (aSAH) is a devastating disease with an overall case-fatality of 40- 50% (van Gijn *et al.* 2001). The incidence of aSAH is increasing concistently with age (de Rooij *et al.* 2007, Fogelholm 1981). However, the median age of death caused by aSAH is significantly lower being 59 years, compared to 73 years for intracerebral hemorrhage and 81 years for ischemic stroke. It has been estimated that aSAH covers over 25% of all stroke-related years of potential life lost before of age 65 (Johnston *et al.* 1998). Moreover, most of the surviving patients are left with neurological deficits and neuropsychological and cognitive impairments (Molyneux *et al.* 2002, Molyneux *et al.* 2005, Vapalahti *et al.* 1984, Vilkki *et al.* 1989). The factors that influence long-term cognitive outcome after aSAH are clinically important as such factors may be potentially modifiable. This study was carried out to describe in detail the magnetic resonance imaging (MRI) outcome one year after aSAH in patients who were randomly assigned to surgical clipping versus endovascular coil treatment of the ruptured aneurysm. The aim was to discover, if MRI could provide valuable information on patients' recovery potential together with detailed neurological and neuropsychological examination after aSAH.

2. REVIEW OF THE LITERATURE

2.1. Subarachnoid hemorrhage (SAH)

2.1.1. Incidence, etiology and risk factors

Aneurysmal subarachnoid hemorrhage is a serious condition: global mortality ranges from 32 to 67% (Hop *et al.* 1997). Twenty to 30% of the survivors are left with disabling sequelae. Half of the patients who were previously employed cannot return to their previous work after aSAH (Buchanan *et al.* 2000). Another study has showed that 60% of aSAH victims referred to neurosurgical unit can be saved and can recover to normal (Saveland *et al.* 1992). A recent review including 51 studies (33 new) reported an overall incidence of aSAH being approximately 9 per 100 000 (de Rooij *et al.* 2007). However, aSAH is significantly more common disease in Finland and Japan compared to other countries (de Rooij *et al.* 2007, Fogelholm 1981, Inagawa *et al.* 1995, Sarti *et al.* 1991).

The cause for non-traumatic SAH is rupture of an intracranial aneurysm (IA) in more than 80% of cases (van Gijn *et al.* 2001). Risk factors for aSAH are advanced age (Rinkel 2008, Rinkel *et al.* 1998), female gender (Linn *et al.* 1996, Morita *et al.* 2005, Rinkel 2008, Rinkel *et al.* 1998), smoking (Feigin *et al.* 2005, Isaksen *et al.* 2002, Juvela *et al.* 1993) , hypertension (Feigin *et al.* 2005, Feigin *et al.* 2005, Sandvei *et al.* 2009), excessive use of alcohol (Feigin *et al.* 2005), having one or more affected close relatives with aSAH (Rinkel *et al.* 1998, Ronkainen *et al.* 1997) and autosomal dominant polycystic kidney disease (Gieteling *et al.* 2003, Rinkel *et al.* 1998, Ronkainen *et al.* 1997). Furthermore, the larger size and irregular shape and certain locations (vertebrobasilar, posterior and anterior communicating arteries) of the aneurysm have been listed to increase the risk of rupture in asymptomatic patients with incidental cerebral aneurysm (Wiebers *et al.* 2003).

2.1.2. Cerebral aneurysms

Intracranial arterial aneurysms (IA) are not congenital, but develop in the course of life. An estimated frequency of cerebral aneurysm for an average adult without specific risk factors is 2-3% (Rinkel *et al.* 1998) and the percentage increases with

age. Most cerebral aneurysm are saccular and arise at sites of arterial branchings, usually at the base of the brain, either on the circle of Willis itself or at nearby branching points. The risk of rupture increases along the size of an aneurysm, but most ruptured aneurysms are small, less than 10 mm (Rinkel *et al.* 1998). Reports of IA in some patients with rare mendelian disorders such as autosomal dominant polycystic kidney disease, Ehlers-Danlos syndrome type IV, Marfan syndrome, neurofibromatosis type 1 and fibromuscular dysplasia suggest that IAs are more common in subjects with these diseases than in the general population (Schievink 1997, Schievink *et al.* 2005, Wills *et al.* 2003). There are different basic types of intracranial aneurysms: saccular or “berry” aneurysms, fusiform aneurysms, blood blister-like aneurysms and dissecting aneurysms. Saccular aneurysms are the most common type and they are true aneurysms, i.e., they are dilations of vascular lumen due to weakness of all vessel wall layers. The aneurysmal sac itself is usually composed only of intima and adventitia. The adventitia may be infiltrated by lymphocytes and phagocytes. Trombotic debris is often present in the lumen of aneurysmal sac (Okazaki 1989). The occurrence, growth, thrombosis, and even rupture of intracranial saccular aneurysms can be explained by abnormal hemodynamic shear stresses on the walls of large cerebral arteries, particularly at the branching points of the arteries (Strother *et al.* 1992). It has been recently suggested that before rupture, the wall of saccular cerebral artery aneurysm undergoes morphological changes associated with remodeling of the aneurysm wall. Some of these changes, e.g. smooth muscle cell proliferation and macrophage infiltration, may reflect ongoing repair attempts that thus could be enhanced with pharmacological therapy (Frosen *et al.* 2004, Frosen *et al.* 2006).

2.1.3. Nonaneurysmal subarachnoid hemorrhage

SAH of unknown origin, usually a perimesencephalic type of SAH (pmSAH), represents 9% to 15% of cases of SAH patients (Kassell *et al.* 1990). In pmSAH, the origin of the bleeding remains unclear and various pathogenetic mechanisms, such as small cerebellar or pontine venous angiomas, capillary telangiectasias, intramural hematomas of the basilar artery or specific anatomic variations of the perimesencephalic venous drainage system have been discussed as possible explanations for nonaneurysmal pmSAH (Ikeda *et al.* 1998). Patients with pmSAH

have been shown to regain independence for activities of daily life and have a normal life expectancy, and they are not at risk for rebleeding. However, up to 25% of these patients are left with symptoms including headache or dizziness, fatigue, forgetfulness and irritability (Greebe *et al.* 2007).

2.2. Vascular anatomy of the brain, circle of Willis and typical aneurysms

2.2.1. Components of circle of Willis

The knowledge of normal vascular anatomy of the brain and angiographic findings of each individual patient are important in analyzing MR images after aSAH. With the familiarity of these factors, it is possible to determine the most probable etiology of the lesions detected on late CT or MR imaging after aSAH (e.g. ischemic lesions in the vascular territory of the ruptured aneurysm and ischemic lesions in the other, remote vascular territories and to differentiate the ischemic lesions from the lesions induced by surgical manipulation) (Hadjivassiliou *et al.* 2001, Kivisaari *et al.* 2001).

The anastomotic ring that connects both halves of the “anterior” circulation with each other and with the vertebrobasilar system is called the circle of Willis. The circle of Willis lies above the sella turcica within the interpeduncular and suprasellar cisterns. A complete circle of Willis is an arterial polygon; a nonagon or a nine-sided structure. The complete circle of Willis consists of two internal carotid arteries (ICAs), two anterior cerebral arteries (ACAs), the anterior communicating artery (AComA), two posterior communicating arteries (PComAs), the basilar artery (BA) and two posterior cerebral arteries (PCAs). Moreover, the middle cerebral arteries (MCA) are a continuum of the ICA distal to branching point of the ACAs. The different variations and incompleteness of circle of Willis are common. Most of the “berry” or saccular aneurysms arise from the branching points of these vessels (Osborn 1999). **Figure 1** shows the complete circle of Willis**.**

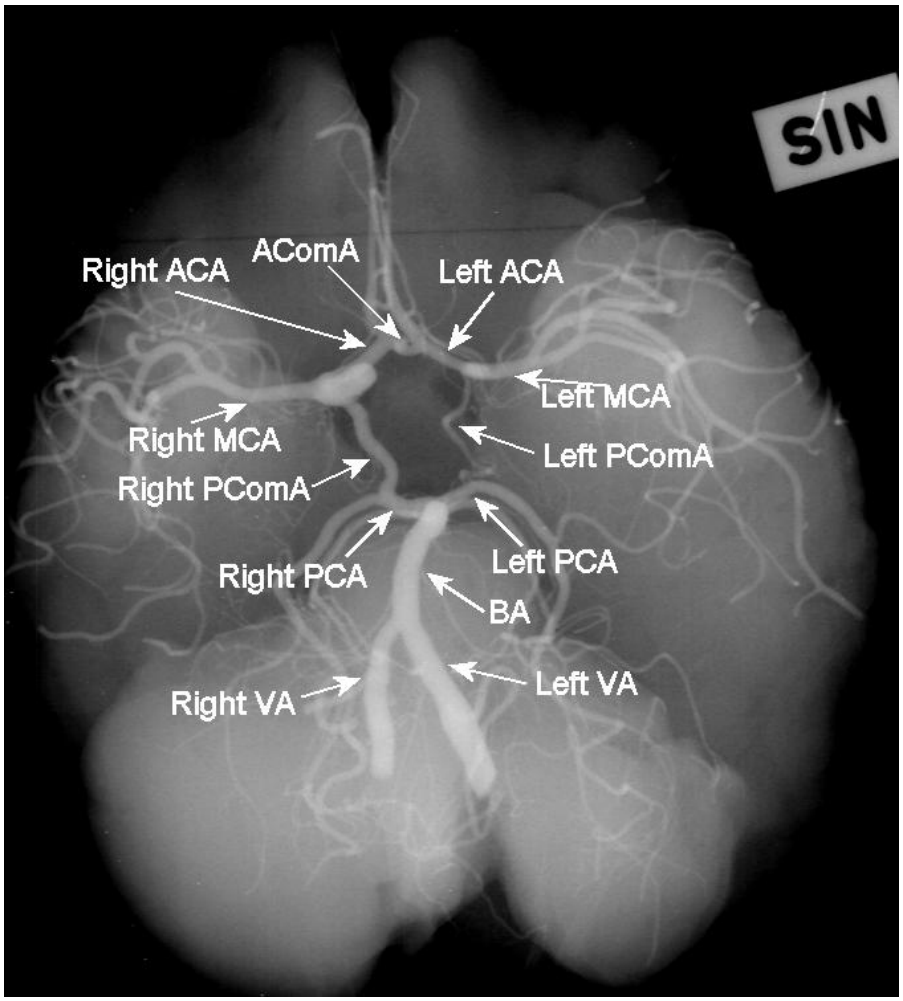

Figure 1. Cerebral cast angiography demonstrating a complete circle of Willis, basilar artery, distal vertebral arteries (VA)s and right and left middle cerebral arteries.

2.2.2. Typical sites for cerebral saccular aneurysms and aneurysm detection

In Finland, the following aneurysm locations have recently been reported: AComA 31.5%, MCA 33.1%, PComA 12.4%, ICA 8.1%, distal ACA 5.7%, VBA 9.3% (van Munster *et al.* 2008). According to a recent study from eastern Finland with 1068 aSAH patients (59% of these were female), the most frequent sites for cerebral sporadic, ruptured intracranial aneurysms (IA)s were reported as following; ICA (ICA and PComA) 23%, ACA (A1, AComA, A2-A5) 35%, MCA (M1, Mbif, M2-M5) 32%, VA

(VA and posterior inferior cerebellar artery (PICA)) 3%, BA (BA bifurcation) 6% and PCA 1% (Huttunen *et al.* 2009). However, the most frequent site for unruptures sIAs was the MCA bifurcation (39-44% of the unruptured aneurysms). In Finland, the predominance of MCA aneurysms has also been reported in other series (Fogelholm 1981, Pakarinen 1967), while forensic reviews report slightly different locations for ruptured cerebral aneurysms; 20-27% ACA, 26-34% MCA, 37-46 % ICA and 8-13% VBA (Rinkel *et al.* 1998).

Noninvasive imaging studies such as spiral computed tomographic angiography (CTA) or high-resolution magnetic resonance angiography (MRA) imaging can provide an overview of the carotid siphon and major arteries at the base of the brain. Detailed examination of the circle Willis, especially visualizing its' small but important perforating branches still relies on the high resolution conventional digital subtraction angiography (DSA). Because the circle of Willis constitutes the best potential source of collateral blood in occlusive vascular disorders, awareness of its normal anatomy is essential, even though the vascular supply can widely vary in an individual patient. Accurate angiographic evaluation is also an integral part of preoperative planning before surgery or endovascular treatment of the ruptured aneurysm.

2.2.3. Cortical branches of the supratentorial cerebral arteries and their vascular territories

The distal segment of the ACA, the pericallosal arteries, gives rise to the cortical and callosal branches. The callosal branches supply the rostrum, genu and the body of the corpus callosum. These branches are joined posteriorly by the splenial branches of the PCA. In the most frequent disposition, the cortical area of supply of the ACA is the medial surface of the hemisphere extending to the superior frontal sulcus and the parieto-occipital sulcus. On the orbitofrontal surface, the arterial territory includes the medial orbital gyri. At the most, the cortical ACA territory reaches the inferior frontal sulcus, and at the least, it includes only the anterior part of the frontal lobe (Osborn 1999, Tatu *et al.* 1998).

The MCA is divided anatomically into four segments: horizontal segments (M1), insular segments (M2), opercular segments (M3; the first ascending branch is sometimes historically called the “candelabra” because the angiographic appearance resembles a branched candlestick) and cortical branches (M4).The MCA begins its

division into cortical branches at the base of the Sylvian fissure, extends over the surface of the hemisphere and forms M4 segments. The most frequent area of supply of the MCA extends from the lateral surface of the hemisphere to the superior frontal sulcus, the intraparietal sulcus, and the inferior temporal gyrus. On the orbitofrontal surface, the arterial territory includes the lateral orbital gyri. The maximum area covers the whole lateral surface of the hemisphere, reaching the interhemispheric fissure. The minimum territory is confined between the inferior frontal and the superior temporal sulci (Osborn 1999, Tatu *et al.* 1998).

As the PCA approaches the dorsal surface of the midbrain, it gives rise to cortical branches. The branches include the hippocampal arteries and the splenial artery that anastomose with the distal part of the pericallosal artery to supply the splenium of the corpus callosum. The most frequent cortical distribution of the PCA includes the inferomedial surfaces of the temporal and occipital lobes extended to the parieto-occipital fissure. In general, the parieto-occipital and calcarine arteries supply the posterior one third of the brain, along with the interhemispheric fissure including the primary visual cortex. At the most, the cortical supply can extend as far as the superior temporal sulcus and the upper part of the precentral sulcus, and at the least, the supply can extend only as far as the medial face of the occipital lobe, limited by the parieto-occipital fissure (Osborn 1994, Osborn 1999, Tatu *et al.* 1998).

2.2.4. Perforating branches of the circle of Willis and Middle Cerebral artery

Important perforating branches arise from every part of the circle of Willis and middle cerebral artery: 1. From *anterior cerebral arteries* arise the medial lenticostriatae arteries and quite often the recurrent artery of Heubner, which can supply the caudate nucleus head, anterior limb of the internal capsule and part of the basal ganglia. 2. From *anterior communicating artery* arise perforating brances to supply the superior surface of the optic chiasm and anterior hypothalamus. These branches may have a significant vascular territory that includes part of the corpus callosum, columns of the fornix, parolfactory areas, lamina terminalis and hypothalamus. 3. From *posterior communicating arteries* arise number of small, but important perforating branches, the anterior thalamoperforating arteries to supply part of the thalamus, the infralenticular limb of the internal capsule and optic tracts. 4. From *distal basilar artery and proximal posterior cerebral arteries* arise numerous

small perforating arteries. These branches, the posterior thalamoperforating arteries and the thalamogeniculate arteries supply the midbrain and thalamus. 5. From the *middle cerebral artery* arise the lateral lenticulostriatal arteries, which supply the substantia innominata, lateral aspect of the anterior commissure, most of the putamen and lateral globus pallidus, the superior half of the internal capsule and adjacent corona radiate, and the body and the head (except the anterior inferior portion) of the caudate nucleus. Portions of the optic radiations and arcuate fasciculus are also supplied by these branches (Osborn 1999).

2.2.5. Circulation of the brainstem and cerebellum

The cerebellar arterial supply depends on three long arteries. The posterior inferior cerebellar artery (PICA) gives rise to two branches and vascularises the inferior vermis and the inferior and posterior surfaces of the cerebellar hemispheres. The anterior inferior cerebellar artery (AICA) supplies the anterior surface of the simple, superior, and inferior semilunar lobules as well as the flocculus and the middle cerebellar peduncle. The superior cerebellar artery (SCA) divides into medial and lateral branches and vascularises the superior half of the cerebellar hemispheres, vermis and the dentate nucleus. These three cerebellar arteries also take part in the vascularisation of the brainstem. The territory of the SCA often includes the upper part of the pontine tegmentum. The PICA takes part in the lateral and posterior arterial groups of the medulla. The AICA supplies the middle cerebellar peduncle and often the lower part of the pontine tegmentum (Duvernoy 1999, Osborn 1999, Tatu *et al.* 1996). However, the vascular anatomy of the posterior fossa can be extremely variable in different individuals.

2.3. Treatment

2.3.1. Natural history of ruptured cerebral aneurysms

Once an aneurysm has ruptured, rebleeding is the most feared complication. Rebleeding peaks in the first few days after the initial bleeding (Kassell *et al.* 1983, Pakarinen 1967). Rebleeding is more frequent in patients with poor clinical condition and those with large aneurysms. If an aneurysm is not treated, the risk of rebleeding

within 4 weeks is estimated to be 35-40% (Hijdra *et al.* 1987). The outcome after aSAH is very poor without treatment. In the historical Finnish series by Pakarinen, the mortality at first recurrence was 64% and at second recurrence it had risen to 86% (Pakarinen 1967).

2.3.2. Clinical assessment of an aSAH patient

The clinical condition of a patient needs to be evaluated acutely after aSAH, since severity of bleeding is the most important prognostic factor for clinical outcome (Koivisto *et al.* 2000). The Hunt & Hess grading scale (Hunt *et al.* 1966) is the most common system for grading the clinical condition of the patient and it is widely used for aSAH patients as following: Grade 0= Asymptomatic, no bleeding, I= Asymptomatic, or minimal headache and/or slight nuchal rigidity, II= Moderate to severe headache, nuchal rigidity, no neurological deficit other than cranial nerve palsy, III= Drowsiness, confusion, or mild local deficit, IV= Stupor, moderate to severe hemiplegia, possibly early decerebrate rigidity, and vegetative disturbances, V= Deep coma, moribund appearance. Also the Glasgow Coma Scale (GCS) is commonly used in clinical practise, (Teasdale *et al.* 1976) and it has further been modified in the World Federation of Neurosurgical Societies (WFNS) classification (Report of Word Federation Of Neurological Surgeons Committee, 1988).

Since the natural history of the ruptured aneurysm is poor, an early treatment should be performed (Fogelholm 1981). The treatment options for excluding a ruptured aneurysm from the circulation are microneurosurgical clipping (Krayenbuhl *et al.* 1970) and endovascular procedures, e.g. coiling (Molyneux *et al.* 2005).

2.3.3. Surgical Treatment of ruptured aneurysms

The goal of surgical treatment of IAs is to isolate the aneurysm from the circulation, while preserving the normal blood flow through parent artery and branch vessels. Surgical treatment is best performed in a microsurgical operation, where a neurosurgeon places a clip across the aneurysm neck (Yasargil *et al.* 1975). This was first done by W. Dandy in 1938 (Dandy 1938), but only in 1960s, after the introduction of operation microscope and improved neurointensive-care, the results of surgery for ruptured aneurysms reached an acceptable level of morbidity and

mortality in good-grade patients (Dandy 1938, Kassell *et al.* 1982, Langmoen *et al.* 1999, Vapalahti *et al.* 1984). Most of the ruptured aneurysms are surgically operable. However the location, size and the configuration of the ruptured aneurysm may sometimes complicate the operation (Hernesniemi *et al.* 1993). Posterior circulation aneurysms can be difficult lesions to be treated by surgery, and they have potential for high morbidity and mortality (Rosengart *et al.* 2007), particularly in elderly patients or patients in poor neurological condition (Schievink *et al.* 1995). Anecdotal clinical series have reported other surgical techniques, such as external wrapping, coating of IAs and the use of the excimer laser-assisted nonocclusive anastomosis technique (ELANA) for surgical treatment of ruptured aneurysms not suitable for conventional surgery (Bederson *et al.* 2009, Muench *et al.* 2007). Modern surgical clips are nonferromagnetic and safe for MR imaging (Kanal *et al.* 1999).

2.3.4. Endovascular treatment of ruptured aneurysms

Endovascular techniques were first used for aneurysms that were considered inoperable or in patients whose previous surgical treatment had failed (Guglielmi *et al.* 1992, Malisch *et al.* 1997). In 1991 Guglielmi and his co-workers introduced an electrically detachable coil system (GDC) which started the endovascular treatment era of ruptured IAs (Guglielmi *et al.* 1991, Guglielmi *et al.* 1991). GDCs are pushed into the aneurysm sac through a microcatheter, and they can be repositioned, retrieved, or replaced by a coil of different size until the situation is considered satisfactory. GDCs are detached from the deploying wire by electrolysis. The standard coil embolization techniques have developed further since GDCs and other detachable platinium coils. For example soft coils, 2D and 3D shaped coils (Lubicz *et al.* 2005, Slob *et al.* 2005), liquid embolic materials (Molyneux *et al.* 2004), remodelling techniques (Moret *et al.* 1997) and endovascular stents have been introduced (Lylyk *et al.* 2005, Tahtinen *et al.* 2009). Embolization with coils has recently been used increasingly for treatment of IAs (Brilstra *et al.* 1999, Molyneux *et al.* 2002, Molyneux *et al.* 2005, Renowden *et al.* 2009, Vinuela *et al.* 1997). A majority of small and moderate sized aneurysms with reasonable neck-aspect ratio are treatable by endovascular means (Vinuela *et al.* 1997). Common reasons for relative unsuitability for endovascular treatment are: aneurysmal size too small/too large, unsuitable neck-aspect ratio, aberrations in intracranial vasculature,

incorporation of distal branches in the aneurysmal neck, aneurysm symptomatic due to mass effect, acute recurrence/re-bleed that follows initial endovascular treatment, and attempted, but unsuccessful prior endovascular treatment. Ruptured cerebral aneurysms deemed unsuitable for endovascular intervention are often difficult to treat surgically (Choudhari *et al.* 2007). Long-term studies evaluating the experience with aneurysm coil embolization during the past decade indicate that embolization of the ruptured aneurysm is a safe and durable treatment method (Koebbe *et al.* 2006, van der Schaaf *et al.* 2005). However, as a result of the lower rates of complete occlusion of the aneurysm after endovascular than surgical treatment (Gerlach *et al.* 2007, Murphy *et al.* 2005, Ogilvy *et al.* 2002), the questions regarding the long-term efficacy of coiling and the possibility of higher rates of rebleedings and recurrence remain (Molyneux *et al.* 2009, Raftopoulos 2005). A recent study shows that virtually all aneurysm reopenings develop within the first 6 months after coiling. Thus no prolonged imaging follow-up is routinely suggested for those aneurysms that are adequately occluded during this time (Rooij *et al.* 2009). Endovascular coils are nonferromagnetic and thus safe for MR imaging (Shellock *et al.* 1997).

2.3.5. Combination treatment of ruptured aneurysms

Although most aneurysms can be clipped microsurgically or coiled endovascularly, a subset of patients may require a combined (crossover) approach. Multimodality approaches are best used with complex aneurysms in which conventional therapy with a single modality has failed (Lawton *et al.* 2008, Thielen *et al.* 1997).

2.3.6. Treatment for associating non-ruptured aneurysms

Unruptured, associated aneurysms are found in up to 30% of patients with aSAH (Huttunen *et al.* 2009, Investigators 1998, Juvela *et al.* 2000, Rinne *et al.* 1994). Different national cohorts of aSAH patients differ with respect of age of the patient and the number and sites of associated aneurysms. When Dutch and Finnish population were compared, multiple aneurysms were more frequent in Kuopio (27.8%) than in Utrecht (14.8%) (van Munster *et al.* 2008). According to local study, multiple MCAAs, found in 20% of the patients with aneurysms, were common in this Finnish population (Rinne *et al.* 1996). A large multicenter study, *ISUIA- Unruptured*

Intracranial Aneurysm: Risk of Rupture and Risks of Surgical Intervention Study, showed that the likelihood of rupture of (unruptured) IAs that were less than 7 mm in diameter was exceedingly low in group of patients who had no history of aSAH from a different aneurysm and was substantially higher among those patients with a history of aSAH from a different aneurysm (Wiebers *et al.* 2003). A coexisting or associated nonruptured aneurysm of all sizes in patients with aSAH due to another treated aneurysm carry a higher risk for future hemorrhage than similar sized aneurysms without a prior SAH history. Other factors that favour treatment for unruptured aneurysms include several factors: a young patient with a long life expectancy, a family history of aneurysm rupture, large aneurysms, symptomatic aneurysms, observed aneurysm growth, and established low treatment risks (Bederson *et al.* 2000).

2.3.7. Consequences and complications of aSAH (Acute impact to brain, hematomas, vasospasm, microcirculatory dysfunction, delayed ischemic neurological deficit and hydrocephalus)

19 - 22% of patients with aSAH presents with an intracerebral hematoma (ICH) (Kivisaari *et al.* 2001, Tokuda *et al.* 1995). The clinical outcome of aSAH patients with ICH is worse than that of aSAH patients without ICH (Bailes *et al.* 1990, Hauerberg *et al.* 1994).

Vasospasm following cerebral aneurysm rupture is one of the most devastating sequelae and is traditionally thought to present the most common cause of delayed ischemic neurological deficits (DIND) (Fisher *et al.* 1977) and a common cause of morbidity and mortality in the patients who survive the initial bleeding. Vasospasm is a frequent complication in the early clinical course after aSAH, occurring in 40 to 70% of patients (Schuknecht *et al.* 1999).

The peak frequency of cerebral ischemia is from 5 to 14 days after aSAH. Although DIND has traditionally been interpreted to be caused by vasospasm (Fergusen *et al.* 2007, Fisher *et al.* 1980) and arterial narrowing, recent studies show that arterial narrowing is neither a necessary nor a sufficient condition (Rabinstein *et al.* 2004, Rabinstein *et al.* 2005, Weidauer *et al.* 2007). Not all patients with DIND have macrovascular vasospasm and there are other mechanisms, such as hypovolemia, hypotension (Chang *et al.* 2000, Wijdicks *et al.* 1985), impaired

fibrinolytic activity, inflammatory and endothelium-related processes leading to the activation mechanisms of the coagulation cascades and formation of microtrombosis and thus leading to development of DIND (Vergouwen *et al.* 2008). Predictors for ischemic lesions in the vascular territory other than the ruptured aneurysm are the total amount of subarachnoid blood (Brouwers *et al.* 1992, Rabinstein *et al.* 2004) and loss of consciousness at the time of hemorrhage (Brouwers *et al.* 1992, Hop *et al.* 1999), which suggests that the global ischemia during the initial event could well be the key factor (van der Schaaf *et al.* 2006). The triple H-treatment including induced hypertension, hypervolemia and hemodilution, is usually the intervention strategy, although controlled trials are missing (Bederson *et al.* 2009). Oral nimodipine have been indicated to reduce poor outcome related to aSAH (Allen *et al.* 1983). The value of other calcium antagonists, whether administrated orally or intravenously, remains still uncertain (Bederson *et al.* 2009). Neurointerventional treatments such as transluminar balloon angioplasties and infusions of intra-arterial vasodilating agents such as nicardipine or nimodipine are also widely used in many units treating patients after aSAH (Hoh *et al.* 2005, Rabinstein *et al.* 2004, Tejada *et al.* 2007), but the effectiveness of these therapies is not well established (Bederson *et al.* 2009). Treatment of aSAH patients with several pharmacological agents such as aspirin, enoxaparin, tirilizad, magnesium sulphate, ebselen, endothelin-1a antagonists and the role of statins have been recently published, but the benefits of these therapies still remain unclear and further studies are needed (Bederson *et al.* 2009). Systemic hypothermia has been used in several clinical settings to protect the brain against ischemic injuries, but its role in treating aSAH patients has not been established (Bederson *et al.* 2009, Todd *et al.* 2005).

The concept of early brain injury (EBI) has been introduced only recently and refers to the immediate injury to the brain as a whole, occurring within the first 72 hours of the ictus, secondary to aSAH. Therefore EBI refers to the events that occur in the brain before the development of vasospasm, including elevation of intracranial pressure, reduction of cerebral blood flow, suppression of cerebral perfusion pressure, fall in brain oxygenation and neuronal cell death. It can be suggested that the etiology of vasospasm may be linked to that of EBI, because they share many of the same characteristics (Kusaka *et al.* 2004). Major early injuries after the initial bleeding are breakdown of blood– brain barrier (BBB) and formation of brain edema (Doczi 1985). There are currently a number of pathways that have been implicated to

EBI and breakdown of BBB including the apoptotic cell death occurring in neurons and in cerebral endothelial cells, inflammatory and ischemic pathways (Cahill *et al.* 2006, Doczi 2001). MRI has been described as a powerful tool for the non-invasive detection of EBI. In experimental models, the use of apparent diffusion gradients demonstrates cellular swelling after a propagating wave of ischemia, which could be seen spreading throughout the ipsilateral and contralateral hemispheres (Busch *et al.* 1998). Animal studies using SAH models have demonstrated profound hippocampal neuronal loss (up to 30%) within relatively short period of time. It is believed that the loss of hippocampal neurons occur secondary to the global ischemia, which occurs at the time of SAH (Park *et al.* 2004). EBI has been speculated to present a combination of physiological insults to the brain, resulting in global ischemia, BBB breakdown, edema and cellular death signalling. These changes occur acutely and chronically although after 72 hours vasospasm becomes the main protagonist. The consequences of EBI can be seen in immediately and in the long term (Cahill *et al.* 2006, Cahill *et al.* 2009).

Chronic hydrocephalus is a well-known complication following aSAH occurring in 10-30% of patients (Dehdashti *et al.* 2004, Gruber *et al.* 1999, Jartti *et al.* 2008, Tapaninaho *et al.* 1993). Well established risk factors for chronic hydrocephalus requiring a shunt placement include: advanced age, Hunt and Hess Grades IV-V, Fisher Grades 3-4, intraventricular bleeding and acute hydrocepahalus on admission (Dehdashti *et al.* 2004, Dorai *et al.* 2003, Tapaninaho *et al.* 1993). Additionally, vertebrobasilar origin of the ruptured aneurysm, postoperative complications (Tapaninaho *et al.* 1993) and clinical vasospasm and endovascular treatment (Dorai *et al.* 2003) have also been reported as risk factors for shunt-dependent hydrocephalus. A recent study reported a relative risk reduction for hydrocephalus in aSAH patients, in whom the fenestration of lamina terminalis had been performed in the surgical operation (Komotar *et al.* 2009).

2. 4. Diagnostic Imaging in acute SAH

2.4.1. Computed tomography (CT) and CT angiography (CTA)

Computed tomography scanning is the first imaging procedure when SAH is suspected. Blood detected in the basal cisterns on CT highly suggests a ruptured aneurysm (van Gijn *et al.* 1980) in patients without trauma. CT scanning has a high ability to detect the extravasated blood in the basal cisterns and the local maxima of the blood may suggest the most probable location of the ruptured aneurysm (van der Jagt *et al.* 1999). Timing of the CT scan after bleeding is associated with the probability of recognizing a hemorrhage on CT scans, which is 85% after 5 days, 50% after 1 week, 30% after 2 weeks (mostly patients with hematomas), and almost nil after 3 weeks (van Gijn *et al.* 1982). Fisher grading has been widely applied to quantify the amount of blood in cisterns: Grade 1= no blood detected, Grade 2= diffuse blood, vertical blood layers (interhemispheric, ambient, lateral sylvian cisterns), <1mm thick, Grade 3= localized clot and/or vertical blood layers > 1mm thick, Grade 4= intracerebral or intraventricular clot with diffuse or no subarachnoid blood. Because Fisher developed the grading system only for his own research purposes, the actual blood clot thicknesses referred in his scale are not directly applicable in clinical use. Consequently, Grades 1-2 are usually referred as mild and moderate bleeding and Grades 3-4 are referred as severe bleeding (Fisher *et al.* 1980, Friedman *et al.* 2002). The amount of extravasated blood on the initial CT scan is related with subsequent vasospasm, delayed cerebral ischemia and clinical outcome (Bell *et al.* 1980, Fisher *et al.* 1980, Kistler *et al.* 1983, Suzuki *et al.* 1980). After SAH has been diagnosed, the multidetector computed tomography angiography (MDCTA) is usually immediately performed to detect the ruptured aneurysm. Sixty-four-row MDCTA can provide prompt and accurate diagnostic and anatomic information in the setting of SAH with an excellent detection rate in acute ruptured aneurysms (Kangasniemi *et al.* 2004, Nijjar *et al.* 2007, Pechlivanis *et al.* 2005). Recently, subtraction 3D CTA has been compared favourably with DSA for detection and characterization of IAs (Li *et al.* 2009, Sakamoto *et al.* 2006). When 64-slice CTA is used in the evaluation of aSAH, the information obtained is usually adequate to determine treatment modality allocation in two-thirds of the cases (Agid *et al.* 2006,

Miley *et al.* 2008) and the possibility of coil embolization can be reliably determined with multidetector CTA (Papke *et al.* 2007, Westerlaan *et al.* 2007).

2.4.2. Digital subtraction angiography (DSA)

Conventional cerebral angiography is still the gold standard for aneurysm detection (van Gijn *et al.* 2001). Cerebral DSA is relatively safe and the rate of neurologic complications seems to have decreased in the modern era with smaller angiographic catheters, new contrast materials and DSA allowing smaller volumes of radiographic contrast per injection. The combination of DSA with 3D rotational angiography (3DRA) is currently the most sensitive technique to detect untreated aneurysms and should be performed in suspicious cases of SAH where the aneurysm is not depicted by 64 MDCTA, because 64 MDCTA may occasionally miss aneurysms less than 3-4 mm in size (McKinney *et al.* 2008). With intraarterial DSA, the prevalence of permanent neurologic deficit has been reported to be 0.3% in 1992 (Waugh *et al.* 1992). Heiserman et al. (1994) prospectively evaluated one thousand consecutive cerebral angiographic procedures performed using transfemoral catheterization and film-screen methods. The overall incidence of neurologic deficits was 1.0 % and the incidence of persistent deficit was 0.5 % (Heiserman *et al.* 1994). All complications occurred in patients presenting with a history of stroke, TIA or carotid bruit, a patient population known to be at risk for atherosclerotic changes. However, the risk of permanent neurological complication associated with cerebral angiography in patients with SAH is significantly lower, 0.07-0.9% (Cloft *et al.* 1999, Dion *et al.* 1987). In addition to neurological complications other angiographic complications are possible following DSA including hematomas and pseudoaneurysms of the puncture site, local or systemic infections, thrombosis of the femoral artery, renal damage and adverse reactions with the use of contrast.

Angiographic studies serve not only to identify one or more aneurysms as potential causes in a patient with aSAH, but also to study the anatomical configuration of the aneurysm in relation to adjoining arteries, which allows optimum selection of treatment (coiling or clipping) (van Gijn *et al.* 2007). The 3DRA furthermore improves the detection of small aneurysms, especially locating on the anterior communicating artery (van Rooij *et al.* 2008, van Rooij *et al.* 2008). The 3DRA with modern software helps to reconstruct the surface luminar anatomical

conditions of the aneurysm and it has been demonstrated to have a good correlation to surgical anatomy (Tanoue *et al.* 2000).

2.4.3. MRI and MR angiography (MRA)

Because of the greater availability and feasibility of CT imaging in patients with suspected subarachnoid hemorrhage, only a few studies of MRI in the acute phase after aSAH have been reported. These suggest that during the first few hours and days, MR with proton density and fluid attenuation recovery (FLAIR) images are as sensitive as CT imaging (Fiebach *et al.* 2004). After the initial days, when hyperdensity on CT scans decreases, MR is better for detecting blood, with FLAIR and T2* and SWI images being most sensitive techniques (Mitchell *et al.* 2001, Thomas *et al.* 2008, van Gijn *et al.* 2007). Although conventional angiography remains the gold standard for aneurysm detection, sometimes non-invasive techniques are used for detection of ruptured aneurysm. 3D time-of- flight (TOF) magnetic resonance angiography (MRA) does not require contrast material and it is the most convenient diagnostic study not carrying essentially any risks. MRA-TOF has been mainly used for aneurysmal screening of people at high risk of aneurysms (Ronkainen *et al.* 1997, van Gijn *et al.* 2007), but the procedure is less feasible for patients who are restless or need mechanical ventilation, and therefore less suitable in acute subarachnoid hemorrhage. Moreover, MR angiography is rarely sufficient for treatment planning. However, standard cross-sectional MR is the best method to demonstrate the presence of thrombus within the aneurysmal sac (Curnes *et al.* 1993). MR-TOF angiography can detect IAs as small as 2-3 mm in diameter, although the detectability is lower for small aneurysms (Okahara *et al.* 2002). Compared to DSA, the sensitivity of 1.5-T MRA in detection of IAs has been demonstrated to be between 79% and 97% and the specificity of 91-100% has been reported (Okahara *et al.* 2002, White *et al.* 2001). Its sensitivity is equivalent to that of CTA and is dependent of aneurysm size with one study suggesting a minimum size of 5 mm for a clinically useful degree of sensitivity for both techniques (White *et al.* 2001). Three-Tesla (3T) MRA is becoming more widely available in clinical practise and it has been shown to be superior to 1.5- T in depiction of IAs, especially small aneurysms (Gibbs *et al.* 2004). For imaging IAs, 3.0-T TOF MR angiography also offers better image quality than 3.0-T CE MR angiography using the elliptical-centric

technique (Gibbs *et al.* 2005). It is essential to distinguish between intradural and extradural location of the aneurysm, because extradural aneurysms that involve the cavernous segment of the ICA have little or no risk for the hemorrhage. Therefore there is no need to preventively treat for SAH and they are commonly just followed (Kupersmith *et al.* 1992). However, the ICA is surrounded by bone, the double dural ring (proximal and distal), the optic nerve, the third cranial nerve and the cavernous sinus, which contribute to its complex anatomical structure. Contrast-enhanced (CE) MRA and multiplanar reformat (MPR) are very useful techniques for determining the location of juxta-dural ring aneurysms (Tsuboi *et al.* 2007) and CE 3D constructive interference in steady state (CISS) MR imaging is useful for the differentiation between paraclinoid and cavernous sinus aneurysms (Hirai *et al.* 2008).

2.5. Imaging in subacute aSAH

In the subacute stage (days 5-20 after aSAH), the diagnosis of delayed cerebral ischemia most often requires repeat CT scans and laboratory tests to rule out hydrocephalus and other systemic reasons (e.g. abnormal electrolytes, infection) as a cause of the deterioratation of a aSAH patient. Various methods have been used to measure cerebral blood flow and cerebral perfusion including CT, MRI, positron emission tomography (PET), single photon emission computed tomography (SPECT), xenon CT, and transcranial Doppler sonography (TCD).

Because of the reported morbidity associated with transporting critically ill patients outside of the intensive care unit (ICU), the portable CT scanners for the ICU have recently been introduced and found to be feasible and cost-effective (Masaryk *et al.* 2008). Radiographic assessment of vasospasm after aSAH by quantitative techniques such as PET and xenon CT, offer tools to identify areas at increased risk for infarction. MRI is more sensitive in detecting early changes in the brain, especially with diffusion weighted imaging. Transcranial Doppler sonography, perfusion-CT, perfusion-MRI and even DSA are used to detect early cerebral ischemia by increased blood flow velocity, prolonged mean transit time (MTT) or arterial narrowing (Bederson *et al.* 2009).

2.5.1. CT and MR perfusion imaging

Perfusion computed tomography (PCT) is a relatively new technique that allows rapid qualitative and quantitative evaluation of cerebral perfusion by generating maps of cerebral blood flow (CBF), cerebral blood volume (CBV) and mean transit time (MTT). The technique is based on the central volume principle (CBF = CBV/ MTT) and requires the use of commercially available software employing complex deconvolution algorithms to produce the perfusion maps (Hoeffner *et al.* 2004). MDCTA with PCT can assess the location and severity of cerebrovascular vasospasm and its related perfusion abnormalities. It can identify severe vasospasm with risk of delayed ischemia and can thus guide to the invasive treatment (Binaghi *et al.* 2007, Sviri *et al.* 2006, Sviri *et al.* 2006, Yoon *et al.* 2006). Cerebral blood flow alterations are common after aSAH, although it has also been reported that decreased cerebral perfusion by itself may not be sufficient to cause DIND (Dankbaar *et al.* 2009). A recent study suggested that there may be perfusion abnormality also without macrovascular vasospasm in the watershed areas or in the vicinity of sulcal cloth. Also cerebral hyperperfusion alterations have been described following vasospasm-induced infarctions (Aralasmak *et al.* 2009). Another recent study, performed on stroke patients suggested, that increased contrast concentration improves peak opacification of tissue, indicating that CTP evaluation is better performed with the highest available concentration contrast agent (Silvennoinen *et al.* 2007).

Review of the literature yielded only a small number of perfusion-weighted MRI (PW-MRI) studies in patients with aSAH analysing haemodynamic changes in regard to the presence of vasospasm (Leclerc *et al.* 2002, Shimoda *et al.* 2001), but a recent study shows that PW-MRI might also reveal early impairment of cerebral autoregulation in patients after aSAH by means of regional CBF (rCBF) and regional CBV (rCBV) (Hattingen *et al.* 2008).

2.5.2. Diffusion weighted imaging (DWI)

Even in the first few minutes after acute arterial occlusion, DWI trace sequences change into a hyperintense signal and there is a fall in the apparent diffusion coefficient (ADC) values (Beauchamp *et al.* 1998). The main pathophysiological

explanation is the existence of cytotoxic edema due to proton pump failure. As a result, water moves from the extracellular spaces into the cells. The resultant cellular swelling leads to a drop in ADC. With a combination of PWI and DWI imaging it is possible to detect areas with a perfusion–diffusion mismatch which represents areas of misery perfusion where the tissue is ischaemic but not yet infarcted. This ‘‘tissue at risk’’ concept derives from studies of ischaemic stroke, grossly identifies the ischaemic penumbra (Wu *et al.* 2005). Quantitative measurements of ADC are more sensitive than DWI for detection of even mild changes in water diffusivity. It has been shown that patients with vasospasm, including the patients without symptoms, presented abnormalities on DWI with a reduction of the ADC prevalently in the white matter (Condette-Auliac *et al.* 2001). Being able to detect the early abnormalities on DWI with parenchymal involvement in asymptomatic patients prior to symptomatic vasospasm might help in preventing the DIND (Condette-Auliac *et al.* 2001). A recent study also reported a finding of global vasogenic edema in subacute stage after aSAH, with elevated ADC values in normal appearing T2-weighted MR images (Liu *et al.* 2007).

2.5.3. Positron emission tomography (PET), single photon emission computed tomography (SPECT), Xenon-CT and transcranial Doppler (TCD)

Positron emission tomography (PET) is the oldest standard for quantitative evaluation of rCBF and cerebral autoregulation after aSAH (Kawai *et al.* 2008, Powers *et al.* 1985). Naderi et al. demonstrated in 1994 that brain perfusion SPECT is a nontraumatic, noninvasive, nonallergic, and inexpensive method for predicting cerebral vasospasm (Naderi *et al.* 1994). Xenon-CT measures CBF directly and low CBF values have been found to be associated with the development of ischemic areas (Yonas *et al.* 1989). However, PET and SPECT require more time compared to PCT and thus, they may be unsuitable for restless patients with unstable conditions in clinical practise. Xenon CT (Xe-CT) is a practical technique which may be performed bedside and may be used to assess cerebral blood flow response to a changing variable e.g. vasoactive drug treatment (Carlson *et al.* 2009). Transcranial Doppler ultrasonography (TCD) is based on the alterations of blood flow velocities which correlate to arterial narrowing and thus, in theory, also to CBF and clinical deterioration (Aaslid *et al.* 1984). TCD is an old, inexpensive, non-invasive, easily

repeatable bedside method used to assess indirectly the cerebral perfusion. However, it is an operator-dependent technique (Horn *et al.* 2001) and a recent study concluded that its overall sensitivity for identifying patients at high risk for DIND is limited (Carrera *et al.* 2009).

2.6. Late Imaging after aSAH

2.6.1. Computed tomography, CT angiography

CT scanning is widely available, easily repeatable, has short study time, and is sensitive to detect ischemic lesions and hydrocepahalus. Moreover, CT is less sensitive to motion artefacts compared to MRI due to considerably shorter scanning time. CT imaging results correlate strongly with clinical outcome (Juvela *et al.* 2005, Naidech *et al.* 2009, Vilkki *et al.* 2004) and most imaging studies after aSAH have been thus far made by using CT. Clip and coil artefacts cause a problem in determining the exact occlusion rates after both endovascular and surgical treatment of aSAH, and there are only a few studies using postoperative CTA for controlling the occlusion rate of the aneurysm. With CTA, the streak artefacts from the coils harass inevitably the perianeurysmal area and aneurysmal occlusion rates cannot be satisfactorily evaluated by CTA (Masaryk *et al.* 2000). However, recent studies reporting the role of CTA for post-operative evaluation of aneurysmal occlusion rates after surgical clipping suggest that CTA might be considered valuable in patients treated with titanium clips (Chen *et al.* 2009, Uysal *et al.* 2009). However, for evaluating the aneurysmal occlusion rates CTA is heavily debated and not commonly used in clinical practise.

2.6.2. Digital subtraction angiography

Conventional digital subtraction angiography (DSA), especially with 3D rotational angiography (van Rooij *et al.* 2008), remains as the gold standard for postoperative imaging of IAs. A literature review from 1979-1999 with more than 1500 clipped aneurysms reported a 5.2 % incomplete occlusion after surgical clipping (Thornton *et al.* 2000). According to a recent study, postoperative DSA detects unplanned vessel occlusions and findings of incomplete occlusions of the aneurysm in one sixth of the

patients, and posterior circulation aneurysms and large or giant-size aneurysms seem to be more prone to incomplete clipping (Kivisaari *et al.* 2004). Significantly better primary angiographic results have been reported after surgical than endovascular treatment with anterior circulation aneurysm (Murphy *et al.* 2005, Vanninen *et al.* 1999). The ISAT study reported complete occlusion rates of 66%; neck remnants or subtotal occlusion rates of 26% and incomplete occlusion rates were detected in 8% of endovascularly treated patients at one year after aSAH (Molyneux *et al.* 2005).

2.6.3. Magnetic resonance imaging and MRA

Magnetic resonance imaging is a powerful tool for diagnosing central nervous system disorders. There are a few contraindications to MRI. These include the presence of cardiac pacemakers, implanted neurostimulators, cochlear implants, metal in the eye, and older ferromagnetic IA clips, which might be displaced by the magnetic field (Shellock *et al.* 1991). MRI of the nervous system offers the following advantages over CT: superior tissue contrast, the ability to obtain images in multiple planes, the absence of artefacts caused by bone, vascular imaging capability and the absence of ionizing radiation. Patients with chronic kidney disease, who need contrast-enhanced (CE) imaging studies, have been traditionally selected to MR imaging with gadolinium-based contrast-media instead of using CT with iodinated contrast media in order to avoid the development of contrast-induced nephropathy (CIN). However, recently the administration of Gd-based contrast agents has been associated with a severe, potentially fatal, adverse reaction, termed nephrogenic systemic fibrosis (NSF), in patients with moderate to severe renal insufficiency (Sadowski *et al.* 2007, Thomsen 2007) and thus the safety questions of the contrast media still remain partly unsolved. However, MR imaging with CE is rarely needed to obtain the diagnostic information of the brain after aSAH.

The disadvantage of MRI is a longer scanning time compared to CT, which makes MRI more sensitive to motion artefacts and less practical for patients whose condition is unstable or who are restless. MRI involves imaging of the proton, the positively charged spinning nucleus of hydrogen atoms that are abundant in tissues containing water, proteins, lipids, and other macromolecules. A MR image represents a display of spatially localized signal intensities. These signal intensities, represented

on the final image as points of relative brightness or darkness, depend on the strength of the magnetic field and the imaging technique, called the pulse sequence, as well as on tissue characteristics, including the T1 and T2 relaxation times, the density of mobile protons, and other factors, such as magnetic susceptibility, chemical shift, and blood flow. Tissues with a large amount of freely mobile water usually appear dark in T1-weighted images but bright in proton-density-weighted and T2-weighted images. Fluids such as cerebrospinal fluid appear very dark in T1-weighted images, intermediate in proton-density-weighted images, and very bright in T2-weighted images. For most clinical studies, all three types of images are used because each contributes to the diagnosis of normal and abnormal structures. On the other hand, T2-weighted images may be better for detecting necrosis and cyst formation in a tumor, and T1-weighted images may be best for detecting subacute hemorrhage. T1-weighted images can be obtained quickly, typically in just a few minutes. The use of the fast spin-echo imaging techniques has shortened the scanning times. For cerebral ischemia, MR Imaging is traditionally considered superior to CT scanning in specificity and sensitivity and the advantages of MRI compared to CT become more pronounced when brain stem or cerebellum has to be evaluated (Awad *et al.* 1986, Edelman *et al.* 1993, Gilman 1998). The appearance of hemorrhage on MRI is heterogeneous and varies according to the age hemorrhage, reflecting the mix of magnetically active products of hemoglobin breakdown and the physical state of the clot (Gomori *et al.* 1988). Hematomas that are three or more days old or older usually have bright components in T1-weighted images at 1.5 T representing extracellular methemoglobin, whereas chronic lesions (over three weeks old) contain dark areas in images because of hemosiderin and ferritin. These features make MRI more sensitive than CT for the detection of older collections of blood; intracerebral, sulcal and extra-axial (Zyed *et al.* 1991). Superficial siderosis of the central nervous system results from hemosiderin deposition in the subpial layers of the brain and spinal cord. A clinical history of subarachnoid hemorrhage is often absent. Patients present with slowly progressive gait ataxia and sensorineural hearing impairment. Superficial siderosis is detected on MR images as a rim of hypointensity on T2-images, enveloping the cortical fissures, the surface of cerebellum and brainstem (Kumar 2007). Moreover, T2*-weighted images and susceptibility-weighted images (SWI) are very powerful to detect superficial areas of low intensity of the hemosiderin in the chronic phase after aSAH (Imaizumi *et al.*

2003, Thomas *et al.* 2008). Non-heme iron is abundantly present in the brain in three different forms: "low molecular weight" complexes, iron bound to "medium molecular weight complexes" metalloproteins such as transferrin, and "high molecular weight" complexes as ferritin and hemosiderin. Ferritin-bound iron is the main storage form of iron and is present predominantly in the extrapyramidal nuclei where its amounts normally increase as a function of age. Ferritin is water soluble and shortens both T1 and T2 relaxation, with results as a signal change on the MR images. Hemosiderin, a degradation product of ferritin, is water-insoluble with a stronger T2 shortening effect than ferritin. The larger cluster size of hemosiderin and its water-insolubility explain a lack of significant T1-shortening effect on T1-weighted images. Thus, in MRI, typical hypointense rims can be observed under the brain surface on T2-weighted images. In contrast, on T1-weighted images, the findings are less obvious and if present, would be shown as hyperintense rims over the brain (Vymazal *et al.* 2000).

Small, bright foci in the white matter are common incidental findings in T2-weighted images, especially in elderly patients. Vascular white matter hyperintensities (WMH) represent one of the main neuroimaging findings in individuals older than 65 years and their clinical significance is still poorly understood (Schmidt *et al.* 1992). Cognitive performance, especially executive functions seem to associate with WMHs (Jokinen *et al.* 2006). Periventricular caps and small, bright subcortical dots correlate with and are risk factors for cerebrovascular disease and cognitive decline (Awad *et al.* 1986, Kertesz *et al.* 1988). Excessive leukoaraiosis has been associated with e.g. cognitive impairment, difficulties in walking and urinary incontinence (Kuo *et al.* 2004). Leukoaraiosis is defined as small vessel white matter ischemic changes on T2-weighted images with no signal changes on T1-weighted images, and it can be scored threepoint score as following: absent, punctuate and/or early confluent and confluent (Schmidt *et al.* 1999). These lesions correspond histopathologically with small areas of minor perivascular damage, reduced myelination, and thinning of the neuropil (Fazekas *et al.* 1991). Dilated perivascular (Virchow-Robin) spaces not associated with lesions in the neuropil are preferentially located in the basal ganglia and midbrain (Heier *et al.* 1989). They do not appear bright in proton-density-weighted images (as opposed to true white-matter lesions) and increase in frequency with age, but after adjustment for the effect of age, they have no known clinical correlation.

Non-ferromagnetic platinum coils are inert and induce practically no susceptibility artefact on MRI when a short echo time is utilized (Walker *et al.* 2005). MRA has been used in follow-up studies of previously coiled aneurysms. A vast majority of embolized patients are eligible to be monitored solely by non-contrast three-dimensonal TOF-technique (Kahara 2006). The sensitivity of 3D TOF MRA compared with DSA for detection of residual aneurysm has ranged between 71% and 97% and the specificity in ruling out residual filling in aneurysms from 89% to 100%, respectively (Okahara *et al.* 2004, Westerlaan *et al.* 2005). Because of the typical susceptibility artefact (diameter typically 20-30mm) a surgical clip causes (Romner *et al.* 1989) MRA TOF cannot be applied for detection of residual aneurysm after surgical clipping.

2.7. Lesions detected on late MR Imaging after aSAH

In analyzing MR images after aSAH, it is essential to be familiar with the vascular anatomy and arterial territories of the brain. On the basis of knowledge of normal vascular anatomy and angiographic findings of each patient, it is possible to determine the most probable etiology of the lesions detected on CT or MR imaging (Hadjivassiliou *et al.* 2001, Kivisaari *et al.* 2001). Ischemic lesions in parental artery territory (vascular territory of the ruptured aneurysm) and other vascular territories (a damage often caused by vasospasm), can thus be differentiated. Late structural brain damage seen on MR imaging can also be associated with the primary hemorrhage itself: superficial siderosis and residual signs of hematoma. Knowledge of surgical techniques used in each case is important when lesions in MR images are interpreted to be caused by surgery. A majority of the retraction injury lesions are located in the basal aspect of the frontotemporal lobes (Hadjivassiliou *et al.* 2001, Kivisaari *et al.* 2001). Patients suffering from aSAH have more lesions in the brain tissue detected by MRI at 2 to 6 years from ictus than might be suspected on the basis of early CT studies. A Finnish study concluded that 81% of surgically treated aSAH patients presented with increased signal intensity on T2-weighted images, consistent with infarction; 48% of the patients had lesions in the frontal lobes (Kivisaari *et al.* 2001). However, CT performed 3 months postoperatively revealed hypodense areas on the scans in only 57% of these patients and showed lesions in the frontal lobes in only 16% of the patients (Kivisaari *et al.* 2001).

2.7.1. Ischemic lesions in the vascular territory of the ruptured aneurysm

Different patterns of cerebral infarcts (CI) can have different pathophysiology. Single cortical or lenticulostriatal infarction in the vascular territory of the ruptured aneurysm can be related to primary bleeding or complications of surgery or angiography and embolization, such as large-vessel occlusion, perforator vessel occlusion, arterial rupture or dissection (Rabinstein *et al.* 2005). Recent studies, particularly those using MRI, report the frequent occurrence of subcortical, often apparently asymptomatic ischemic areas (Kivisaari *et al.* 2001, Shimoda *et al.* 2001). Rabinstein et al. have introduced the two most common patterns of ischemic lesions after aSAH; 1. single cortical infarction in the area of the ruptured aneurysm and; 2. multiple infarctions, often including bilateral and subcortical lesions. It is still unclear, if these two patterns represent different pathophysiological mechanisms or different degrees of severity of the same vascular process (Rabinstein *et al.* 2005). Simple classification for CI after aSAH (single versus multiple, cortical versus deep versus combined) has been shown to give useful prognostic information and a recent study showed that aSAH patients with combined deep and cortical CI was associated with the worst prognosis (Naidech *et al.* 2009). According to the vascular anatomy of each aSAH patient, it can be evaluated if the detected ischemic lesion locates in the vascular territory of the ruptured aneurysm (Tatu *et al.* 1996, Tatu *et al.* 1998).

2.7.2. Ischemic lesions in the vascular territory other than the ruptured aneurysm

Unlike the tromboembolic stroke or sudden arterial occlusion, cerebral ischemia after aSAH usually has a gradual onset and it often involves more than the territory of the parent or a single cerebral artery or one of its branches (Rabinstein *et al.* 2005). The clinical manifestations evolve gradually and consist of hemispheric focal deficits in a quarter of patients, a reduction in the level of consciousness in another quarter and both signs in the remaining half (Hijdra *et al.* 1986). According to the vascular anatomy of each aSAH patient, it can be determined if the detected ischemic lesion locates in the vascular territory other than that of a ruptured aneurysm (Tatu *et al.* 1996, Tatu *et al.* 1998).

2.7.3. Focal laminar cortical infarcts following aSAH

The recently described infarct pattern after aneurysmal aSAH includes cortical band-like lesions. In contrast to territorial infarcts or lacunar infarcts in the white matter which develop as a result of moderate or severe proximal and/or distal vasospasm visible on angiography, the cortical band-like lesions adjacent to sulcal clots may also develop without evidence of vessel occlusion or macroscopic vasospasm, implying a vasospastic reaction of the most distal superficial and intraparenchymal vessels (Dreier *et al.* 2002, Naidech *et al.* 2006, Rabinstein *et al.* 2004, Weidauer *et al.* 2008).

2.7.4. Lesions related to hematoma and superficial siderosis

Residual signs of hematoma on late MRI after aSAH can be easily detected with the help of admission CT scan or control scans after treatment; high-signal-intensity (SI) lesion on T2-images correlating the primary CT finding. Local or more widespread sulcal siderosis is often present and 8 to 72% incidence of hemosiderin after aSAH has been previously published (Imaizumi *et al.* 2003, Kivisaari *et al.* 2001). A recent study showed that the extent of hemosiderin deposition was significantly associated with several factors, including age, CT findings and poor prognosis. Furthermore, T2*-weighted MRI demonstrated more hemosiderin deposits in the subarachnoid spaces and cisterns with aneurysms treated with coil embolization than aneurysms treated with clipping and craniotomy (Imaizumi *et al.* 2003).

2.7.5. Retraction injury due to surgical manipulation

Knowledge of the surgical techniques used in each individual case is important when high-SI lesions on T2-weighted MR images are interpreted to be caused by surgery. A typical retraction injury does not follow the vascular anatomy of the brain. A majority of the retraction injury lesions are located in the basal and superficial aspects of the frontotemporal lobes. The volumes of the focal encephalomalasia due to retraction injury typically vary from large areas adjacent to sylvian fissure to small areas of resected gyrus rectus (Hadjivassiliou *et al.* 2001, Kivisaari *et al.* 2001). The

orbital surface of the frontal lobe can show individual anatomical variations (Duvernoy 1999, Tamraz 2006). Nonetheless, the gyrus rectus is easily identified and often it shows focal atrophy due to surgical resection. A wide variety of surgical approaches has been reported for clipping the ruptured anterior circulation aneurysms, e.g. the pterional approach (Solomon 2001), the lateral supraorbital approach (Hernesniemi *et al.* 2005), the orbitozygomatic approach (Zabramski *et al.* 1998) and the anterior interhemispheric approach (Yeh *et al.* 1985). In the ACA area, the most important factor in selecting the side of approach is the dominance of A1s in preoperative imaging; the side of the dominant A1 is often preferred. If a large ICH is present, the side of ICH is used to prevent bilateral gyrus rectus resection, regardless of the A1 dominancy or other anatomical features. In case of the posterior circulation aneurysms, e.g. the pterional route, subtemporal (Hernesniemi *et al.* 2005) lateral suboccipital (Orakcioglu *et al.* 2005) and anterior petrosectomy (Figueiredo *et al.* 2006) approaches have been used. Presence of other aneurysms may influence selection as clipping of all available aneurysms should be attempted through the same exposure (Hernesniemi *et al.* 2008).

2.7.6. Ventricular dilation, permanent shunts

Ventricular dilation after aSAH is usually related to hydrocephalus, however, ventricular dilation is often combined with sulcal dilation (Vilkki *et al.* 1989), a finding similar to the diffuse brain atrophy detected in patients who survive a severe traumatic brain injury (Poca *et al.* 2005). As a rough planimetric estimate of ventricular size, the cella media index (CMI) and the width of the third ventricle have been used (Jartti *et al.* 2008). CMI can be calculated when the width of the lateral ventricles is divided by the width of the outer layer of the skull. Evans index, where maximal frontal horn width diameter is divided by the maximal width of the frontal skull has also been used to assess ventricular dilation (Zhang *et al.* 2008).

2.7.7. Presence of lacunar infarctions and leukoaraiosis

MR is superior to CT to detect small lacunar lesions (lesions in the basal ganglia, thalamus and white matter), particularly those located deep in the perforator areas and in the brain stem and cerebellum (Awad *et al.* 1986, Edelman *et al.* 1993, Gilman

1998). Some of these lesions, especially those located in putamen and claustrum can be asymptomatic (Shimoda *et al.* 2001). In the recent CT and MRI based analyses 20-39% of all infarcts after aSAH are lacunar type (Rabinstein *et al.* 2005, Shimoda *et al.* 2001, Weidauer *et al.* 2007). Many older people have age-related changes in white matter on brain MRIs (Breteler *et al.* 1994, Pantoni *et al.* 1995). Incidences of leukoaraiosis have been previously reported in 32-60% of aSAH patients (Hadjivassiliou *et al.* 2001, Kivisaari *et al.* 2001).

2.8. Volumetric Magnetic Resonance Imaging

Many MRI-based clinical trials have used quantitative measurements of the brain tissue volumes. These volumetric studies have been concentrated mainly to neurodegenerative processes, such as Alzheimer's disease, stroke and multiple sclerosis, where recent or emerging therapies have been evaluated with volumetric MRI (Ciumas *et al.* 2008, Teipel *et al.* 2008). Various methods are currently available to study volumetric changes in the brain. Most of these structural analyses are performed using high-resolution three-dimensional T1-weighted images. Volumetric analyses can be performed by manually or semimanually delineating regions of interest (ROI), however, manual methods are time-consuming and rater-dependent. Moreover, sometimes the focus of interest is in the structural changes occuring in the whole brain instead in one specific structure and thus several methods that enable the assessment of the whole brain have been developed. These include deformation-based morphometry (DBM) (Ashburner *et al.* 1998, Gaser *et al.* 2001), which provides information about global differences in brain shape, tensor-based morphometry (TBM) (Good *et al.* 2001), which provides information about local shape differences in the brain and voxel- based morphometry (VBM) (Ashburner *et al.* 2000, Good *et al.* 2001), which compares neuroanatomical differences on a voxel by voxel basis, and methods for measuring the cortical thickness (MacDonald *et al.* 2000).

2.8.1. Manual Volumetry

Manual volumetric methods are currently the gold standard to determine the brain structural volumes and they have been widely used in the clinical studies of cognitive disorders (AD and MCI), often concentrating to temporomesial structures;

entorhinal cortex (Insausti *et al.* 1998), hippocampus and amygdala (Soininen *et al.* 1994). In the manual measurements the ROI is manually defined in consecutive slices covering the specific anatomical structure, (e.g. hippocampus) or a specific detected lesion (e.g. ischemic lesion) on brain MRI. The volume then is determined from summing all voxels contained in the ROI across all slices and multiplying the structure or lesion areas by the sum of the section and gap thicknesses. Manual measurements have further been developed to semiautomatic, commercial methods such as EasyMeasure (Bendel *et al.* 2006).

2.8.2. Voxel-based morphometry

The most widely published automated postprocessing method to date is voxel-based morphometry (VBM). The method is based on a low-dimensional spatial transformation of brain scans into a common reference space to get rid of global differences in brain size and shape. After segmentation, differences in grey matter (GM) volumes remaining on a local scale after accounting for global differences are the parameters of interest that drive a voxel-based univariate statistic (Ashburner *et al.* 2000). In a modified form of VBM, the normalization process is iterated such that the final normalization parameters are driven by brain grey matter only. This modification aims to increase the validity of the results by reducing the influence of non-brain tissue (Good *et al.* 2001). It is also possible to assess changes in white matter (WM) and cerebrospinal fluid (CSF), and VBM can be used for longitudinal evaluations of brain volume changes. The method of VBM is demonstrated on **Figure 2**. To determine the anatomical locations of reduced GM, the Montreal neurological Institute (MNI) coordinates obtained from the peak voxels are transferred into Talairach space using the mni2tal routine (http://imaging.mrc-cbu.cam.ac.uk/imaging/MniTalairach). The anatomical locations of the peak voxels in the significant clusters are determined by using the Talairach Daemon Applet (Lancaster *et al.* 2000) and further verified from anatomical brain atlases (Duvernoy 1999, Tamraz 2006).

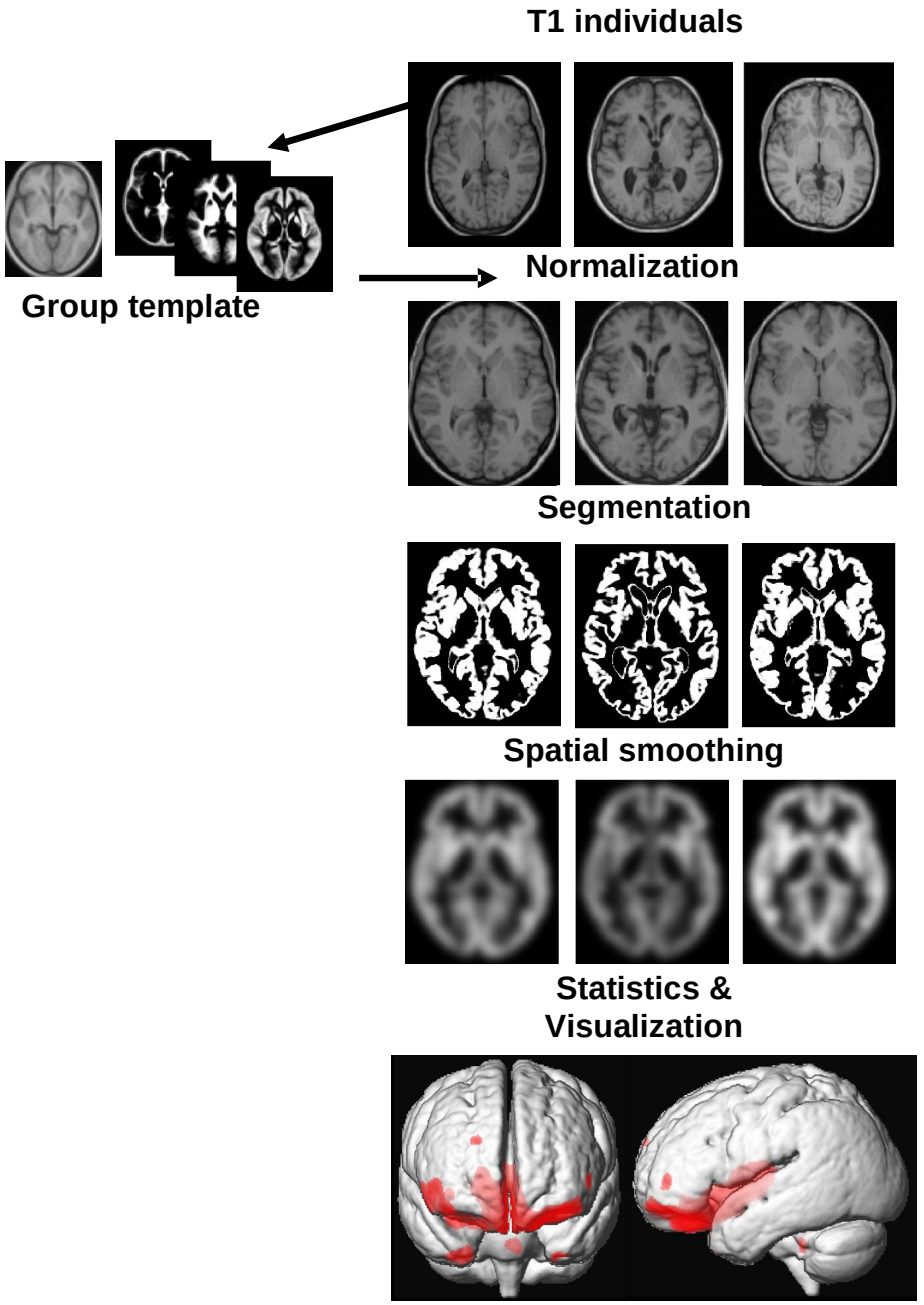

Figure 2. Steps of VBM are demonstrated above.

2.9. Methods for outcome assessment

2.9.1. Clinical outcome scales and prognostic factors

The clinical outcome is usually evaluated at the outpatient department by a neurosurgeon, usually two to three months after aSAH and treatment of the ruptured aneurysm. The Glasgow Outcome Scale (GOS) (Jennett *et al.* 1975) is often used as a rough outcome measure. GOS scores are graded as following: GOS V= Good recovery, GOS IV= Moderate disability; disabled, but independent, GOS III= Severe disability; conscious but disabled, GOS II= Persistent vegetative state, GOS I= Death. There are other rough categorical outcome grading systems such as old Rankin Outcome scale (Rankin 1957) which have also been used for assessment of the clinical outcome.

The main determinant of outcome is the severity of the initial bleed (Broderick *et al.* 1994, Hop *et al.* 1997, Koivisto *et al.* 2000). The clinical and cognitive outcome is related to the several well-established pre- and postreatment clinical factors: higher Hunt and Hess grade, advanced age, a high Fisher score, preoperative hydrocephalus, clinical vasospasm, and larger aneurysm, all favoring the poorer outcome (Hernesniemi *et al.* 1993, Hoh *et al.* 2004, Kassell *et al.* 1990, Koivisto *et al.* 2000 , Molyneux *et al.* 2005, Salary *et al.* 2007). Massachusetts General Hospital grade incorporates prognostic factors such as age, Hunt and Hess grade, size and location of the aneurysm, and Fisher grade which alone may not demonstrate statistical association, but may add incrementally to the risk of poor outcome of a patient (Hoh *et al.* 2004). Clipping of an anterior cerebral artery aneurysm has been associated with a higher impairment rating (Bornstein *et al.* 1987). Furthermore, high blood glucose levels (Kruyt *et al.* 2009), occurrence of hypovolemia and hypotension (Chang *et al.* 2000) and elevated blood D-dimer (Juvela *et al.* 2006) have been correlated with worse outcome.

2.9.2. Neuropsychological outcome

The long-term neuropsychosocial effects of aSAH are considerable, even in patients who regain functional independence (Wermer *et al.* 2007). Many patients surviving from aSAH are left with persisting neurological and cognitive impairments

(Bellebaum *et al.* 2004, Hackett *et al.* 2000, Kreiter *et al.* 2002, Mayer *et al.* 2002, Ogden *et al.* 1997) and half of the surviving patients cannot return to their previous work (Powell *et al.* 2002). During the past decade, there have been many studies reporting functional outcome; cognitive function and quality of life (QOL). Neuropsychological testing is a feasible outcome measure (Anderson *et al.* 2006, Egge *et al.* 2005) in patients after aSAH, especially with good clinical outcome. However, good neurological outcome (GOS V) score does not exclude persisting neuropsychological deficits, and even 62% of GOS V patients suffer cognitive impairments (Hutter *et al.* 1993). Global cerebral edema and diffuse brain damage and left-sided infarction or frontal medial infarctions are important risk factors for cognitive dysfunction after aSAH (Kreiter *et al.* 2002, Vilkki *et al.* 1989).

2.9.3. Quality of life

Quality of life (QOL) constitutes a criterion of evaluation that describes the daily life tasks in physical, physiological, and social fields of health and has been measured in outcome studies after aSAH. The information has been collected with regard to the QOL by semistructured interview and different quality of life scores, for example EURO QOL (EQ-5D) (Brooks 1996, Brooks 1996, Hutter *et al.* 1993, Ogden *et al.* 1997) or validated instruments (Hop *et al.* 1998, Hop *et al.* 2001, Hutter *et al.* 2001).

3. AIMS OF THE STUDY

The general aim of the study was to determine the MRI outcome and to compare it in aneurysmal subarachnoid hemorrhage (aSAH) patients who were randomly assigned to endovascular versus surgical treatment of acutely ruptured intracranial aneurysms.

The more specific fourfold aims were:

I: To prospectively evaluate, with MR imaging, the long-term outcome of the brain after endovascular versus neurosurgical treatment for aSAH.

II: To evaluate and compare the volumes of temporomesial structures (amygdala and hippocampus) after endovascular and surgical treatment of aSAH.

III: To assess the regional atrophic patterns of the brain and their clinical and neuropsychological relevance after aSAH due to a ruptured anterior cerebral artery aneurysm by employing voxel-based morphometry (VBM).

IV: To quantify the possible late (atrophic) ventricular and other cerebrospinal fluid (CSF) space dilation in patients with aSAH and to correlate the cognitive outcome with the degree of enlarged CSF spaces.

4. PATIENTS AND METHODS

4.1. Study design and study inclusion criteria and patients

The study design was approved by the Ethical Committee of the University of Kuopio and Kuopio University Hospital. During the original study period between February 1, 1995 and December, 1999, all patients who were admitted to Kuopio University Hospital because of SAH were assessed as candidates for the prospective randomized study.

CT was performed to all candidates to confirm the diagnosis of SAH. After CT an informed consent from the patient or from the patients' closest relative were obtained. The final recruitment into the study was made after the diagnostic angiography, where the diagnosis of aneurysmal SAH was confirmed. All patients with ruptured IAs suitable for both endovascular and surgical treatment were consecutively included. The exclusion criteria for enrollment into the study were the following: 1. Age> 75 years; 2. Bleeding > 3 days previously; 3. Large hematoma requiring urgent surgery; 4. Mass effect of the aneurysm causing neurological deficit; 5. A previous aneurysmal surgery.

Based on the diagnostic angiography, the aneurysm was not considered as suitable for endovascular treatment and thus not randomized if: 1. the neck of the aneurysm was wider than the fundus; 2. the aneurysm was fusiform; 3. the neck and its' relationship to parent vessel and adjacent branches were not distinguishable; 4. the size of the aneurysm was < 2 mm (less than the smallest coil available). The patients' suitability for endovascular treatment and randomization was assessed according to the morphology of the aneurysm that had most probably ruptured (size and the irregularity of the aneurysm and the localization of hemorrhage detected on CT). Randomization procedure was performed in three different categories according to the pretreatment clinical condition of the patient (Hunt & Hess Grade I-II, Grade III, and Grade IV-V) in order to avoid the selection bias. Sealed envelopes were allocated for each group of patients in randomization procedure.

4.2. Fisher- and Hunt and Hess Grades and clinical vasospasm

Every patient had preoperative CT scans, which were evaluated in consensus by a neurosurgeon (T.K) and a neuroradiologist (R.V) for assessment of the Fisher grade (Fisher *et al.* 1980) and possible hydrocephalus. The Fisher grades were further dichotomized into grades 0-2 (minor/moderate bleeding) and grades 3-4 (severe bleeding). The Hunt and Hess grades were assessed by one of six resident neurosurgeons (with 1-6 years of experience) and confirmed by two senior neurosurgeons. Clinical criteria for symptomatic vasospasm (assessed by one of 7 senior neurosurgeons) were a decrease of Glasgow Coma Scale by ≥2 scores or appearance of new localizing symptoms (dysphasia or hemiparesis); other reasons for deterioration, e.g. hydrocephalus, metabolic disorders, post-operative bleeding and infections being ruled out.

4.3. Diagnostic angiography and embolization procedure

The diagnostic angiography was performed via the femoral artery through a 6-F-introducer. Digital subtraction angiography equipment (Polytron; Siemens Medical Engineering Group, Erlangen, Germany) with a 1024 x 1024 matrix was used. The internal carotid and vertebral arteries were selectively catherized. Angiography was followed by the immediate random assignment and if indicated, endovascular treatment during the same session. At angiography, the site, orientation and morphology of the aneurysm were carefully evaluated and the size of the aneurysm and the width of the neck were measured with a digital caliber using two coins as a reference. In all grade IV-V patients and majority of grade III patients, embolization was performed with use of general anesthesia. In patients with grade I-II and in some of the grade III patents, no method of sedation was used. During the procedure, systemic administration of heparin (initial bolus of 5000 IU in the first 5 patients and 2500 IU in the remaining patients, followed by 1000 IU after an hour and according to the measured activated clotting time thereafter). The endovascular procedures were performed by two interventional neuroradiologists (1 and 3 years of experience in neurointerventions in the beginning of the study). A 6 F guiding cathether was advanced to ICA near the level of skull base or to the upper cervical portion of the vertebral artery. A microcatheter (Tracker-10 or Tracker-18; Target Therapeutics,

Fremont, California, USA) with two tip markers and a Dasher-14, usually followed by a Dasher-10 guidewire (Target Therapeutics, Fremont, California, USA) were used for hyperselective catheterization of the aneurysmal sac. By using a distal roadmap control, care was taken not to touch the aneurysmal wall with the guidewire or the catheter. A continuous, pressurized flush of heparinized saline solution was maintained in both the guiding catheter and the microcathetheter. Once catheterization had been achieved, the aneurysmal sac was filled with Guglielmi detachable coils (GDCs; Target Therapeutics, Fremont, California, USA), which can be electrically detached. Complete occlusion of the aneurysmal sac and neck was always attempted. The largest coil, selected according the measured aneurysm diameter, was positioned first to form a basketlike frame in the aneurysm. The smaller coils were then sequentially delivered into the aneurysm until the lumen was completely occluded and flow inside the aneurysm as well the secundary pouch was arrested. If the size of selected coil proved to be unsuitable, the GDC system allowed removal of the coil and repositioning of the mesh to an optimal position. Oral administration of aspirin (250 mg daily) was continued for 3 months after embolization. After endovascular treatment, the follow-up DS angiographs were performed 3, 12 and 36 months after aSAH.

4.4. Surgical treatment

Surgical procedures were performed under balanced anesthesia with hyperventilation by a team consisting of 7 senior neurosurgeons (10-30 years of experience in neurosurgery) with a collective experience of approximately 2000 aneurysm operations. All patients received corticosteroids and mannitol. Pterional, subtemporal, frontal interhemispherical or lateral suboccipital approaches were used depending on the location of the aneurysm. A standard microsurgical method was used for clipping the aneurysmal neck with Sugita (Mizuho Medical Co., Tokyo, Japan) or Yasargil (Aesculap AG & Co. KG, Tuttlingen, Germany) aneurysm clip. If feasible, the aneurysm was opened, coagulated or both. Follow-up angiography was scheduled after surgical clipping during the primary hospitalization, and in case of neck-remnant, 12 months after clipping.

4.5. Patient care after treatment

After the randomization procedure and treatment, both endovascular and surgical patients were treated in the intensive care unit and neurosurgical ward in a similar manner. The hypervolemic therapy, which was ascertained with Swan-Ganz catheter placement and measurements of the pulmonary capillary wedge pressure was used. Regardless of the treatment modality, prolonged bed-rest (10 days), corticosteroids and intravenous nimodipine were used in every patient. Symptoms of vasospasm were recorded on daily basis.

4.6. Follow-up protocol: MR Imaging

4.6.1. Conventional MRI protocol

Patients underwent 1.5 Tesla MRI (Magnetom Vision; Siemens Medical Systems, Erlangen, Germany) with a circular-polarized head coil. MRI protocol consisted of axial T2 and intermediate-weighted (TR/TE 2625/98-16ms, matrix 260x512, slice thickness 5mm) images, magnetic resonance time of flight angiography for the embolized patients and a three-dimensional T1-weighted-sequence: magnetisation-prepared rapid gradient echo (MPRAGE) sequence (TR/TE/TI 9.7/4/20ms, flip angle 12º, FOV 250mm, matrix 256x 256). All coils and surgical clips were non-ferromagnetic and MRI-safe.

4.6.2. MRI Analysis

All MRI examinations were analyzed in a consensus by a neuroradiologist (R.V.), a neurosurgeon (T.K.) and a resident (P.B.) with15, 13 and 2 years of experience in interpretation of MRI images on the time. Blinded reading was not possible because of characteristic clip and coil artefacts. The presence of any high-SI lesions on T2 and intermediate-weighted images (low-signal-intensity on 3D T1-weighted images) was visually evaluated and lesion volumes were measured. The most probable etiology of the high-SI lesion was determined and classified in consensus with knowledge of all clinical, radiological and surgical details of the patient. CT-scans and angiographic images were available during the MRI evaluation.

The following factors were analyzed and quantified according to anatomical locations (Tatu *et al.* 1996, Tatu *et al.* 1998). Ischemic lesions in 1. parental artery territory (vascular territory of the ruptured aneurysm) and 2. other vascular territories, based on knowledge of normal vascular anatomy and angiographic findings of the individual patient; 3. Superficial siderosis and residual signs of hematoma; 4. Signs of retraction injury due to surgical manipulation and instrumentation; 5. Ventricular size and possible hydrocephalus; 6. Parenchymal lesions associated with intraventricular catheter and permanent shunt placement and 7. Previous infarctions, degree of possible previous atrophy, and presence of lacunar infarctions and leukoaraiosis.

The parental artery of the ruptured aneurysm was classified as: 1. anterior cerebral artery (ACA), 2. middle cerebral artery (MCA), 3. internal carotid artery (ICA), or 4. vertebrobasilar artery (VBA). If the ruptured aneurysm was located in the AComA or the basilar tip, the bilateral vascular territories of frontopolar, callosomarginal, and pericallosal arteries and posterior cerebral arteries were considered as parental arteries. Ischemic lesions in vascular territories other than the parental arteries were considered to represent general vasospastic etiology. Signs of parenchymal or Sylvian hematoma were evaluated with help of primary CT-scans. The convexity of the brain, basal cisterns and Sylvian region were evaluated for possible signs of superficial siderosis. Approximate adjustment for ventricular size was made visually on consensus reading. As a rough measure of ventricular size, the modified cella media index (mCMI) was calculated as the maximum diameter of the lateral ventricles/ intraparenchymal diameter at the same level. Degree of leukoaraiosis was scored as: absent, punctuate/ early confluent or confluent (Schmidt *et al.* 1999). Volumes of ischemic and retraction lesions were measured by a single interpreter (P.B., based on the initial concensus reading) on a PACS workstation (SECTRA EE, version 10.2.P4; Linköping, Sweden) by drawing a region of interest according to the lesion margin on each T2 weighted image and by multiplying the lesion areas by the sum of the slice (5 mm) and gap (1.5 mm) thickness.

4.6.3. Volumetric MRI

The sequence for the volumetric analyses was scheduled as an additional sequence at the end of the imaging, if the patient was cooperative and there were no movement artefacts in the basic images and the patient was willing to stay extra time in the MR scanner.

The 3D T1 sequence needed for volumetry was obtained using the magnetisation-prepared rapid gradient echo (MPRAGE) sequence (TR/TE/TI 9.7/4/20ms, flip angle 12º, FOV 250mm, matrix 256 x256). The coronal slices (thickness 2.0 mm) included the whole cerebrum.

4.6.4. Semiautomatic volumetry (Study II)

Standard neuroanatomical landmarks (such as AC-PC line, hemispheres and orbits) were used to reconstruct coronal slices (thickness 2 mm) perpendicular to the long axis of the left hippocampus (HC). These sixteen-bit Siemens format images were converted to the ANALYZE format (MAYO Foundation, Minnesota, USA). In study II, the volumes of the amygdalae (AM) and HC were manually measured by a single observer. To maintain blind assessment and confidentiality, data was registered and coded by subject numbers only. The intraclass correlation coefficients for intrarater reliability (bilateral measurements of 10 patients) were 0.94 for the AM and 0.88 for the HC volumes. The point counting method (EasyMeasure, version 1.0, MariArc, Liverpool, UK) was used to calculate the volumes of the hippocampus and the amygdala. The point-counting method consisted of overlaying a systematic array of the test points (one point per 9 pixels) completely over each slice. Instances in which a point, in fact a cross, lies within the area of interest, are recorded by clicking a computer mouse. Subsequently, the total number of the test points is multiplied by the volume of the test point (17.17 mm^3). Boundaries of the HC and AM were identified with the use of the neuroanatomy atlas (Martin 1996) and previously published research (Watson *et al.* 1992). The point counting of the structures proceeded from anterior to posterior.

The amygdaloid volume consisted of the volumes of the central nucleus, the corticomedial nucleus and the basolateral nucleus. Hippocampal volumetry included the dentate gyrus, the cornus ammonis (hippocampus proper) and the subiculum.

Defining of the hippocampus started from the first appearance below the amygdala and continued till the most posterior slice on which the temporal horn and the body of the ventricles were separated. The method of the volumetry is shown on **Figure 3.**

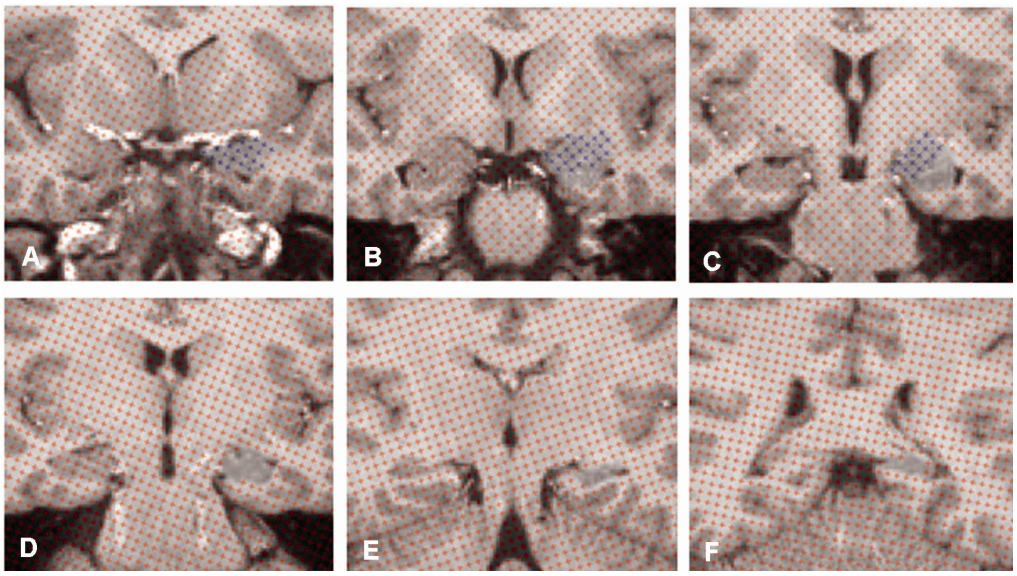

Figure 3. The method of volumetry. Coronal three-dimensional T1-weighted images from anterior to posterior demonstrate the marked structures of left amygdala (A through C, blue crosses) and left hippocampus (B through F, no crosses) in a healthy 23-year-old female control individual.

The coronal intracranial area was measured at the level of the anterior commissure (the reference slice). This intracranial area has been noted to give a reliable correlation to the whole brain volume (Laakso *et al.* 1998). To remove the influence of the head size to the volumes of nuclei, the volumes were normalized by dividing the volume of the nucleus with the slice volume of the intracranial area (volume of the structure/intracranial area in reference slice)*100 (Pennanen *et al.* 2004). Normalized volumes were further defined as "ipsilateral" or "contralateral" according to the side (right or left) the ruptured aneurysm was filling from. In midline (basilar and AComA) aneurysms ipsilateral side was defined as the side where the surgery or endovascular cathetrization was performed.

4.6.5. Voxel-based morphometry (studies III - IV)

Optimized VBM analysis (Ashburner *et al.* 2000, Good *et al.* 2001) was performed using the VBM2 (study III) toolbox (http://dbm.neuro.uni-jena/vbm/) under SPM2 (Wellcome Department of Imaging Neuroscience, London, UK; www.fil.ion.ac.uk/spm). The VBM procedure started with creating a customized template and customized prior probability maps using the standard procedure of VBM-toolbox: normalization to the MNI T1-weighted template provided by SPM, resampling the voxel size to 2 x 2 x 2 mm, segmenting the images into gray matter (GM), white matter (WM), and cerebrospinal fluid (CSF), smoothing both the normalized images and the segments with 8 mm Gaussian kernel, averaging the smoothed images and segments.

In order to define the normalization parameters for spatial normalization and absolute volumes of different tissue types, the original images were segmented into GM, WM and CSF using the customized prior probability maps. The absolute volumes of GM, WM, and CSF were calculated from the segments, and they were further summarized to obtain the total intracranial volume (ICV) and the GM/ICV and CSF/ICV ratios were calculated from these values. The normalization parameters were estimated using these GM segments and the customized GM template. The original images were then normalized using the estimated normalization parameters, and were resampled to 2 x 2 x 2 mm. The normalized images were further segmented into GM, WM, and CSF using the customized prior probability maps. Finally, the GM-segments were modulated and smoothed with a 12 mm Gaussian kernel.

VBM Group analyses (Study III) were performed in SPM2 including age, sex and intracranial area as nuisance covariates in order to compare the GM volumes between the patients and controls. Between group differences were assessed using a t-test with a height threshold of $P<0.05$, corrected for multiple comparisons by the family-wise error (FWE) or by the false discovery rate (FDR-method) (Genovese *et al.* 2002) method. When surgical and endovascular patients were compared in VBM-analysis, the group differences were assessed using a t-test with a height threshold of $P<0.05$, corrected for multiple comparisons by the false discovery rate (FDR) method, because no voxels survived the conservative FWE-method. Only those clusters exceeding a size of 50 voxels were included in the analysis. To determine

the anatomical locations of reduced GM, the MNI coordinates obtained from the peak voxels were transferred into Talairach space using the mni2tal routine (http://imaging.mrc-cbu.cam.ac.uk/imaging/MniTalairach). The anatomical locations of the peak voxels in the significant clusters were found using the Talairach Daemon Applet (Lancaster *et al.* 2000) and further verified from an anatomical brain atlas (Duvernoy 1999).

In study III, the aim was to examine the differences in grey matter volumes between the patients and controls with respect to the side of the treatment (craniotomy or endovascular cathetherization) and the contralateral side. Therefore, the MR images of the patients in whom the approach of the treatment was on the left hemisphere (17 out of 37) were flipped around the anterior-posterior axis using MRIcro (www.sph.sc.edu/comd/rorden/mricro.html) prior to any data analysis. Furthermore, same proportion of controls (12 out of 30), matching with the patients' age in decades, had their images similarly flipped.

In study IV, for quantitation of the ventricular size at the group-level, an averaged normalized CSF segment image was calculated using the segmentation routine provided by VBM5 toolbox in SPM5 for both patients and control individuals. Using these averaged CSF-images, a ventricular ROI was manually traced (by P.B) for both groups with MriCro (http://www.sph.sc.edu/comd/rorden/mricro.html) and the average volumes of the ventricles were calculated for patient and control individual groups.

4.7. Follow-up protocol: Clinical Outcome, Neuropsychological evaluation

Clinical outcome and GOS one year after aSAH were assessed by a single neurosurgeon (T.K.). Detailed neuropsychological examination was performed by a single neuropsychologist (H.H.) one year after aSAH. Two experienced neuropsychologists (M.Ä. and T.H.) further interpreted the neuropsychological test results using the normative data.

The comprehensive evaluation included tests of general intelligence, memory and selected language abilities and assessment of attention and flexibility of mental processing as explained in the following: General intellectual ability: On the basis of subtests of the Wechsler Adult Intelligence Scale-Revised (WAIS-R) (Wechsler 1981) the scores for general verbal and nonverbal ability and total intelligence quotients

were calculated. The Modified Boston Naming test (Lezak MD 2004) was used to examine naming ability and the Finnish version of the Verbal Fluency Test on letters (Borkowski *et al.* 1967) was used to evaluate word fluency. Learning and memory: Memory was tested by the Wechsler Memory Scale (WMS) (Wechsler 1974). The Memory Quotient was calculated to assess short-term memory performance. Delayed recall of Logical Memory Subtest (Wechsler 1974) and the Visual Reproduction Subtest (Wechsler 1974) was asked 45 minutes later. Nonverbal memory was also assessed by the Rey Complex Figure Test (Lezak MD 2004). Attention and flexibility of mental processing and psychomotor speed: The Stroop Test (Golden 1978) (form A, B and C) and the Trail Making Test (Reitan 1958) (part A and B) were used to evaluate sustained attention and resistance to interference. The Finger Tapping test was used to assess simple psychomotor speed. Neuropsychological examination was divided into four different cognitive domains (general intellectual functioning, memory, language and executive functions). Impairment in any of the four cognitive domains was defined on the basis of normative data, where the scores fell below the normal range in either measure of the domain. General intellectual functioning was estimated on the basis of five subtests of the Wechsler Adult Intelligence Scale-Revised (WAIS-R) (Wechsler 1981). Language was evaluated with a shortened version of the Boston Naming Test and Verbal Fluency test (Lezak MD 2004). Memory was assessed with the Logical Memory and Visual Reproduction subtests (immediate and delayed recall) from Wechsler Memory Scale (WMS) (Wechsler 1974). Percent retention scores (calculated by dividing the delayed recall score by immediate recall score) were the measures for verbal and visual memory. Executive functions were assessed with the Trail Making Test and the Stroop Test (Golden 1978, Reitan 1958). In order to extract the executive component in these tests, a difference score was calculated by subtracting the time taken in Trail Making A from the time taken in Trail Making B. A similar calculation was performed for recorded times for colour naming and the interference part of the Stroop Test. The neuropsychological test results were then further dichotomized.

4.8. Study populations

4.8.1. Original study population and MRI study population (study I)

Altogether 168 patients were randomized according to the study protocol; 86 patients were allocated to surgical treatment and 82 were allocated to endovascular treatment. MR imaging was scheduled to all allocated patients one year after aSAH. **Figure 4** shows the flowchart of the study population. The final MRI study population consisted of 138 aSAH patients. The demographic data of the MRI study population is shown on **Table 1**.

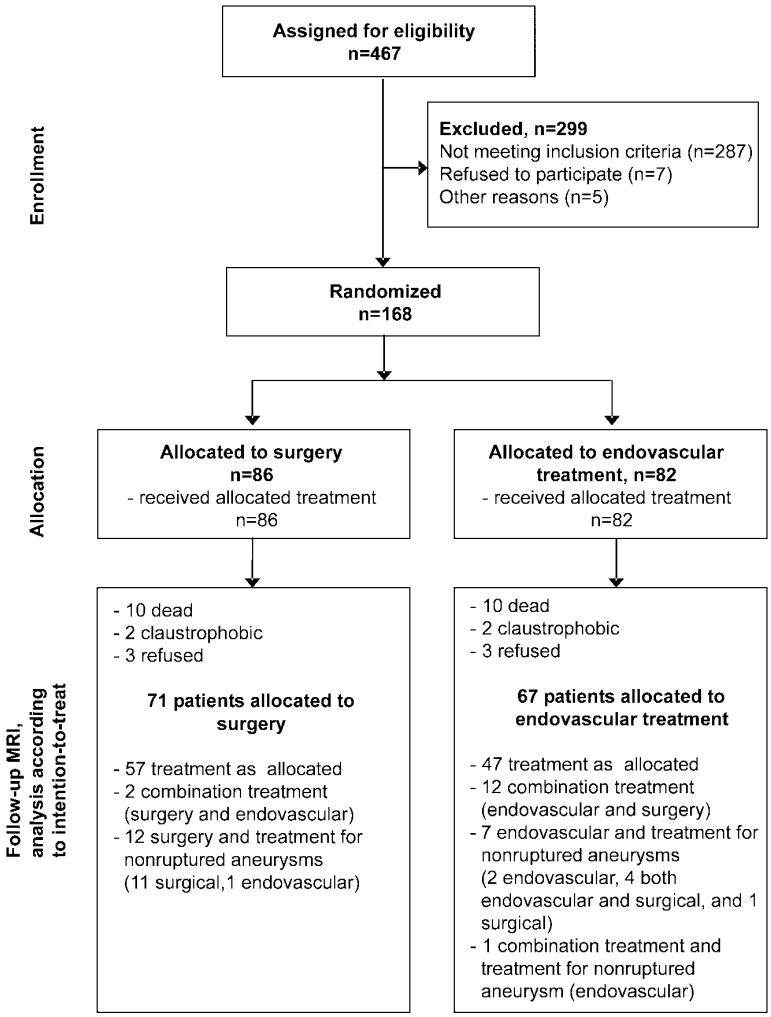

Figure 4. The flowchart of the original study population.

Table 1. Baseline Characteristics of Patients with 12 Month MRI According to Intention to Treat

Characteristic	Embolization n = 67	p	Surgery n = 71
Male/female	35/32	0.131	28/43
Age, mean±SD (yrs)	50 ± 13	0.485	51 ± 13
Hunt & Hess grade		0.774	
I-II	45 (67.2%)		49 (69.0%)
III	15 (22.4%)		17 (23.9%)
IV-V	7 (10.4%)		5 (7.0%)
Fisher grade		0.187	
0-2	28 (41.8%)		22 (31.0%)
3-4	39 (58.2%)		49 (69.0%)
Clinical Vasospasm	18 (26.9%)	0.058	30 (42.3%)
Ruptured aneurysm site		0.094	
Anterior circulation	59 (88.1%)		68 (95.8%)
Posterior circulation	8 (11.9%)		3 (4.2%)
Size of the ruptured aneurysm, mean ± SD (mm)	6.3 ± 2.9	0.697	6.5 ± 2.9

p-value indicates statistical significance between patients intended to treat endovascularily vs. surgically.

4.8.2. Combination treatment of the ruptured aneurysm and treatment of additional associated nonruptured aneurysms

Altogether 15 of the 138 (10.9%) patients who underwent follow-up MRI, have had combination treatment (both endovascular and surgical) of the ruptured aneurysm. The indications for combination treatment were failure in the primary treatment procedure or revascularisation of the aneurysm in follow-up DS angiography. Combination treatment was required more frequently in the endovascular group (n=13, 19.4%) than in the surgical group (n=2, 2.8%, p=0.002). Thirty-five of the138 (25.4%) patients had 54 nonruptured aneurysms, which were treated using the same criteria currently recommended (Bederson *et al.* 2000): embolization in 6, surgery in 23, combination treatment in 3 and angiographic follow-up in 22 cases. All analyses where treatment groups (surgical. vs. endovascular) were compared with each other were performed according to intention-to-treat and also repeated after excluding patients with combination treatment or additional treatment for nonruptured aneurysms.

4.8.3. Volumetric study populations (studies II, III and IV)

Altogether 77 patients from the randomized population (33 endovascular, 36 surgical and 8 combination treatment patients) underwent three-dimensional T1-weighted examinations. In study II, 77 volumetric measurements were available. In study IV 76 volumetric measurements were available; one volumetric study had to be excluded, because the scanning area on T1-weighted volumetric sequence did not cover the whole cerebrum. Study III consisted of 37 ACA volumetric patients (after exclusion of 5 ACA patients whose associated unruptured aneurysms had been treated before MRI). The demographic data of the volumetric study population is shown on **Table 2**.

Table 2. Patient and Control Individual Characteristics in Volumetric Study Population

	Controls n = 30	Aneurysmal SAH n = 77	Endovascular patients n = 41	p	Surgical patients n = 36
Age, years ± SD	54.1 ± 15.5	50.2 ± 14.8	50.1 ± 14.3	0.963	50.3 ± 15.5
Sex female	18 (60%)	43 (55.8%)	20 (48.7%)	0.183	23 (63.9%)
male	12 (40%)	34 (44.2%)	21 (51.2%)		13 (36.1%)
Fischer Grade					
0 - 2		28 (36.4%)	16 (39.0%)	0.604	12 (33.3%)
3 - 4		49 (63.6%)	25 (61%)		24 (66.7%)
Hunt & Hess Grade					
I - II		55 (71.4%)	28 (68.3%)	0.459	27 (75.0%)
III		17 (22.1%)	9 (22.0%)		8 (22.2%)
IV - V		5 (6.5%)	4 (9.8%)		1 (2.8%)
Aneurysm location					
ACA		42 (54.5%)	23 (56.1%)	0.409	19 (52.8%)
MCA		11 (14.3%)	4 (9.8%)		7 (19.4%)
ICA		16 (20.8%)	8 (19.5%)		8 (22.2%)
VBA		8 (10.4%)	6 (14.6%)		2 (5.6%)
Aneurysm size			6.12 ± 2.82	0.685	6.39 ± 2.93
Neck size			2.83 ± 0.99	0.487	2.67 ± 1.04

ACA indicates anterior cerebral artery, AComA, pericallosal artery. MCA; middle cerebral artery. ICA; internal carotid artery, ophthalmic artery, PComA, anterior choroidal artery. VBA indicates vertebrobasilar arteries. p indicates the difference between endovascular vs. surgical aSAH patients according to intention to treat.

4.8.4. Neuropsychological study population (studies I-IV)

The neuropsychological examination was available from 116 out of 138 (84.1%) patients, who underwent the one year MRI. In the volumetric study populations, 76 out of 77 (98.7%, study II), all 37 ACA patients (study III) and 75 out of 76 (98.7%, study IV) underwent the neuropsychological examination.

4.8.5. Control individuals (Studies II, III and IV)

30 healthy control individuals matching their age and gender to the volumetric study population (studies II - IV) were also imaged for volumetric purposes with the same MRI equipment than the aSAH patients. The demographic data of the control individuals is also shown on Table 2.

4.9. Statistics

All analyses were performed with the statistical package for Windows (SPSS, Inc., Chicago, IL, USA, versions 11.5- 16). The intention-to-treat analysis was used in all comparisons of endovascular and surgical patients. In addition to intention-to-treat analyses, the censored analyses were also performed after excluding patients having combination treatment for ruptured aneurysm or treatment for additional, nonruptured aneurysms.

In general, all continuous variables were tested for normal distribution with the Kolmogorov-Smirnov 1-sample test (level of statistical significance difference at $p<0.1$). The Chi-Square test was used for categorical data and dichotomized variables. The Student t-test was used to compare normally distributed data and Mann-Whitney-U test was used to compare nonparametric, continuous-scale data for non-normally distributed variables. Spearman and Pearson correlation coefficients were used to assess correlation between nonparametric continuous-scale variables. Differences were considered to be statistically significant, if the two-tailed p value was <0.05. The multiple comparisons were corrected with Bonferroni adjustment (Norman G 1994) and the significant p-value in these analyses using the same parameter twice was $0.05/2 =0.025$. The group differences in volumetric analyses are

based on t-test statistics with a height threshold of $P<0.05$ and explained in more detail in paragraph 4.6.3.

5. RESULTS

5.1. Comparability of the study groups

According to the intention to treat analysis, in the MRI-study population with 138 patients, the endovascular and surgical treatment groups did not show any statistically significant differences in their age or sex distribution, nor in their Hunt & Hess Grades, Fisher grades, size or location of the ruptured aneurysm or preoperative hydrocephalus (study I). The endovascular and surgical treatment groups remained also balanced in a censored analysis after excluding the patients who had undergone combination treatment or treatment for additional nonruptured aneurysms. Moreover, the different treatment groups did not show statistically significant differences in abovementioned parameters (studies II, III and IV) in volumetric studies. The control individual group was used in volumetric comparisons (studies II-IV) and the control individuals were statistically balanced in terms of age and gender. In study III, all aSAH patients (n=37: 20 endovascular, 17 surgical) and controls (n=30) were balanced for age and sex in comparison between aSAH patients and controls. The final group analyses in study III were performed after excluding patients with crossover treatment (5 endovascular patients) and after this exclusion there was a male dominance in the endovascular subgroup (12 of 15, 80%) vs. controls (13 of 30, 43.3%; p=0.020). The surgical group and controls remained gender balanced.

The volumetric study population mostly consisted of patients with good recovery; 66 patients had good outcome and ten patients (7 surgical, 3 endovascular) had moderate disability. Moreover, the clinical outcome was better in the volumetric subgroup compared to the original study population.

The mean interval between aSAH and MRI was 15.8 ± 8.5 months (range 9-64 months). The diagnostic quality of the MRI examinations was excellent in 134 (97.1%) and suboptimal, but diagnostic in 4 (2.9%) examinations.

5.2. Brain parenchymal lesions detected on late MR imaging and comparison of surgical vs. endovascular treatment modalities (Study I)

One year after aSAH only 44 (31.9%) patients (29, 43.3% endovascular, 15, 21.2% surgical) had normal MRI of the brain or the finding was analogous to the admission CT-scan. Parenchymal high SI-intensity lesions on T2 and intermediate weighted images of different etiology were seen in 38 (56.7%) endovascular and in 56 (78.9%) surgical patients (p=0.005). In patients with higher H & H and Fisher grades, parenchymal lesions were seen significantly more often than in patients with lower grades. MRI-detectable parenchymal lesions of different etiologies are demonstrated on **Tables 3 and 4**.

Table 3. Number of Parenchymal MRI lesions One Year After aSAH in Patients Intended to Treat Endovascularily vs. Surgically

	Embolization n = 67	P	Surgery n = 71
Parenchymal lesions altogether	38 (56.7%)	0.005	56 (78.9%)
H & H			
I- III	31/60 (52.7%)	0.003	51/66 (77.3%)
IV- V	7/7 (100%)	-	5/5 (100%)
Fisher			
0 - 2	12/28 (42.9%)	0.144	14/22 (63.6%)
3 - 4	26/39 (66.7%)	0.034	42/49 (85.7%)
Anatomical locations:			
Frontal lobe	34 (50.7%)	0.018	50 (70.4%)
Temporal lobe	15 (22.4%)	0.002	34 (47.9%)
Parietal lobe	8 (11.9%)	0.212	14 (19.7%)
Occipital lobe	2 (3.0%)	0.953	2 (2.8%)
Thalamus and basal ganglia	7 (10.4%)	0.057	16 (22.5%)
Brain stem and cerebellum	4 (6.0%)	0.037	0 (0%)

P value indicates statistical significance between patients intended to treat endovascularily vs. surgically.

Table 4. Brain MRI Findings According to the Etiology of the Lesion 1 year After aSAH in Patients Intended to Treat Endovascularily vs. Surgically

	Embolization, n=67	P	Surgery, n=71
MRI findings	**n (%)**		**n (%)**
Any Ischemic deficits	19 (28.4%)	0.005	37 (52.1%)
Parental artery territory	15 (22.4%)	0.003	33 (46.5%)
Cortical involvement	13 (19.4%)		29 (40.8%)
Perforator artery territory	6 (9.0%)		15 (21.1%)
More than one lesion	4 (6.0%)	0.178	9 (12.7%)
Other vascular territory	7 (10.4%)	0.379	11 (15.5%)
Cortical involvement	8 (11.9%)		16 (22.5%)
Perforator artery territory	4 (6.0%)		3 (4.2%)
More than one lesion	3 (4.5%)	0.757	4 (5.6%)
Superficial brain retraction deficits	10 (14.9%)	<0.001	40 (56.3%)
Deficit caused by preoperative ICH	15 (22.4%)	0.683	18 (25.4%)
Superficial siderosis	28 (41.8%)	0.778	28 (39.4%)

Note. P value indicates statistical significance between patients intended to treat endovascularily vs. surgically. Perforator artery territory includes the branches of the thalamoperforating arteries, thalamogeniculate arteries (from posterior communicating arteries, basilar artery and posterior cerebral arteries), medial lenticulostriatae arteries and recurrent artery of Heubner (from anterior cerebral arteries and anterior communicating arteries) and lateral lenticulostriatae arteries (from middle cerebral artery).

5.2.1. Ischemic lesions in the parental artery territory

High-signal-intensity lesions on T2 and intermediate-weighted images indicating infarction in the vascular territory of the ruptured aneurysm were seen in 15/67 (22.4%) endovascular and in 33/71 (46.5%) surgical patients (p=0.003). Four endovascular and 7 surgical patients had two separate infarctions and 2 surgical patients had three separate infarctions in the parental artery territory. In patients who had infarctions, the mean volume of the infarcted tissue was 17.6cm^3 (range 0.14-121.5cm^3) in the endovascular group, and 20.9cm^3 (range 0.09-261.5cm^3) in the surgical group (p=0.209). In all patients included, the mean volume of the infarcted tissue in the parental artery territory was 3.9cm^3 (range 0.0-121.5 cm^3) after

endovascular treatment and 9.7cm^3 (range 0.0-261.5cm^3) after surgical treatment (p=0.002).

5.2.2. Ischemic lesions in other vascular territories

Eighteen out of 67 (26.9%) endovascular and 30/71 (42.3%) surgical patients had symptoms of clinical vasospasm (p=0.058). Brain infarctions in vascular territories other than that of the ruptured aneurysm were seen in 7/67 (10.4%) endovascular and in 11/71 (15.5%) surgical patients (p=0.379). In patients who had remote infarctions, the mean volume of the infarcted tissue was 27.6cm^3 (range 0.17-58.5cm^3) in endovascular and 43.3cm^3 (range 1.29-247.5cm^3) in surgical patients (p=0.821). One endovascular patient had two and 2 patients had three infarctions in remote territories. In the surgical group, one patient had two, 2 patients had three, and one patient had four separate infarctions in remote territories. In all patients, the mean volume of the ischemic lesions in remote vascular territories was 2.9cm^3 (range 0.0-58.5cm^3) after endovascular treatment and 6.7cm^3 (range 0.0-247.5cm^3) after surgical treatment (p=0.373).

5.2.3. Residual signs of hematoma and superficial siderosis

High-signal-intensity lesions on T2 and intermediate-weighted images due to previous intracerebral or sylvian hematoma were detected in 15 (22.4%) endovascular and 18 (25.4%) surgical patients (p=0.683). Signs of superficial hemosiderosis were present in 28 (41.8%) endovascular and 28 (39.4%) surgical patients (p=0.778).

5.2.4. Retraction injury due to surgical manipulation and instrumentation

Lesions in the brain parenchyma due to mechanical surgical trauma were clearly more common after surgical (n=40, 56.3%) than endovascular (n=10, 14.9%) treatment (p<0.001). Retraction injuries were also detected after endovascular treatment because 13 endovascular patients needed additional surgery or nonruptured aneurysms were surgically ligated before MRI. The mean volumes of the

retraction deficits were 4.3cm^3 (range 1.2-10.2cm^3) after endovascular treatment and 8.4cm^3 (range 1.4-32.0cm^3) after surgical treatment (p=0.055).

5.2.5. Lesions caused by shunt device

Compared to endovascular patients (n=4, 6.0%), surgical patients (n=12, 16.9%) more often had a permanent shunt device (p=0.045). Parenchymal lesions induced by a ventricular catheter (temporary drainage or permanent shunt device) were seen in 19 (28.4%) endovascular and 24 (33.8%) surgical patients (p=0.490).

5.2.6. Previous infarctions, brain atrophy, lacunar infarctions and leukoaraiosis

One endovascular patient had an old cortical infarction on admission CT-scan. Previous atrophy was present in one endovascular and two surgical cases (p=0.594). On MRI, at least one lacunar infarction was detected in 12 (17.9%) endovascular and 21 (29.6%) surgical patients (p=0.108). Leukoaraiosis was absent in 42 (62.7%) endovascular and 40 (56.3%) surgical patients; punctuate or early confluent in 24 (35.8%) endovascular and 25 (35.2%) surgical patients; and confluent in 1 (1.5%) endovascular and 6 (8.5%) surgical patients (p=0.171).

5.2.7. Demonstrative Images of the typical findings detected on MRI one year after aSAH

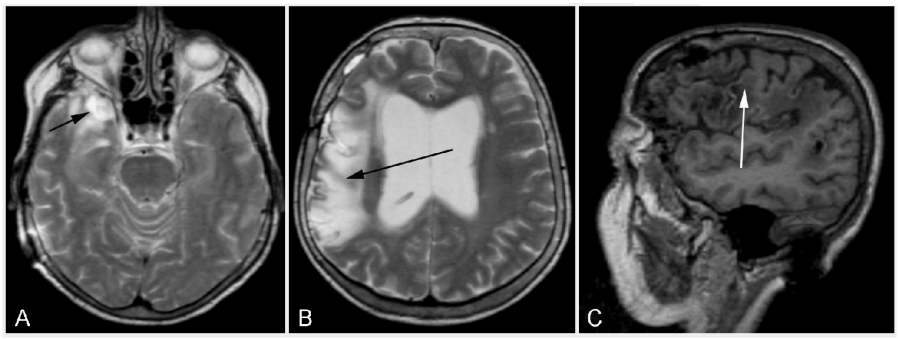

Figure 5. Axial T2-weighted (A, B) and sagittal T1-weighted (C) MR images show small retraction deficit in apex of the right temporal lobe (short arrow) and cortical infarction (long arrow) in the parental artery of the ruptured aneurysm after surgery of right MCA aneurysm.

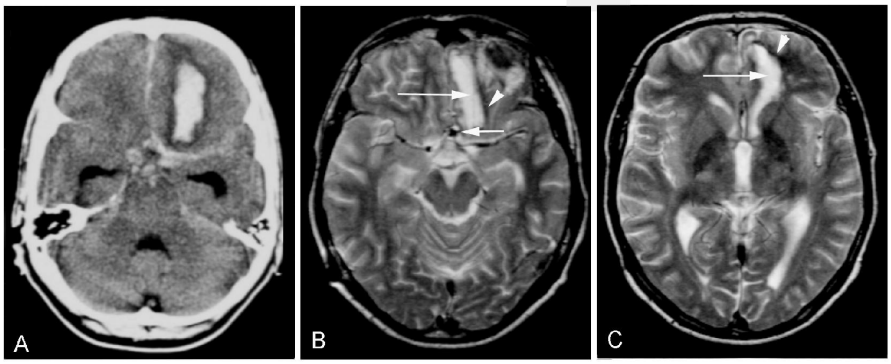

Figure 6. Axial CT scan shows SAH after ruptured right AComA aneurysm with left frontobasal hematoma (A). Axial T2-weighted MR images (B, C) show high-SI lesion owing to previous frontobasal hematoma (long arrow) with low-SI hemosiderin rim (arrowhead). A local signal loss (short arrow) is detected after endovascular coil treatment in the location of AComA.

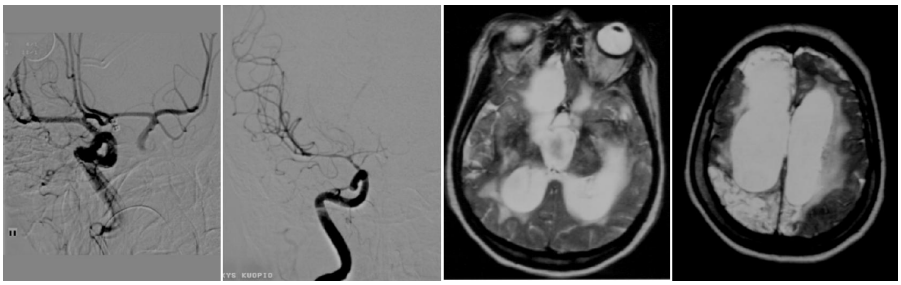

Figure 7. DSA images show successful embolization result of right AComA aneurysm treatment and severe symptomatic vasospasm occurring one week after aSAH and treatment. T2-weighted MR images show severe outcome of vasospasm after endovascular treatment with widespread lesions one year after aSAH with poor clinical outcome.

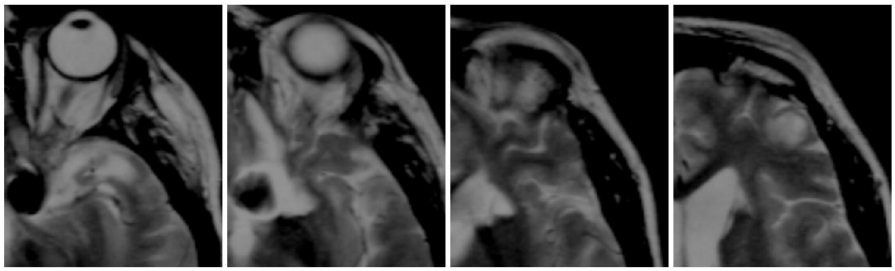

Figure 8. Left AComA aneurysm has been treated with surgery. Zoomed axial T2-images show retraction deficits on the frontal and temporal lobe surfaces and frontobasal area. A small perforant infarction in the caudate nucleus can also be detected.

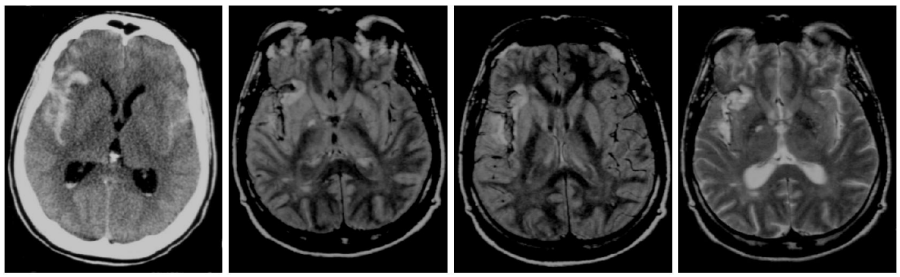

Figure 9. The right ICA aneurysm has been ruptured with blood maxima in the right sylvian fissure. A small lesion owing to previous hematoma can be detected on PD and T2-weighted images. Superficial siderosis and cortical band-like hyperintensity are present in the sylvian fissure. A small perforant infarction can be detected in the parental artery territory of the right ICA.

5.3. Temporomesial structures: Hippocampus and Amygdala (study II)

The volumes of the amygdalae of three out of 77 patients had to be excluded from analysis because of the clip artefact after the surgery. No disturbing artefacts due to clips or coils were detected in the regions of hippocampi. When comparisons between treatment groups were performed, crossover patients (n=8) and those patients whose non-ruptured aneurysms had been treated before the one year MRI (n=9) were excluded from the analysis. After exclusion, thirty endovascular and thirty-one surgical patients were included in the final analysis comparing the actual treatment modalities.

5.3.1. Temporomesial volumes; aSAH patients vs. control individuals

When comparing the normalized volumes of the hippocampi and amygdalae, differences between aSAH patients and controls were seen in the measured volumes of right (23.2 ± 3.9 vs. 24.7 ± 3.7, p=0.072) and left HC (21.3 ± 3.5 vs. 23.7 ± 3.6, p=0.002) and right (18.4 ± 4.9 vs. 21.0 ± 3.9, p=0.012) and left AM (18.8 ± 4.1 vs. 20.5 ± 3.7, p=0.045) after aSAH, the last three volumes being significantly smaller in the aSAH patients.

5.3.2. Temporomesial volumes in endovascular and surgical subgroups vs. controls

Comparisons of the temporomesial volumes between the endovascularly treated patients and normal controls did not reach significant differences: Right AM (20.7 ± 4.38 vs. 20.96 ± 3.91, p=0.790); left AM (19.66 ± 2.90 vs. 20.52 ± 3.67, p=0.319); Right HC (23.56 ± 4.43 vs. 24.71 ± 3.71, p=0.281); Left HC (21.79 ± 3.76 vs. 23.67 ± 3.64, p=0.055). However, the corresponding comparisons between the surgically treated patients and controls revealed the following differences: Right AM (16.31 ± 4.82 vs. 20.96 ±3.91, p< 0.001); left AM (18.97 ± 3.69 vs. 20.52 ± 3.67, p= 0.111); Right HC (22.50 ± 3.73 vs. 24.71 ± 3.71, p=0.024); Left HC (20.81 ± 3.70 vs. 23.67 ± 3.64, p=0.004).

5.3.3. Temporomesial volumes and the side of the treatment

Among all the aSAH patients, smaller ipsilateral (17.8 ± 5.0) than contralateral amygdaloid volumes (19.4 ± 3.9, p=0.008) were observed. In the surgical subgroup (n=31) the difference between the mean volumes of the ipsilateral and contralateral amygdalae was evident (15.7 ± 5.1 vs. 19.4 ± 2.9, p=0.001), while in the endovascular subgroup (n=30), no such difference in the normalized volumes of the ipsilateral (20.3 ± 4.1) and contralateral (20.0 ± 3.1) amygdalae was found (p=0.650). There was no difference in the ipsi- and contralateral volumes of hippocampi. Ipsilateral amygdaloid volumes were (after Bonferroni correction) smaller after surgical (15.7 ± 5.1) than after endovascular (20.3 ± 4.3) treatment of aSAH (p<0.001). There were no differences in volumes of contralateral amygdalas or neither hippocampi between the different treatment groups.

5.4. VBM analysis of patients after treatment of ruptured anterior cerebral artery aneurysm (Study III)

5.4.1. Clinical outcome and conventional MRI findings

Forty-two aSAH patients from the volumetric study population presented with a ruptured ACA aneurysm. Patients whose associated nonruptured aneurysms had

been treated before MRI were excluded. The VBM study population thus consisted of 37 patients (17 surgical, 20 endovascular treatment) with ruptured ACA aneurysm, all of them having a good or moderate clinical outcome (GOS V or IV). A VBM analysis was applied to compare the patients and controls. All volumetric ACA patients also underwent a detailed neuropsychological assessment. The final group analyses for comparison the endovascular and surgical patients were performed after excluding patients with crossover treatment (5 endovascular patients).

5.4.2. VBM results: All ACA patients vs. controls

In comparison of all ACA patients to controls, the five endovascular patients receiving additional surgical treatment were included in the analysis to demonstrate the gray-matter atrophy detected after aSAH due to ruptured ACA aneurysm, regardless of the treatment modality itself.

The GM/ICV ratios proved to be reduced in aSAH patients (0.359 ± 0.027) compared to controls (0.378 ± 0.027, p=0.008) and the CSF/ICV ratios were increased in aSAH patients (0.410 ± 0.036) compared to controls (0.384 ± 0.033, p=0.003), reflecting general brain atrophy. In VBM analysis, when aSAH patients were compared to age-matched controls, a widespread bilateral atrophy was shown in the orbitofrontal cortex and inferior frontal gyrus, the gyrus rectus and thalamic and hypothalamic areas. Smaller clusters of atrophy were also detected in the ipsilateral temporal lobe pole, the ipsilateral superior frontal gyrus, the ipsilateral middle frontal gyrus (2 small areas) and the dorsal pons. Results are shown on **Table 5** and **Figure 10.**

Table 5. Areas of reduced gray matter in ACA aneurysm patients one year after SAH compared to controls

Brain region	**C / I**	**MNI coordinates** (x,y,z)	***k***	***T* value**
1*. All aSAH patients (n=37)*				
Orbitofrontal cortex	C / I	-34, 55, -18 / 36, 51, -19	50937	9.92 / 8.46
Inferior frontal gyrus	C / I	-34, 44, -18 / 34, 44, -18	*	6.57 / 5.50
Gyrus rectus	C / I	-8, 32, -24 / 6, 26, -24	*	6.44 / 6.78
Thalamus	C / I	-5, -7, 1 / 7, -7, -2	*	6.15 / 5.73
Hypothalamus	C / I	-3, -1, -8 / 4, -4, -8	*	5.23 / 5.42
Caudate nucleus, head	I	12, 17, 1	*	5.53
Brainstem, dorsal pons	C / I	-2, -37, -35 / 2, -37, -39	1546	6.73 / 5.21
Temporal lobe pole, superior temporal gyrus	I	35, 18, -45	328	6.60
Superior frontal gyrus	I	21, 64, 28	272	5.99
Middle frontal gyrus	I	52, 45, -5	112	5.52
Middle fontal gyrus	I	40, 62, 8	84	5.30
2. Surgical aSAH (n=17)				
Orbitofrontal cortex	C	-34, 51, -16	40800	7.58
Gyrus rectus	C / I	-8, 32,-24 / 6, 26, -24	*	6.30 / 6.57
Caudate nucleus	I	12, 15, 1	*	13.30
Thalamus	C / I	-6, 17, -8 / 6, 17, -7	*	6.25 / 10.68
Hypothalamus	C / I	-3, 5, -11 / 8, 5, -11	*	7.36 / 12.26

Hippocampus	I	33, -12, -16	11437	8.52
Parahippocampal gyrus	I	21, -35, -6	*	8.12
Superior temporal gyrus, temporal lobe pole	C	-30, 18, -46	496	8.01
Middle frontal gyrus	I	50, 49, -4	1639	7.79
Orbitofrontal cortex	I	39, 53, -17	*	7.53
Superior temporal gyrus, temporal lobe pole	I	28, 17, -45	648	7.78
Brainstem, dorsal pons	C	-2, -37, -35	235	6.03
Posterior orbital gyrus	I	36, 29, -21	239	5.97
Inferior frontal gyrus	C	-50, 48, 5	106	5.83
Anterior insula	I	38, 13, -5	197	5.72
Superior frontal gyrus	I	21, 63, 29	74	5.71
3. Embolized aSAH (n=15)				
Orbitofrontal cortex	C	-34, 54, 19	793	7.60
Orbitofrontal cortex	I	32, 51, -22	1049	8.43
Thalamus	C	-5, -7, 1	1616	6.27

C= contralateral, I=ipsilateral to ruptured aneurysm treatment side, MNI coordinates x,y,z of anatomical structures in each cluster refer to Montreal Neurological Institute (MNI) space. *k*= cluster extent in voxels. * =cluster extent in voxels is included in the number reported above. T-value = statistical significance of GM volume loss of the corresponding MNI coordinate, assessed using a t-test (T-value) with a height threshold of $P < 0.05$, corrected for multiple comparisons by the family-wise error (FWE) method. In larger clusters, several coordinates of local maximas and their corresponding T-values are reported.

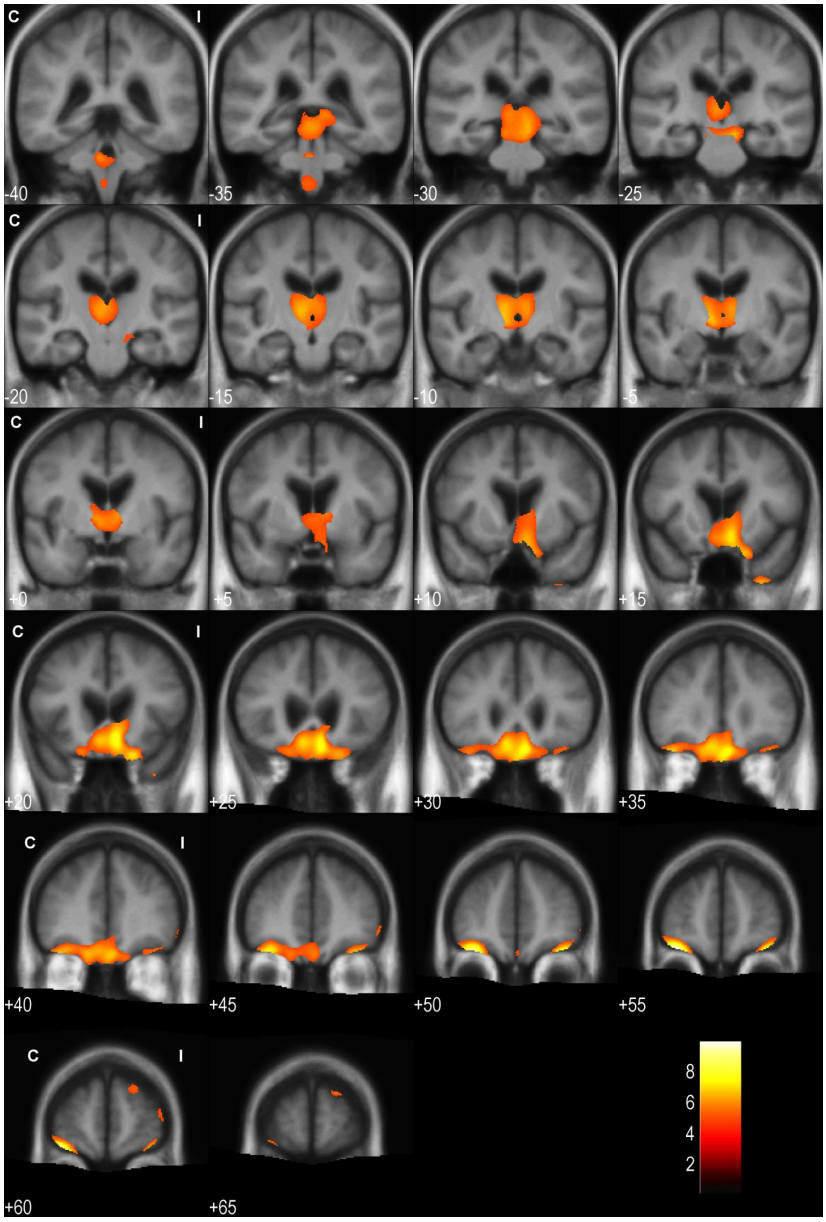

Figure 10. Areas of atrophy in aSAH patients (n=37) after treatment (20 endovascular, 17 surgical) of ruptured ACA aneurysm compared to controls. VBM analysis, $p< 0.05$, corrected with the family-wise error (FWE) method. The ipsilateral (I) treatment side is oriented to the right; contralateral (C) side is to left. T-values (from t test statistics) are represented by the colour bar. The results are demonstrated on an averaged and smoothed image.

5.4.3. VBM results: Surgical ACA patients vs. controls

Areas of brain atrophy were quite similar both between all aSAH patients and surgically treated subgroup of aSAH patients. After surgical treatment, additional atrophy was detected in the ipsilateral hippocampus, parahippocampal gyrus, anterior insula and caudate nucleus: a finding not detected in the analysis made with all aSAH patients and controls (**Table 5**, **Figure 11A**). An averaged image of the normalized T1-weighted MRIs of the surgical group was calculated to illustrate the average clip artefact in the area of AComA **(Figure 12)**, an area clearly more restricted than the bilateral orbitofrontal and hippocampal regions of observed atrophy.

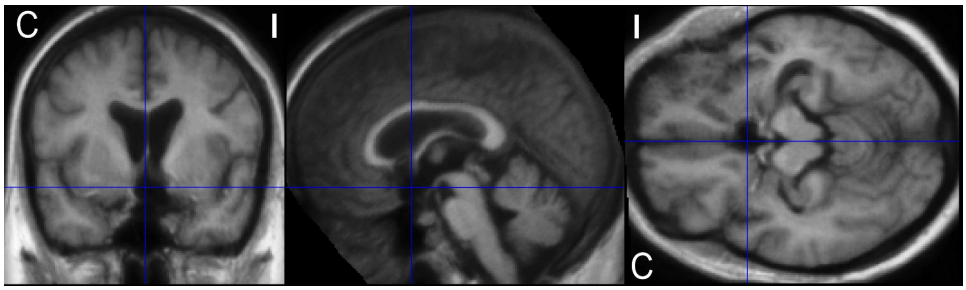

Figure 12. The size and location of an average clip artefact is demonstrated in three planes in an averaged, T1-weighted MR image calculated from the surgical patient population (n=17) after treatment of ruptured ACA aneurysm.

5.4.4. VBM results: Endovascular ACA patients vs. controls

When comparing the endovascularly treated aSAH patients with controls, the analysis revealed atrophy in both ipsilateral and contralateral areas of the orbitofrontal cortex. A small atrophic cluster was also detected in the contralateral thalamus. The results are shown on Table 5 and **Figure 11B**.

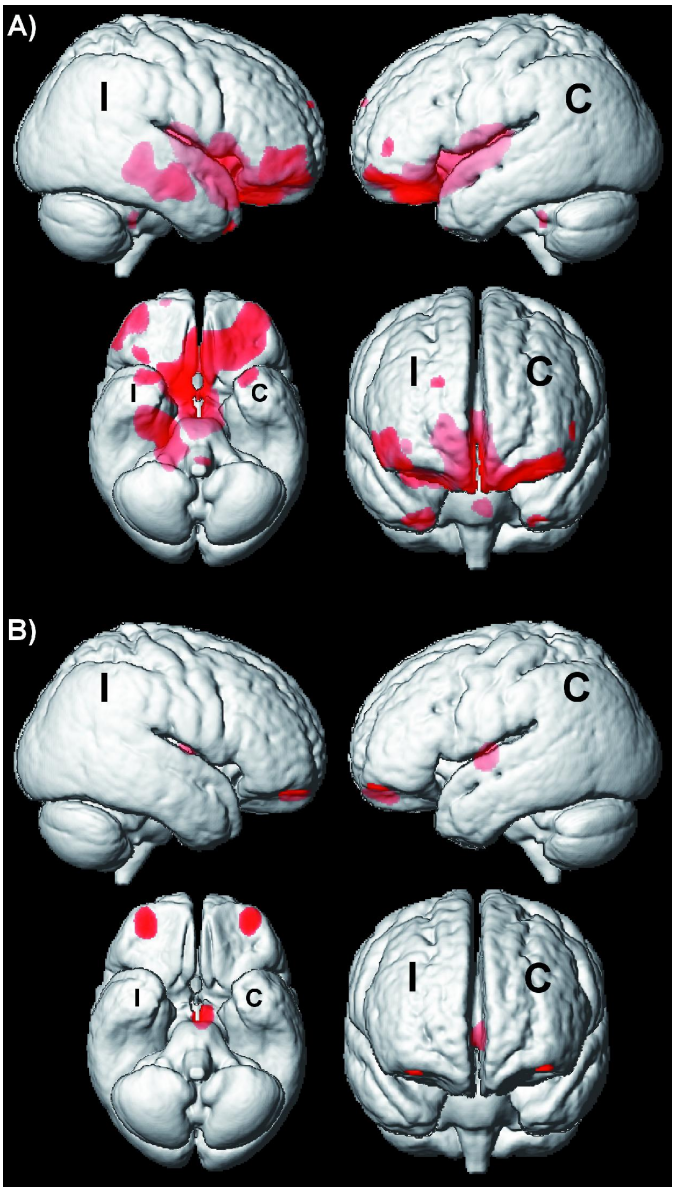

Figure 11. A: Areas of atrophy (red) after surgical treatment of aSAH patients with ruptured ACA aneurysm (n=17) compared to controls. B: Areas of atrophy (red) after endovascular treatment of aSAH patients with ruptured ACA aneurysm (n=15) compared to controls. The ipsilateral (I) treatment side is oriented to the right; contralateral (C) is to the left. The VBM analyses are performed using t test statistics, $p<0.05$, corrected with the FWE method. The results are shown on an averaged and smoothed image.

5.4.5. VBM results: Endovascular ACA patients vs. surgical ACA patients

When comparing the endovascularly treated patients to the surgically treated patients, the GM/ICV ratios did not significantly differ between treatment groups, p=0.193, nor did the CSF/ICV ratios significantly differ between treatment groups, p=0.249. When compared to endovascularly treated patients, VBM analysis revealed statistically significant atrophic gray matter areas in surgically treated patients only in the hemisphere ipsilateral to surgical approach. Areas of atrophy were detected in the ipsilateral hippocampus and amygdala, in ipsilateral thalamic and hypothalamic regions, and in small areas in ipsilateral insula, temporal lobe pole, middle temporal gyrus and frontal subcentral gyrus.

5.5. Ventriculomegaly and enlargement of CSF volumes after aSAH (Study IV)

5.5.1. Patients and controls, preoperative hydrocephalus and permanent shunt-device

The study IV was performed to compare the CSF volumes between 76 volumetric aSAH patients and 30 age and gender matched control individuals. Preoperative hydrocephalus was detected in 16 (40.0%) out of 40 endovascular and 11 (30.6%) out of 36 surgical patients, p=0.390. A permanent shunt device was present in four (1 endovascular, 3 surgical, p=0.255) patients. The mean interval between aSAH and shunt operation was 4.75 ± 2.87 weeks (range 1-8 weeks).

5.5.2. Degree of ventriculomegaly and enlarged CSF-spaces

The mCMI measurements were available in all patients from original MRI population (n=138) and CSF/ICVs from all volumetric patients (n=76). The mCMI proved to be higher in patients with aSAH when compared to the age and sex matched control individuals. The more detailed analyses of the CSF volumes in 76 patients were in line with the rough planimetric measurements: the mean volume of the ventricular system (obtained from manually drawn ROI-analysis) was 64.14 cm^3 in the aSAH patients, being 31.4 % larger compared to the volume in control

individuals (44.00 cm^3). The ICV values were comparable between the aSAH patients and controls. The CSF/ICV ratios were 35.58 ± 7.00 in aSAH patients compared to 30.36 ± 6.25 in controls, p=0.001. The mCMI correlated with CSF/ICV ratios (r= 0.495, p< 0.001). Moreover, the GM/ICV- ratios and WM/ICV-ratios were lower in aSAH-patients compared to the control individuals. **Figure 13** illustrates on a group level that both the ventricles and the cortical sulci are enlarged in the aSAH patients compared to control population.

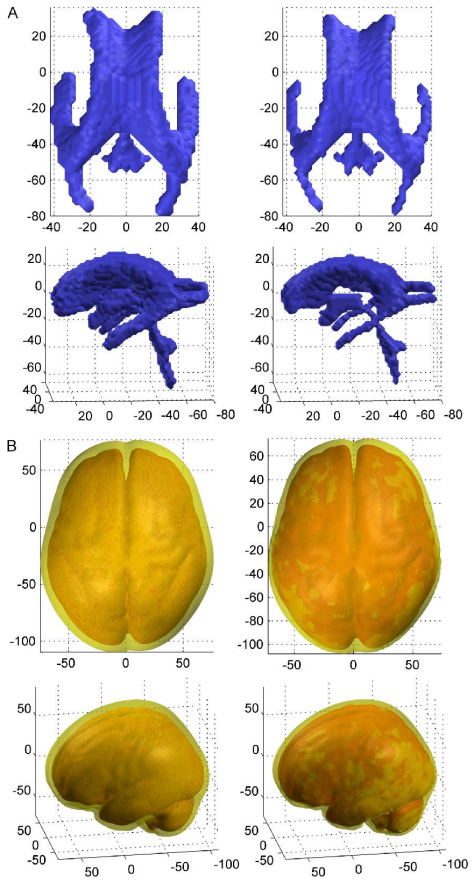

Figure 13. Three-dimensional render images of the averaged ventricular system and the superficial sulcal CSF-segments are illustrated in MNI space. Image axes represent the MNI coordinates. A: The mean ventricular system of aSAH patients (n=76) shown on the left side and control individuals (n=30) shown on the right side, cranial and lateral views. B: The mean superficial CSF-segments of aSAH patients (n=76) shown on the left side and control individuals (n=30) shown on the right side, cranial and lateral views.

5.5.3. Associations between ventricular and sulcal enlargement and clinical and other radiological features

The mCMIs (n=138 aSAH patients) were comparable between the treatment groups: 0.23 ± 0.1 after endovascular and 0.23 ± 0.1 after surgical treatment. The treatment method did not significantly affect the measured CSF/ICV ratios (n=76); CSF/ICV was 34.49 ± 7.7 after endovascular treatment and 36.78 ± 6.0 after surgical treatment (p= 0.289).

At the time of MRI clinical or radiological evidence of raised intracranial pressure could not be detected among any of the patients studied. There were no differences in mCMI or CSF/ICV ratios when the patients with or without the permanent shunt device were compared.

Patients with originally higher Hunt & Hess and Fisher grades showed more pronounced mCMIs than did patients with lower Hunt & Hess and Fisher grades. Higher Fisher grade was also associated with higher CSF/ICV ratios and patients with preoperative hydrocephalus tended to have higher CSF/ICV ratios. Associations between enlarged CSF spaces and contributing factors (such as preoperative hydrocephalus, Hunt & Hess and Fisher grades) are demonstrated on **Table 6.**

Table 6. Associations of Clinical and Radiological findings with enlargement of ventricles and other CSF volumes after aSAH

Descriptive	Mean mCMI	p	Mean CSF/ICV	p
Preoperative hydrocephalus		< 0.001		0.051
no (n=27)	0.21 ± 0.06		34.44 ± 7.57	
yes (n=49)	0.28 ± 0.06		37.64 ± 5.35	
Hunt & Hess grade		< 0.001		0.293
I-II (n=55)	0.21 ± 0.06		34.98 ± 7.54	
III-V (n=21)	0.29 ± 0.05		37.15 ± 5.18	
Fisher grade		0.001		0.014
0-2 (n=27)	0.20 ± 0.06		32.75 ± 7.75	
3-4 (n=49)	0.25 ± 0.06		37.13 ± 6.10	

Note. For calculation mCMI- indexes and the t-test was used. mCMI refers to maximal ventricular width/ maximal intracranial width ratio measured from the same axial T2-weighted slice. CSF refers to CSF volume determined by SPM5. ICV= Total intracranial volume (contains gray matter, white matter and CSF segments) measured by SPM5. For CSF/ICV indexes the Mann-Whitney-U-test was used. For calculations of mCMI, n=138, and for calculations of CSF/ICVs, n=76.

5.6. Correlations of MRI-detectable findings and neuropsychological outcome (Studies I-IV)

5.6.1. Neuropsychological analysis of the MRI study population (Study I)

The neuropsychological examination one year after aSAH was available in 116/138 (84.1%) patients with MRI. 17/127 (13.4%) patients with good or moderate clinical outcome refused the neuropsychological examination and in 5/11(45.5%) patients, who had severe neurological deficits or who were in vegetative state the neuropsychological examination was not possible to perform. Clinical and neuropsychological outcome between patients intended to treat endovascularly vs. surgically (n=116) are shown in **Table 7** (containing previously unpublished data).

Table 7. Clinical Outcome and Neuropsychological and associated MRI findings expressed as counts or means ± SD or in 116 patients completing the neuropsychological tests one year after aSAH.

	Endovascular patients n = 55	p	Surgical patients n = 61
Clinical Outcome		0.057	
GOS V	49 (89.1%)		44 (72.1%)
GOS IV	4 (7.5%)		14 (23.0%)
GOS III	2 (3.8%)		3 (4.9%)
Neuropsychological findings			
Any neuropsyc. deficit detected	29 (52.7%)	0.019	45 (73.8%)
Deficit in general intellectual functioning	4 (7.5%)	0.099	11 (18.0%)
Memory deficit	22 (40.0%)	0.062	35 (57.4%)
Verbal deficit	19 (35.8%)	0.574	25 (41.0%)
Deficit in executive functions	12 (21.8%)	0.133	21 (34.4%)
MRI findings			
Frontal lobe lesion	26 (49.1%)	0.032	42 (68.9%)
Temporal lobe lesion	12 (22.6%)	0.015	27 (44.3%)
Parenchymal deficit	30 (56.6%)	0.020	47 (77.0%)
Total Parencymal lesion volume (cm^3)	6.61 ± 24.08	<0.001	13.83 ± 19.29
Ischemic Brain volume (cm^3)	5.99 ± 23.90	0.005	8.69 ± 16.91

Note. The differences between patient groups has been analyzed with X^2- test (categorical data and dichotomous variables) Mann-Whitney-U-test (different lesion volumes). p refers to the comparison in patients after endovascular vs. surgical treatment.

5.6.2. Neuropsychological results and temporomesial volume correlation (Study II)

Among the aSAH patients, age of the patient correlated with all neuropsychological parameters. The hippocampal volumes correlated with a visual memory test (Visual reproduction subtest (Wechsler 1974)) and several tests of attention, flexibility of mental processing, intellectual ability and psychomotor speed. A test of verbal episodic memory (Wechsler 1974) and another visual memory test (Rey) (Lezak 1995) did not correlate with hippocampal volumes. The volumes of the amygdalae did not significantly correlate with neuropsychological test results.

Since the neurocognitive deficits noted among the volumetric aSAH patients were quite similar to those expected in patients with frontal lobe lesions, the correlations between the neuropsychological test results and hippocampal volumes were analyzed separately in patients with and without a frontal lobe lesion. Furthermore, significant correlations were found between the impaired neuropsychological test results and reduced hippocampal volumes in both subgroups of the patients with aSAH.

5.6.3. Neuropsychological test results in volumetric ACA population and their correlation to GM/ICV and CSF/ICV ratios (Study III)

Analysis of neuropsychological data revealed cognitive deficit in at least in one of the four cognitive domains in 20 (54.1%) patients (10 endovascular, 10 surgical, p=0.591). Impairment in executive functions was detected more often after surgical treatment (n=8, 72.7%) than after endovascular treatment (n=3, 27.3%, p=0.033) of a ruptured ACA aneurysm. Ten out of the 11 patients with executive deficits also had a frontal lobe lesion that was detectable by MRI. Memory deficits were detected in 45.0% of the endovascular and 47.0% of the surgical patients. Verbal disturbances were found in 25% of the endovascular and 29.4% of the surgical patients. No differences among treatment groups were observed in cognitive domains other than the executive functions (intelligence, memory, and verbal skills). The VBM-based covariate analyses did not reveal any statistically significant specific areas of atrophy, when the dichotomized neuropsychological deficits in general, or a dichotomized

executive deficits, or a dichotomized GOS, were used as a covariate. The analyses in endovascular and surgical subgroups also failed to reveal any statistically significant specific areas of GM atrophy that could be straightly related to these cognitive deficits.

In patients with at least one neuropsychological deficit, the GM/ICV-ratios (0.354 ± 0.025) were slightly lower and the CSF/ICV ratios (0.420 ± 0.036) were slightly higher when compared to patients with no neuropsychological deficits (GM/ ICV= 0.367 ± 0.029, ns, and CSF/ICV= 0.404 ± 0.035, ns). The patients with a deficit in executive functions (n=11) showed lower GM/ICV-ratios (0.342 ± 0.015) and higher CSF/ ICV ratios (0.433 ± 0.032) compared to patients without an executive defict (GM/ICV= 0.366 ± 0.028, p=0.014 and CSF/ICV= 0.403 ± 0.033, p=0.013).

5.6.4. Clinical outcome, neuropsychological results and CSF volume correlation (Study IV)

GOS II -IV patients had larger ventricles and CSF-spaces (mCMI = 0.29 ± 0.08, CSF/ICV= 38.19 ± 5.81) compared to GOS V patients (mCMI = 0.23 ± 0.06, p<0.001 and CSF/ICV= 35.19 ± 7.12, p=0.237).

In the group of patients with at least one neuropsychological deficit detected, the mCMIs (0.249 ± 0.07) and CSF/ICV ratios (37.45 ± 6.13) were higher compared to those patients without any neuropsychological deficit (mCMI=0.211 ± 0.05, p=0.003 and CSF/ICV= 32.16 ± 7.21, p=0.001). In line with the higher CSF/ICV ratios, the aSAH patients with neuropsychological deficits showed lower GM/ICV ratios than the aSAH-patients without neuropsychological deficits. In separate analyses of each cognitive domain, higher mCMIs and CSF/ICV ratios were detected in the patients with a deficit (**Table 8**).

Table 8. Associations between neuropsychological deficits and enlarged ventricles and other CSF volumes

Descriptive	mCMI (n=116)	*p*	CSF/ICV (n=75)	*p*
Clinical Outcome		< 0.001		0.214
GOS V	0.23 ± 0.06		35.18 ± 7.12	
GOS II - IV	0.29 ± 0.08		38.16 ± 5.81	
Any neuropsychological deficit		0.001		0.001
no	0.21 ± 0.05		32.16 ± 7.21	
yes	0.25 ± 0.01		37.45 ± 6.13	
Verbal deficit		0.003		0.002
no	0.22 ± 0.06		33.78 ± 6.38	
yes	0.26 ± 0.06		38.60 ± 6.38	
Memory deficit		0.040		0.018
no	0.22 ± 0.06		33.61 ± 7.66	
yes	0.25 ± 0.07		37.45 ± 5.61	
Deficit in general intellectual functioning		0.015		< 0.001
no	0.23 ± 0.06		34.29 ± 6.94	
yes	0.27 ± 0.06		42.02 ± 2.68	
Deficit in executive functions		0.001		< 0.001
no	0.22 ± 0.06		33.36 ± 6.80	
yes	0.27 ± 0.06		41.00 ± 4.03	

Note.- Neuropsychological analysis was available (at least from one of the four cognitive domains) on 75 volumetric patients out of 76 and 116 patients out of the population of 138 patients with conventional MRI and modified cella media index(mCMI). CSF refers to the CSF volume determined by SPM5. ICV = Total intracranial volume (contains gray matter, white matter and CSF segments) measured by SPM5. In the statistical analyses the T-test was used mCMI comparisons and Mann-Whitney-U-test was used for CSF/ICV comparisons; p refers to statistical significance between different GOS/neuropsychological deficit subgroups. GOS=Glasgow Outcome scale.

5.7. The effect of age and MRI and neuropsychological outcome (studies I, II and IV)

5.7.1. Age and MRI and neuropsychological deficits

There were no statistically significant correlations between the MRI detectable lesion volumes (total parenchymal lesion volume, retraction volume or ischemic lesion volume) and age of the patient. However, in our study population, the 44 (21 male, 23 female) patients without focal parenchymal lesions were significantly younger (mean age 44.8 ± 2.4 years) compared to the control individuals (54.1 ± 5.5 years, p=0.006). To compare the late atrophy in aSAH patients without focal MRI abnormalities with age and gender matched control individuals, we selected a balanced subgroup of younger controls (n=18; 9 male, 9 female, mean age 44.0 ± 11.3), and found out that significantly higher CSF/ICV ratios were detected in aSAH patients (31.39 ± 7.52) compared to CSF/ICV ratios in controls (26.56 ± 4.05, p=0.027). There was no significant difference in mCMIs, when comparing the aSAH patients without focal parenchymal deficit (mCMI=0.21 ± 0.06) and the subgroup of younger controls (mCMI=0.19 ± 0.03, p=0.353). The age of the patient correlated significantly with all separate neuropsychological parameters with a single exception: the correlation coefficient between the age of a patient and memory quotient was not found, r= -0.090, p=0.338. Patients with dichotomized neuropsychological deficit were older (mean age 55.6 ± 13.1 years) than patients with normal cognitive profile (mean age 42.3 ± 14.1 years, p<0.001). Furthermore, in a separate analysis age of the patient was found to strongly associate with all of the four cognitive domains (general intellectual functioning, memory, language and executive functions).

5.7.2. Age and temporomesial structures

In the matched control population, the following correlation coefficients between the age of the individual and the measured temporomesial volumes were obtained: AM right (r=-0.41, p=0.03), AM left (r=-0.52, p=0.004), HC right (r=-0.60, p=0.001), HC left (r=-0.60, p=0.002).

In the aSAH population correlation between age and both ipsi- and contralateral hippocampal volumes was somewhat lower: HC ipsilateral (r=-0.31, p=0.006) and HC

contralateral (r=-0.33, p=0.003). The volumes of amygdalae, in terms, did not correlate with age significantly.

5.7.3. Age and ventricular and sulcal CSF spaces

In study IV the ventricular and sulcal CSF volumes between the aSAH patients and control individuals were analyzed in three different age groups. Age of the patient and control individuals was categorized into three different age groups; young individuals (under 45 years), middle-aged individuals (45-65) and elderly individuals (more than 65 years) and the volumes of these individuals were separately compared. As expected, age of the patient was significantly correlated with larger ventricles and CSF-spaces: mCMI, r=0.416, p<0.001, and CSF/ICV, r=0.718, p<0.001. This finding was constant in all three different age groups when compared to matched control individuals. **Figure 14** demonstrates the associations between the CSF/ICV ratios and the age of the individual.

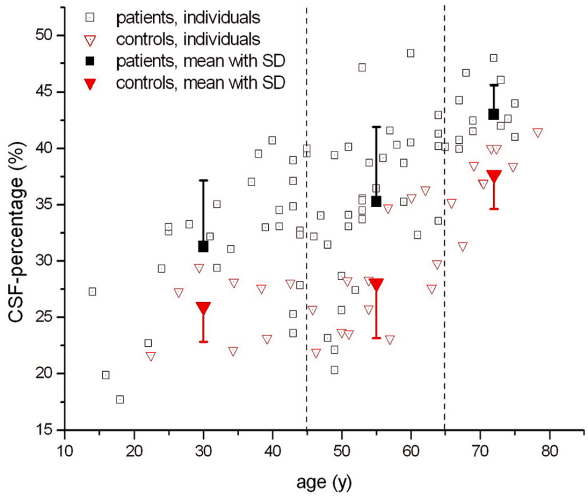

Figure 14. CSF/ICV ratios in relation to the age of the patient and control individuals. The mean CSF/ICV ratios with ± SD are demonstrated in three age groups; young individuals (under 45 years), middle-aged individuals (45-65) and elderly individuals (more than 65 years).

6. DISCUSSION

6.1. One-year MRI Outcome after aSAH: Surgical versus Endovascular treatment (Study I)

The past 15 years have seen a revolution in the treatment of IAs. The development of the Guglielmi detachable coils introduced a potential alternative treatment for IAs in certain patient populations. Although not replacing open surgery, the continued improvements have allowed aneurysms that previously were amenable only to open clip ligation to be safely treated with durable long-term outcomes (Koebbe *et al.* 2006). The main advantage of endovascular coiling is that the craniotomy is avoided and recovery after treatment is more rapid. The major disadvantage is that the recanalizing of the aneurysm may occur as observed at long-term follow-ups (Molyneux *et al.* 2009, Nieuwkamp *et al.* 2009).

Most of the long term radiological outcome studies of the brain parenchyma after aSAH have been performed after surgical clipping (Kivisaari *et al.* 2001, Romner *et al.* 1989) and by using CT (Hoh *et al.* 2004, Orbo *et al.* 2008, Rabinstein *et al.* 2005). The present study is the first prospective, randomized study focusing to late MRI-detectable structural brain damage after endovascular or surgical treatment of aSAH. The study suggests a higher incidence of brain parenchymal lesions in surgically treated patients than in endovascularly treated patients with aSAH, especially in the frontotemporal areas. These parenchymal lesions are of clinical importance, because their volumes clearly correlated with neuropsychological test performance. Many lesions were surgery-related brain retraction injuries, but in the surgical group there was also a significantly higher incidence of ischemic lesions in the parental artery territory of the ruptured aneurysm than in the endovascular group. Probably the main parental and small perforating arteries are more prone to spasm, occlusions or thromboembolism during the surgical procedure.

In remote vascular territories, probably representing more generalized form of global vasospasm, no difference in the incidence of ischemic lesions was found between the two treatment modalities. It has been suggested that endovascular treatment could carry a higher risk for vasospasm, because the blood degradation products in the sulci might cause chemical irritation to the leptomeningeal arteries, compared to open surgery where some of the subarachnoidal blood may be removed (Gruber *et al.* 1998). In the present study, no beneficial effect of surgical clot removal

was observed, but instead surgical patients tended to have a higher incidence of clinical vasospasm. However, equal frequency and size of ischemic lesions were detected in remote vascular territories, both in cortical branch and perforator artery territories.

Knowledge of the surgical techniques in each individual case was important when etiologies of the parenchymal lesions were evaluated. A majority of the retraction injury lesions were located in the basal aspect of the frontotemporal lobes. A typical retraction injury does not follow the vascular anatomy of the brain. In the acute phase of aSAH, the brain is generally swollen with edema, in addition to the mass effect of the possible hematoma and hydrocephalus, making the surface of the brain especially vulnerable.

The clinical significance of the persisting blood degradation deposits on brain surface remains unclear, but clinical manifests such as cerebellar ataxia, sensorineural hearing loss and myelopathy have been suggested (McCarron *et al.* 2003). Surprisingly, in this study signs of hematomas and superficial siderosis were significantly more frequent than reported earlier (Kivisaari *et al.* 2001) and almost equal in both treatment groups, suggesting no obvious beneficial effect of surgical cisternal rinsing.

A study by Hadjivassilou et al. suggested that coiling might cause less structural damage to brain parenchyma (Hadjivassiliou *et al.* 2001) than surgical clipping. The International Subarachnoid Aneurysm Trial (ISAT) demonstrated that endovascular coiling is more likely to result in independent survival than neurosurgical clipping in good grade patients with anterior circulation aneurysms suitable for both treatment modalities at one year after aSAH. According to ISAT study, the risk of death at 5 years was still significantly lower in coiling group than in the clipping group, but the proportion of the survivors who were independent did not differ between the two groups any more (83% endovascular and 82% neurosurgical) (Molyneux *et al.* 2009).

In the present study, the results are reported primarily according to intention-to-treat analysis. However, repeating all the analyses after censoring the patients with combination treatment or additional treatment for nonruptured aneurysms did not produce notable changes in the statistically significant differences between the treatment groups. Thus, in the light of the long term MRI-findings, these results may provide further support to other studies; showing less structural damage on the brain parenchyma (Hadjivassiliou *et al.* 2001) and reduced mortality after endovascular

treatment compared to surgical treatment of the ruptured aneurysm (Molyneux *et al.* 2009). In a certain group of patients, a finding of fewer parenchymal lesions could be a factor, in combination with other criteria, when choosing an optimal treatment method for patients with aSAH, although complete occlusion of the aneurysm may require additional surgical treatment in some patients.

6.2. Temporomesial volume loss after aSAH (Study II)

Hippocampus and amygdale volumes have been widely studied in various neuropsychiatric disorders, since these structures play a vital role in processing memory formation and stress and emotional regulation (Geuze *et al.* 2005). Stress, hypoxia and increased glutamate have been associated with damage to the hippocampus (Fujioka *et al.* 2000, Kalviainen *et al.* 1998, Villarreal *et al.* 2002). Animal studies using SAH models have demonstrated profound hippocampal neuronal loss (up to 30%) within relatively short period of time. It is believed that the loss of hippocampal neurons occur secondary to the global ischemia, which occurs at the time of SAH (Park *et al.* 2004). This is probably exacerbated by BBB breakdown and brain edema. Hippocampal structures seem to have a more pronounced vulnerability to global brain ischemia than the temporal lobe in general (Fujioka *et al.* 2000). Significantly reduced hippocampal volumes have been reported after traumatic brain injury (TBI) and this volume reduction is not always related to the severity of the injury (Bigler *et al.* 2002). In our clinical work, we have observed by visual estimation that the temporomesial volumes seem sometimes atrophic after aSAH, even if there are no focal parenchymal lesions on MRI.

In the present study, focusing in temporomesial volumes, it was found that aSAH and its treatment were followed by atrophy in temporomesial structures. The AM ipsilateral to the ruptured aneurysm was smaller in patients after surgical than endovascular treatment. The treatment modality did not significantly affect the measured HC volumes. Furthermore, a clear correlation was demonstrated between neuropsychological performance and reduced temporomesial volumes. This is interesting since, in the MRI protocol used, the volumetric sequence was scheduled to the end of the imaging as an extra sequence, if the patient was cooperative and willing to stay extra time in the scanner, a fact favouring the good grade patients to be included to this volumetric study**.** The patients with suboptimal recovery and

severe neurological deficits could not participate in the longer MRI examination protocol necessary to volumetric analysis. Thus the clinical outcome was better in this volumetric population than in most of the aSAH populations (Hackett *et al.* 2000). Therefore, the results cannot be generalized in a straightforward manner to all aSAH patients. The damage that aSAH causes to the temporomesial structures is probably as severe or even more pronounced in patients with poorer outcomes. However, in the patients with poor outcome, the clinical consequences of temporomesial volume loss would probably vanish among the major neurologic deficits, making the possible volumetric measurements irrelevant.

In spite of the seemingly good clinical outcome in this volumetric study sample, the temporomesial volume study clearly demonstrated neuropsychological impairments correlating with reduced temporomesial volumes one year after aSAH. Although the volumetric study focused on the reduced temporomesial volumes after aSAH, two thirds of the patients also have other radiologically documented lesions on brain MRI, most of these locating in the frontal lobes. However, the presence of a frontal lesion was not significantly associated with the hippocampal volumes measured. As expected, the presence of a frontal lesion was significantly associated with worse results on the neuropsychological tests. A further analysis was made regarding the correlations between the neuropsychological test results and hippocampal volumes separately in patients with and without a frontal lesion. Significant correlations were found between impaired neuropsychological test results and reduced hippocampal volumes in both subgroups of the patients with or without a frontal lobe lesion after aSAH, suggesting that the detected hippocampal volume loss seems to be associated with impaired neuropsychological performance regardless of a possible coexisting MRI-detectable lesion in frontal lobes. Those correlations were seen in a larger number of the tests applied in patients with a frontal lobe lesion, indicating that the effect of the hippocampal volume loss is probably more pronounced in patients with a documented frontal lobe lesion. A possible explanation is that the changes in hippocampal volumes are also associated with more widespread brain changes that affect several aspects of cognition and are not specific to memory. The relation between hippocampus and memory performance is well established (Squire *et al.* 2004). In our study, the correlations between neuropsychological test results and hippocampal volumes were somewhat unexpected. Namely, significant correlations were consistently found between

hippocampal volumes and several tests of attention, flexibility of mental processing, intellectual ability and psychomotor speed. On the other hand only one out of three memory tests correlated with hippocampal volumes. It can be assumed assumed that both the temporomesial volume loss and other local parenchymal lesions together contribute to the development of neurocognitive deficits which are often detected in patients after aSAH.

6.3. Brain atrophy after ruptured ACA aneurysm and treatment (Study III)

The ACA is a common location for cerebral aneurysms and accounts 35% of ruptured aneurysms in recent report of Kuopio database of 1068 aSAH patients (Huttunen *et al.* 2009). According to Proust et al. 80% of ACA aneurysm patients admitted to hospital in good clinical status attain favourable clinical recovery (Proust *et al.* 2003). Nevertheless, more than 60% of ruptured ACA aneurysm patients with GOS 1 score may suffer cognitive impairment (Hutter *et al.* 1993). For ACA location of the ruptured aneurysm, most studies report deficits in verbal memory, executive functions and QOL (Bottger *et al.* 1998). In order to optimize the homogeneity of the study population, the VBM study focused on patients with a good or moderate clinical outcome and ruptured ACA aneurysms. Based on the clinical experience and visual and quantitative analyses in conventional MRI, it was noted that especially frontal lobe lesions are frequent in both treatment groups (Bendel *et al.* 2008) and therefore it was hypothetized that on a group level a similar atrophic pattern would be observed due to homogenous location of the ruptured aneurysm, and primary bleeding and treatment approach (both surgical and endovascular). The VBM study elucidates the pathophysiology behind the common cognitive disorders associated with the sequela due to a ruptured ACA aneurysm. It was decided that analyses would be performed separately to all patients, surgical and endovascular subgroups and their age-and gender-matched control individuals. When patients with ruptured ACA aneurysms were compared to age-matched controls, they showed bilateral widespread atrophy in the orbitofrontal cortex and inferior frontal gyrus, gyrus rectus and ipsilateral caudate nucleus. The analyses also revealed atrophy in the thalamic regions and dorsal brainstem when comparing the GM volumes between aSAH patients and controls. Lateral ventricles are principally surrounded by white matter, however there are also areas of central GM structures (the thalamus, caudate and brainstem nuclei)

around the ventricles, and thus the detected thalamic and brainstem atrophy probably represents the more widespread central brain atrophy after aSAH, which has been reported in previous studies (Bendel *et al.* 2009, Mayer *et al.* 2002, Vilkki *et al.* 1989). In line with this finding, the aSAH patients showed significantly higher mean relative CSF volumes and lower relative GM volumes than control individuals. An additional finding after the surgical treatment was hippocampal atrophy ipsilateral to treatment side, as expected according to the former volumetric study focusing to temporomesial structures after aSAH. Atrophy could not be detected in other temporomesial structures, perhaps due to smaller sample size in this study limited to only volumetric ACA patients.

Detailed neuropsychological examination of the ACA study population revealed deficits in several cognitive domains. Impaired general intellectual functions, verbal deficits and memory disturbances were equally common after both treatment modalities, but problems in executive functions were more frequently detected after surgical treatment. In accordance with this finding, the MRI-detectable frontal lobe lesions were more frequent after surgical than endovascular treatment. In a recent study by Proust et al. neuropsychological outcome after treatment of an ACA aneurysm was studied and an increased risk for focal encephalomalacia in the surgical group compared to endovascular one was reported, but with no significant difference in executive functions (Proust *et al.* 2009). Executive functions have long been suspected to depend on the prefrontal cortex, the neocortex at the anterior end of the brain (Miller 2000). Interestingly, in this study, the areas of reduced GM were more pronounced after surgical than endovascular treatment (**Figure 11**). In keeping with these neuropsychological and VBM results, recent studies suggest comparable or even better neuropsychological outcomes (Chan *et al.* 2002, Fontanella *et al.* 2003) after endovascular than surgical treatment of the ruptured ACA aneurysms.

Although brain parenchymal lesions seen on MR images are frequent after aSAH (Bendel *et al.* 2008, Kivisaari *et al.* 2001), especially in frontotemporal areas, it is well known that absence of pathological findings in individuals' MR images does not exclude the possibility of cognitive malfunctioning (Romner *et al.* 1989). Therefore we suggest that these VBM-assisted group comparisons might enlighten clinically significant atrophic patterns detected in the bilateral frontobasal cortical areas and hippocampus ipsilateral to the surgical approach after treatment of ruptured ACA aneurysm. Perhaps these atrophic findings may be also associated with the

observed impaired cognitive outcome. It is notable that the atrophic areas after treatment of ACA aneurysm were found in patients who achieved a good or at least moderate outcome according to GOS, and thus cannot be generalized to aSAH patients with worse clinical outcomes. However, the atrophic findings would most likely be even more pronounced in those patients who were recovering poorly.

6.4. Atrophic enlargement of CSF volumes after aSAH (Study IV)

A recent study concluded that post-traumatic ventriculomegaly is frequently observed in clinical practise in patients surviving from traumatic brain injury (Poca *et al.* 2005). We share this clinical experience and have also detected ventricular dilation in patients after aSAH, as has been reported in the literature (Dehdashti *et al.* 2004, Jartti *et al.* 2008, Sethi *et al.* 2000). Diffuse atrophic brain damage after aSAH has been recognized in clinical practice and it was mentioned in the literature already in 1928 (Bagley 1928).

In study IV, the ventricular and sulcal enlargement after aSAH was quantified and related it to patients′ neuropsychological outcome. It is assumed that this is the first time modern three-dimensional image analysis methods were used in patients who have recovered from aSAH. In the late MRI study, performed one year after aSAH, all patients with clinical and radiological findings suggesting active hydrocephalus had already been treated with a permanent shunt-device. Moreover, there were no differences in ventricular enlargement and sulcal dilation of CSF spaces when the patients with or without the permanent shunt device were compared, suggesting that patients with symptomatic hydrocephalus component had been previously successfully treated. In the aSAH patients, the cortical sulci were also wider than those in the control individuals (**Figure 13**). Therefore it can be suggested that the ventricular dilation together with detected reduced gray and white matter volumes of the brain, observed in the chronic phase after aSAH should be interpreted to represent diffuse brain atrophy rather than chronic hydrocephalus.

The mechanism behind the diffuse brain atrophy after aSAH remains unclear and it can be speculated that it cannot be ischemia only. It has been well established that even in good grade aSAH patients, who do not exhibit clinical or radiological vasospasm and who do not have any obvious complications with regard to surgery or postoperative course, still show long-term psychosocial difficulties (Hutter *et al.* 1999,

Kreiter *et al.* 2002). Up to 50% of the survivors after aSAH never return to their previous employment, which further indicates underdiagnosed injuries sustained at the time of initial bleed (Hutter *et al.* 1999, Kreiter *et al.* 2002). Moreover, absence of focal parenchymal lesions in individuals MR images does not exclude the possibility of cognitive malfunctioning (Romner *et al.* 1989). Diffuse brain atrophy together with reduced temporomesial volumes and specific atrophic patterns after treatment of ruptured aneurysms of certain locations may partly explain this phenomenon (Bendel *et al.* 2009, Bendel *et al.* 2006, Bendel *et al.* 2009). General atrophy may also enhance the neuropsychological deficits caused by focal lesions on brain MRI.

The recent concept of early brain injury (EBI) has been suggested as the primary cause of mortality in aSAH patients (Broderick *et al.* 1994) and EBI has also been suggested to play an important role in subtle changes in behaviour, memory and psychosocial difficulties detected in patients after aSAH (Cahill *et al.* 2006, Cahill *et al.* 2009). EBI and a global ischemic injury at the moment of acute SAH results to raised ICP and decreased CBF and trigger a number of critical pathways initiating acutely after bleeding such as inflammation, hypoxia, apoptosis, oxidative stress and excitotoxicity which all are interrelated with a similar end result, cell death (Park *et al.* 2004). Consequently, a number of mechanisms have been proposed to explain global edema after aSAH. Those mechanisms include diffuse ischemic injury due to transient ictal cerebral circulation arrest (Shigeno *et al.* 1982), diffuse inflammatory or neurotoxic effects of widespread subarachnoid blood and its degradation products on brain tissue (Germano *et al.* 1994), or abnormal autoregulation (Handa *et al.* 1992). A recent study concluded that mild vasogenic global edema with increased ADC-values is a relatively common finding after aSAH in the normal appearing brain tissue (Liu *et al.* 2007). It can be suggested that the diffuse brain atrophy after aSAH detected in this study may be related to these mechanisms of EBI. In this study, higher Fischer grades and preoperative hydrocephalus, factors also reflecting the severity of EBI, were found to associate with increased atrophy. As expected, patients with focal lesions detected on MR imaging showed more pronounced atrophy than those patients without these lesions.

The current study shows that diffuse atrophic ventricular and sulcal enlargement are common sequelae after aneurysmal subarachnoid hemorrhage. Furthermore, enlarged CSF-spaces strongly correlate with neuropsychological test performance. It is probable that diffuse brain atrophy together with focal parenchymal lesions such as

cortical infarctions and retraction lesions all contribute to the development of neurocognitive deficits in patients recovering from aSAH.

6.5. General considerations

The psychological problems faced by aSAH survivors have well been described in the past. Even patients with less severe aSAH often have long-term problems with memory, mood and concentration. Many aSAH survivors never return to their previous employment, which further indicates underdiagnosed injuries probably sustained at the time of initial bleed. The aetiology behind this phenomenon remains partly unclear.

On a group level among aSAH patients, these results have now shown a significant general and temporomesial atrophy, both correlating with neuropsychological outcome of the patients. General atrophy was also detected in a patient group without any obvious MRI-detectable lesions in the brain parenchyma. These diffuse atrophic findings may partly be explained by an early brain injury, EBI, a result of a number of critical, molecular pathways with a similar end result, cell death.

MR imaging and careful analysis of the images after aSAH may help the clinician to predict the clinical recovery potential of the individual patient together with neurological assessment and detailed neuropsychological analysis. Focal MRI-detectable brain parenchymal lesions are common in this patient group and the detected lesion volumes significantly correlate with the cognitive outcome.

Although the case fatality of aneurysmal aSAH has decreased with introduction of recent improved techniques in diagnostic and management strategies, severity of the initial bleeding remains still the most important prognostic factor for clinical outcome of an individual aSAH patient. The only way to significantly improve the outcome of aSAH would be preventing aSAH by diagnosing and treating aneurysms before they rupture.

7. CONCLUSIONS

1. Aneurysmal subrachnoid hemorrhage (aSAH) is frequently followed by permanent lesions in brain parenchyma, a majority of which are related to the primary bleeding, but some are adverse effects of the treatment procedures. Parental artery territory ischemic lesions seem to be more frequent after surgical than after endovascular treatment of the ruptured aneurysm, especially in frontotemporal areas. Lesions associated with surgical retraction occur in more than half of the patients treated surgically.

2. aSAH and its treatment is followed by temporomesial volume loss that can be detected in magnetic resonance imaging one year after aSAH. Amygdaloid volume loss ipsilateral to the ruptured cerebral aneurysm seems to be more pronounced after surgical than endovascular treatment of the aneurysm. The scores of several neuropsychological measurements are correlated with the hippocampal, but not amygdaloid volumes.

3. Gray matter atrophy, principally involving the frontobasal cortical areas and hippocampus ipsilateral to the surgical approach is detected after aSAH and treatment of the ruptured ACA aneurysm. Areas of reduced gray matter are more pronounced after surgical than endovascular treatment. Together with possible focal cortical infarctions and brain retraction deficits in individual patients, this finding may explain the neuropsychological disturbances commonly detected after treatment of ruptured ACA aneurysms.

4. Ventricular and sulcal enlargement together with reduced brain parenchymal volumes are common sequelae after aSAH and indicate general atrophy rather than hydrocephalus. Higher Fisher scores, preoperative hydrocephalus and older age were found to associate with ventricular and sulcal enlargement. Enlarged CSF- spaces correlate with cognitive deficits after aSAH. A simple measure: modified cella media index proved to be a feasible tool to assess the diffuse atrophic brain damage after aSAH.

8. REFERENCES

Aaslid, R., Huber, P., and Nornes, H., 1984. Evaluation of cerebrovascular spasm with transcranial Doppler ultrasound. *J Neurosurg*, 60(1), pp.37-41.

Agid, R., Lee, S.K., Willinsky, R.A., Farb, R.I., and terBrugge, K.G., 2006. Acute subarachnoid hemorrhage: using 64-slice multidetector CT angiography to "triage" patients' treatment. *Neuroradiology*, 48(11), pp.787-794.

Allen, G.S., Ahn, H.S., Preziosi, T.J., Battye, R., Boone, S.C., Boone, S.C., Chou, S.N., Kelly, D.L., Weir, B.K., Crabbe, R.A., Lavik, P.J., Rosenbloom, S.B., Dorsey, F.C., Ingram, C.R., Mellits, D.E., Bertsch, L.A., Boisvert, D.P., Hundley, M.B., Johnson, R.K., Strom, J.A., and Transou, C.R., 1983. Cerebral arterial spasm--a controlled trial of nimodipine in patients with subarachnoid hemorrhage. *N Engl J Med*, 308(11), pp.619-624.

Anderson, S.W., Todd, M.M., Hindman, B.J., Clarke, W.R., Torner, J.C., Tranel, D., Yoo, B., Weeks, J., Manzel, K.W., and Samra, S., 2006. Effects of intraoperative hypothermia on neuropsychological outcomes after intracranial aneurysm surgery. *Ann Neurol*, 60(5), pp.518-527.

Aralasmak, A., Akyuz, M., Ozkaynak, C., Sindel, T., and Tuncer, R., 2009. CT angiography and perfusion imaging in patients with subarachnoid hemorrhage: correlation of vasospasm to perfusion abnormality. *Neuroradiology*, 51(2), pp.85-93.

Ashburner, J. and Friston, K.J., 2000. Voxel-based morphometry--the methods. *Neuroimage*, 11(6 Pt 1), pp.805-821.

Ashburner, J., Hutton, C., Frackowiak, R., Johnsrude, I., Price, C., and Friston, K., 1998. Identifying global anatomical differences: deformation-based morphometry. *Hum Brain Mapp*, 6(5-6), pp.348-357.

Awad, I., Modic, M., Little, J.R., Furlan, A.J., and Weinstein, M., 1986. Focal parenchymal lesions in transient ischemic attacks: correlation of computed tomography and magnetic resonance imaging. *Stroke*, 17(3), pp.399-403.

Awad, I.A., Spetzler, R.F., Hodak, J.A., Awad, C.A., and Carey, R., 1986. Incidental subcortical lesions identified on magnetic resonance imaging in the elderly. I. Correlation with age and cerebrovascular risk factors. *Stroke*, 17(6), pp.1084-1089.

Bagley, 1928. Blood in the cerebrospinal fluid. resultant functional and organic alterations in the central nervous system. A. Experimental data. *Arch Surg*, 17, pp.18-38.

Bailes, J.E., Spetzler, R.F., Hadley, M.N., and Baldwin, H.Z., 1990. Management morbidity and mortality of poor-grade aneurysm patients. *J Neurosurg*, 72(4), pp.559-566.

Beauchamp, N.J., Jr., Ulug, A.M., Passe, T.J., and van Zijl, P.C., 1998. MR diffusion imaging in stroke: review and controversies. *Radiographics*, 18(5), pp.1269-1283; discussion 1283-1265.

Bederson, J.B., Awad, I.A., Wiebers, D.O., Piepgras, D., Haley, E.C., Jr., Brott, T., Hademenos, G., Chyatte, D., Rosenwasser, R., and Caroselli, C., 2000. Recommendations for the management of patients with unruptured intracranial aneurysms: A Statement for healthcare professionals from the Stroke Council of the American Heart Association. *Stroke*, 31(11), pp.2742-2750.

Bederson, J.B., Connolly, E.S., Jr., Batjer, H.H., Dacey, R.G., Dion, J.E., Diringer, M.N., Duldner, J.E., Jr., Harbaugh, R.E., Patel, A.B., and Rosenwasser, R.H., 2009. Guidelines for the management of aneurysmal subarachnoid hemorrhage: a statement for healthcare professionals from a special writing group of the Stroke Council, American Heart Association. *Stroke*, 40(3), pp.994-1025.

Bell, B.A., Kendall, B.E., and Symon, L., 1980. Computed tomography in aneurysmal subarachnoid haemorrhage. *J Neurol Neurosurg Psychiatry*, 43(6), pp.522-524.

Bellebaum, C., Schafers, L., Schoch, B., Wanke, I., Stolke, D., Forsting, M., and Daum, I., 2004. Clipping versus coiling: neuropsychological follow up after aneurysmal subarachnoid haemorrhage (SAH). *J Clin Exp Neuropsychol*, 26(8), pp.1081-1092.

Bendel, P., Koivisto, T., Aikia, M., Niskanen, E., Kononen, M., Hanninen, T., and Vanninen, R., 2009. Atrophic Enlargement of CSF Volume after Subarachnoid Hemorrhage: Correlation with Neuropsychological Outcome. *AJNR Am J Neuroradiol*, Epub ahead of print, Nov 26.

Bendel, P., Koivisto, T., Hanninen, T., Kolehmainen, A., Kononen, M., Hurskainen, H., Pennanen, C., and Vanninen, R., 2006. Subarachnoid hemorrhage is followed by temporomesial volume loss: MRI volumetric study. *Neurology*, 67(4), pp.575-582.

Bendel, P., Koivisto, T., Kononen, M., Hanninen, T., Hurskainen, H., Saari, T., Vapalahti, M., Hernesniemi, J., and Vanninen, R., 2008. MR imaging of the brain 1 year after aneurysmal subarachnoid hemorrhage: randomized study comparing surgical with endovascular treatment. *Radiology*, 246(2), pp.543-552.

Bendel, P., Koivisto, T., Niskanen, E., Kononen, M., Aikia, M., Hanninen, T., Koskenkorva, P., and Vanninen, R., 2009. Brain atrophy and neuropsychological outcome after treatment of ruptured anterior cerebral artery aneurysms: a voxel-based morphometric study. *Neuroradiology*, 51(11), pp.711-722.

Bigler, E.D., Anderson, C.V., Blatter, D.D., and Andersob, C.V., 2002. Temporal lobe morphology in normal aging and traumatic brain injury. *AJNR Am J Neuroradiol*, 23(2), pp.255-266.

Binaghi, S., Colleoni, M.L., Maeder, P., Uske, A., Regli, L., Dehdashti, A.R., Schnyder, P., and Meuli, R., 2007. CT angiography and perfusion CT in cerebral vasospasm after subarachnoid hemorrhage. *AJNR Am J Neuroradiol*, 28(4), pp.750-758.

Borkowski, J., Benton, A., and Spreen, O., 1967. Word fluency and brain damage. *Neuropsychologia*, 5, pp.135-140.

Bornstein, R.A., Weir, B.K., Petruk, K.C., and Disney, L.B., 1987. Neuropsychological function in patients after subarachnoid hemorrhage. *Neurosurgery*, 21(5), pp.651-654.

Bottger, S., Prosiegel, M., Steiger, H.J., and Yassouridis, A., 1998. Neurobehavioural disturbances, rehabilitation outcome, and lesion site in patients after rupture and repair of anterior communicating artery aneurysm. *J Neurol Neurosurg Psychiatry*, 65(1), pp.93-102.

Breteler, M.M., van Swieten, J.C., Bots, M.L., Grobbee, D.E., Claus, J.J., van den Hout, J.H., van Harskamp, F., Tanghe, H.L., de Jong, P.T., van Gijn, J., and et al., 1994. Cerebral white matter lesions, vascular risk factors, and cognitive function in a population-based study: the Rotterdam Study. *Neurology*, 44(7), pp.1246-1252.

Brilstra, E.H., Rinkel, G.J., van der Graaf, Y., van Rooij, W.J., and Algra, A., 1999. Treatment of intracranial aneurysms by embolization with coils: a systematic review. *Stroke*, 30(2), pp.470-476.

Broderick, J.P., Brott, T.G., Duldner, J.E., Tomsick, T., and Leach, A., 1994. Initial and recurrent bleeding are the major causes of death following subarachnoid hemorrhage. *Stroke*, 25(7), pp.1342-1347.

Brooks, R., 1996. EuroQol: the current state of play. *Health Policy*, 37(1), pp.53-72.

Brooks, R., 1996. Quality of life measures. *Crit Care Med*, 24(10), pp.1769.

Brouwers, P.J., Wijdicks, E.F., and Van Gijn, J., 1992. Infarction after aneurysm rupture does not depend on distribution or clearance rate of blood. *Stroke*, 23(3), pp.374-379.

Buchanan, K.M., Elias, L.J., and Goplen, G.B., 2000. Differing perspectives on outcome after subarachnoid hemorrhage: the patient, the relative, the neurosurgeon. *Neurosurgery*, 46(4), pp.831-838; discussion 838-840.

Busch, E., Beaulieu, C., de Crespigny, A., and Moseley, M.E., 1998. Diffusion MR imaging during acute subarachnoid hemorrhage in rats. *Stroke*, 29(10), pp.2155-2161.

Cahill, J., Calvert, J.W., Solaroglu, I., and Zhang, J.H., 2006. Vasospasm and p53-induced apoptosis in an experimental model of subarachnoid hemorrhage. *Stroke*, 37(7), pp.1868-1874.

Cahill, J., Calvert, J.W., and Zhang, J.H., 2006. Mechanisms of early brain injury after subarachnoid hemorrhage. *J Cereb Blood Flow Metab*, 26(11), pp.1341-1353.

Cahill, J. and Zhang, J.H., 2009. Subarachnoid hemorrhage: is it time for a new direction? *Stroke*, 40(3 Suppl), pp.S86-87.

Carlson, A.P. and Yonas, H., 2009. Radiographic assessment of vasospasm after aneurysmal subarachnoid hemorrhage: the physiological perspective. *Neurol Res*, 31(6), pp.593-604.

Carrera, E., Schmidt, J.M., Oddo, M., Fernandez, L., Claassen, J., Seder, D., Lee, K., Badjatia, N., Connolly, E.S., Jr., and Mayer, S.A., 2009. Transcranial Doppler for predicting delayed cerebral ischemia after subarachnoid hemorrhage. *Neurosurgery*, 65(2), pp.316-323; discussion 323-314.

Chan, A., Ho, S., and Poon, W.S., 2002. Neuropsychological sequelae of patients treated with microsurgical clipping or endovascular embolization for anterior communicating artery aneurysm. *Eur Neurol*, 47(1), pp.37-44.

Chang, H.S., Hongo, K., and Nakagawa, H., 2000. Adverse effects of limited hypotensive anesthesia on the outcome of patients with subarachnoid hemorrhage. *J Neurosurg*, 92(6), pp.971-975.

Chen, W., Yang, Y., Qiu, J., Peng, Y., and Xing, W., 2009. Clinical application of 16-row multislice computed tomographic angiography in the preoperative and postoperative evaluation of intracranial aneurysms for surgical clipping. *Surg Neurol*, 71(5), pp.559-565.

Choudhari, K.A., Ramachandran, M.S., McCarron, M.O., and Kaliaperumal, C., 2007. Aneurysms unsuitable for endovascular intervention: surgical outcome and management challenges over a 5-year period following International Subarachnoid Haemorrhage Trial (ISAT). *Clin Neurol Neurosurg*, 109(10), pp.868-875.

Ciumas, C., Montavont, A., and Ryvlin, P., 2008. Magnetic resonance imaging in clinical trials. *Curr Opin Neurol*, 21(4), pp.431-436.

Cloft, H.J., Joseph, G.J., and Dion, J.E., 1999. Risk of cerebral angiography in patients with subarachnoid hemorrhage, cerebral aneurysm, and arteriovenous malformation: a meta-analysis. *Stroke*, 30(2), pp.317-320.

Condette-Auliac, S., Bracard, S., Anxionnat, R., Schmitt, E., Lacour, J.C., Braun, M., Meloneto, J., Cordebar, A., Yin, L., and Picard, L., 2001. Vasospasm after subarachnoid hemorrhage: interest in diffusion-weighted MR imaging. *Stroke*, 32(8), pp.1818-1824.

Curnes, J.T., Shogry, M.E., Clark, D.C., and Elsner, H.J., 1993. MR angiographic demonstration of an intracranial aneurysm not seen on conventional angiography. *AJNR Am J Neuroradiol*, 14(4), pp.971-973.

Dandy, W.E., 1938. Intracranial Aneurysm of the Internal Carotid Artery: Cured by Operation. *Ann Surg*, 107(5), pp.654-659.

Dankbaar, J.W., Rijsdijk, M., van der Schaaf, I.C., Velthuis, B.K., Wermer, M.J., and Rinkel, G.J., 2009. Relationship between vasospasm, cerebral perfusion, and delayed cerebral ischemia after aneurysmal subarachnoid hemorrhage. *Neuroradiology*, 51(12), pp.813-819.

de Rooij, N.K., Linn, F.H., van der Plas, J.A., Algra, A., and Rinkel, G.J., 2007. Incidence of subarachnoid haemorrhage: a systematic review with emphasis on region, age, gender and time trends. *J Neurol Neurosurg Psychiatry*, 78(12), pp.1365-1372.

Dehdashti, A.R., Rilliet, B., Rufenacht, D.A., and de Tribolet, N., 2004. Shunt-dependent hydrocephalus after rupture of intracranial aneurysms: a prospective study of the influence of treatment modality. *J Neurosurg*, 101(3), pp.402-407.

Dion, J.E., Gates, P.C., Fox, A.J., Barnett, H.J., and Blom, R.J., 1987. Clinical events following neuroangiography: a prospective study. *Stroke*, 18(6), pp.997-1004.

Doczi, T., 1985. The pathogenetic and prognostic significance of blood-brain barrier damage at the acute stage of aneurysmal subarachnoid haemorrhage. Clinical and experimental studies. *Acta Neurochir (Wien)*, 77(3-4), pp.110-132.

Doczi, T.P., 2001. Impact of cerebral microcirculatory changes on cerebral blood flow during cerebral vasospasm after aneurysmal subarachnoid hemorrhage. *Stroke*, 32(3), pp.817.

Dorai, Z., Hynan, L.S., Kopitnik, T.A., and Samson, D., 2003. Factors related to hydrocephalus after aneurysmal subarachnoid hemorrhage. *Neurosurgery*, 52(4), pp.763-769; discussion 769-771.

Dreier, J.P., Sakowitz, O.W., Harder, A., Zimmer, C., Dirnagl, U., Valdueza, J.M., and Unterberg, A.W., 2002. Focal laminar cortical MR signal abnormalities after subarachnoid hemorrhage. *Ann Neurol*, 52(6), pp.825-829.

Duvernoy, H., 1999. *The Human Brain Surface, Blood Supply, and Three-dimensional Sectional Anatomy*. 2 nd edition, Springer-Verlag Wien New York.

Edelman, R.R. and Warach, S., 1993. Magnetic resonance imaging (1). *N Engl J Med*, 328(10), pp.708-716.

Egge, A., Waterloo, K., Sjoholm, H., Ingebrigtsen, T., Forsdahl, S., Jacobsen, E.A., and Romner, B., 2005. Outcome 1 year after aneurysmal subarachnoid hemorrhage: relation between cognitive performance and neuroimaging. *Acta Neurol Scand*, 112(2), pp.76-80.

Fazekas, F., Kleinert, R., Offenbacher, H., Payer, F., Schmidt, R., Kleinert, G., Radner, H., and Lechner, H., 1991. The morphologic correlate of incidental punctate white matter hyperintensities on MR images. *AJNR Am J Neuroradiol*, 12(5), pp.915-921.

Feigin, V., Parag, V., Lawes, C.M., Rodgers, A., Suh, I., Woodward, M., Jamrozik, K., and Ueshima, H., 2005. Smoking and elevated blood pressure are the most important risk factors for subarachnoid hemorrhage in the Asia-Pacific region: an overview of 26 cohorts involving 306,620 participants. *Stroke*, 36(7), pp.1360-1365.

Feigin, V.L., Rinkel, G.J., Lawes, C.M., Algra, A., Bennett, D.A., van Gijn, J., and Anderson, C.S., 2005. Risk factors for subarachnoid hemorrhage: an updated systematic review of epidemiological studies. *Stroke*, 36(12), pp.2773-2780.

Fergusen, S. and Macdonald, R.L., 2007. Predictors of cerebral infarction in patients with aneurysmal subarachnoid hemorrhage. *Neurosurgery*, 60(4), pp.658-667; discussion 667.

Fiebach, J.B., Schellinger, P.D., Gass, A., Kucinski, T., Siebler, M., Villringer, A., Olkers, P., Hirsch, J.G., Heiland, S., Wilde, P., Jansen, O., Rother, J., Hacke, W., and Sartor, K., 2004. Stroke magnetic resonance imaging is accurate in hyperacute intracerebral hemorrhage: a multicenter study on the validity of stroke imaging. *Stroke*, 35(2), pp.502-506.

Figueiredo, E.G., Zabramski, J.M., Deshmukh, P., Crawford, N.R., Spetzler, R.F., and Preul, M.C., 2006. Comparative analysis of anterior petrosectomy and transcavernous approaches to retrosellar and upper clival basilar artery aneurysms. *Neurosurgery*, 58(1 Suppl), pp.ONS13-21; discussion ONS13-21.

Fisher, C.M., Kistler, J.P., and Davis, J.M., 1980. Relation of cerebral vasospasm to subarachnoid hemorrhage visualized by computerized tomographic scanning. *Neurosurgery*, 6(1), pp.1-9.

Fisher, C.M., Roberson, G.H., and Ojemann, R.G., 1977. Cerebral vasospasm with ruptured saccular aneurysm--the clinical manifestations. *Neurosurgery*, 1(3), pp.245-248.

Fogelholm, R., 1981. Subarachnoid hemorrhage in middle-Finland: incidence, early prognosis and indications for neurosurgical treatment. *Stroke*, 12(3), pp.296-301.

Fontanella, M., Perozzo, P., Ursone, R., Garbossa, D., and Bergui, M., 2003. Neuropsychological assessment after microsurgical clipping or endovascular treatment for anterior communicating artery aneurysm. *Acta Neurochir (Wien)*, 145(10), pp.867-872; discussion 872.

Friedman, J.A., Goerss, S.J., Meyer, F.B., Piepgras, D.G., Pichelmann, M.A., McIver, J.I., Toussaint, L.G., 3rd, McClelland, R.L., Nichols, D.A., Atkinson, J.L., and Wijdicks, E.F., 2002. Volumetric quantification of Fisher Grade 3 aneurysmal subarachnoid hemorrhage: a novel method to predict symptomatic vasospasm on admission computerized tomography scans. *J Neurosurg*, 97(2), pp.401-407.

Frosen, J., Piippo, A., Paetau, A., Kangasniemi, M., Niemela, M., Hernesniemi, J., and Jaaskelainen, J., 2004. Remodeling of saccular cerebral artery aneurysm wall is associated with rupture: histological analysis of 24 unruptured and 42 ruptured cases. *Stroke*, 35(10), pp.2287-2293.

Frosen, J., Piippo, A., Paetau, A., Kangasniemi, M., Niemela, M., Hernesniemi, J., and Jaaskelainen, J., 2006. Growth factor receptor expression and remodeling of saccular cerebral artery aneurysm walls: implications for biological therapy preventing rupture. *Neurosurgery*, 58(3), pp.534-541; discussion 534-541.

Fujioka, M., Nishio, K., Miyamoto, S., Hiramatsu, K.I., Sakaki, T., Okuchi, K., Taoka, T., and Fujioka, S., 2000. Hippocampal damage in the human brain after cardiac arrest. *Cerebrovasc Dis*, 10(1), pp.2-7.

Gaser, C., Nenadic, I., Buchsbaum, B.R., Hazlett, E.A., and Buchsbaum, M.S., 2001. Deformation-based morphometry and its relation to conventional volumetry of brain lateral ventricles in MRI. *Neuroimage*, 13(6 Pt 1), pp.1140-1145.

Genovese, C.R., Lazar, N.A., and Nichols, T., 2002. Thresholding of statistical maps in functional neuroimaging using the false discovery rate. *Neuroimage*, 15(4), pp.870-878.

Gerlach, R., Beck, J., Setzer, M., Vatter, H., Berkefeld, J., Du Mesnil de Rochemont, R., Raabe, A., and Seifert, V., 2007. Treatment related morbidity of unruptured intracranial aneurysms: results of a prospective single centre series with an interdisciplinary approach over a 6 year period (1999-2005). *J Neurol Neurosurg Psychiatry*, 78(8), pp.864-871.

Germano, A.F., Dixon, C.E., d'Avella, D., Hayes, R.L., and Tomasello, F., 1994. Behavioral deficits following experimental subarachnoid hemorrhage in the rat. *J Neurotrauma*, 11(3), pp.345-353.

Geuze, E., Vermetten, E., and Bremner, J.D., 2005. MR-based in vivo hippocampal volumetrics: 2. Findings in neuropsychiatric disorders. *Mol Psychiatry*, 10(2), pp.160-184.

Gibbs, G.F., Huston, J., 3rd, Bernstein, M.A., Riederer, S.J., and Brown, R.D., Jr., 2004. Improved image quality of intracranial aneurysms: 3.0-T versus 1.5-T time-of-flight MR angiography. *AJNR Am J Neuroradiol*, 25(1), pp.84-87.

Gibbs, G.F., Huston, J., 3rd, Bernstein, M.A., Riederer, S.J., and Brown, R.D., Jr., 2005. 3.0-Tesla MR angiography of intracranial aneurysms: comparison of time-of-flight and contrast-enhanced techniques. *J Magn Reson Imaging*, 21(2), pp.97-102.

Gieteling, E.W. and Rinkel, G.J., 2003. Characteristics of intracranial aneurysms and subarachnoid haemorrhage in patients with polycystic kidney disease. *J Neurol*, 250(4), pp.418-423.

Gilman, S., 1998. Imaging the brain. First of two parts. *N Engl J Med*, 338(12), pp.812-820.

Golden, C., 1978. *Stroop Color and Word Tests*. Chigaco, Ill.: Stoerting.

Gomori, J.M., Grossman, R.I., and Steiner, I., 1988. High-field magnetic resonance imaging of intracranial hematomas. *Isr J Med Sci*, 24(4-5), pp.218-223.

Good, C.D., Ashburner, J., and Frackowiak, R.S., 2001. Computational neuroanatomy: new perspectives for neuroradiology. *Rev Neurol (Paris)*, 157(8-9 Pt 1), pp.797-806.

Good, C.D., Johnsrude, I.S., Ashburner, J., Henson, R.N., Friston, K.J., and Frackowiak, R.S., 2001. A voxel-based morphometric study of ageing in 465 normal adult human brains. *Neuroimage*, 14(1 Pt 1), pp.21-36.

Greebe, P. and Rinkel, G.J., 2007. Life expectancy after perimesencephalic subarachnoid hemorrhage. *Stroke*, 38(4), pp.1222-1224.

Gruber, A., Reinprecht, A., Bavinzski, G., Czech, T., and Richling, B., 1999. Chronic shunt-dependent hydrocephalus after early surgical and early endovascular treatment of ruptured intracranial aneurysms. *Neurosurgery*, 44(3), pp.503-509; discussion 509-512.

Gruber, A., Ungersbock, K., Reinprecht, A., Czech, T., Gross, C., Bednar, M., and Richling, B., 1998. Evaluation of cerebral vasospasm after early surgical and endovascular treatment of ruptured intracranial aneurysms. *Neurosurgery*, 42(2), pp.258-267; discussion 267-258.

Guglielmi, G., Vinuela, F., Dion, J., and Duckwiler, G., 1991. Electrothrombosis of saccular aneurysms via endovascular approach. Part 2: Preliminary clinical experience. *J Neurosurg*, 75(1), pp.8-14.

Guglielmi, G., Vinuela, F., Duckwiler, G., Dion, J., Lylyk, P., Berenstein, A., Strother, C., Graves, V., Halbach, V., Nichols, D., and et al., 1992. Endovascular treatment of posterior circulation aneurysms by electrothrombosis using electrically detachable coils. *J Neurosurg*, 77(4), pp.515-524.

Guglielmi, G., Vinuela, F., Sepetka, I., and Macellari, V., 1991. Electrothrombosis of saccular aneurysms via endovascular approach. Part 1: Electrochemical basis, technique, and experimental results. *J Neurosurg*, 75(1), pp.1-7.

Hackett, M.L. and Anderson, C.S., 2000. Health outcomes 1 year after subarachnoid hemorrhage: An international population-based study. The Australian Cooperative Research on Subarachnoid Hemorrhage Study Group. *Neurology*, 55(5), pp.658-662.

Hadjivassiliou, M., Tooth, C.L., Romanowski, C.A., Byrne, J., Battersby, R.D., Oxbury, S., Crewswell, C.S., Burkitt, E., Stokes, N.A., Paul, C., Mayes, A.R., and Sagar, H.J., 2001. Aneurysmal SAH: cognitive outcome and structural damage after clipping or coiling. *Neurology*, 56(12), pp.1672-1677.

Handa, Y., Hayashi, M., Takeuchi, H., Kubota, T., Kobayashi, H., and Kawano, H., 1992. Time course of the impairment of cerebral autoregulation during chronic cerebral vasospasm after subarachnoid hemorrhage in primates. *J Neurosurg*, 76(3), pp.493-501.

Hattingen, E., Blasel, S., Dettmann, E., Vatter, H., Pilatus, U., Seifert, V., Zanella, F.E., and Weidauer, S., 2008. Perfusion-weighted MRI to evaluate cerebral autoregulation in aneurysmal subarachnoid haemorrhage. *Neuroradiology*, 50(11), pp.929-938.

Hauerberg, J., Eskesen, V., and Rosenorn, J., 1994. The prognostic significance of intracerebral haematoma as shown on CT scanning after aneurysmal subarachnoid haemorrhage. *Br J Neurosurg*, 8(3), pp.333-339.

Heier, L.A., Bauer, C.J., Schwartz, L., Zimmerman, R.D., Morgello, S., and Deck, M.D., 1989. Large Virchow-Robin spaces: MR-clinical correlation. *AJNR Am J Neuroradiol*, 10(5), pp.929-936.

Heiserman, J.E., Dean, B.L., Hodak, J.A., Flom, R.A., Bird, C.R., Drayer, B.P., and Fram, E.K., 1994. Neurologic complications of cerebral angiography. *AJNR Am J Neuroradiol*, 15(8), pp.1401-1407; discussion 1408-1411.

Hernesniemi, J., Dashti, R., Lehecka, M., Niemela, M., Rinne, J., Lehto, H., Ronkainen, A., Koivisto, T., and Jaaskelainen, J.E., 2008. Microneurosurgical management of anterior communicating artery aneurysms. *Surg Neurol*, 70(1), pp.8-28; discussion 29.

Hernesniemi, J., Ishii, K., Niemela, M., Kivipelto, L., Fujiki, M., and Shen, H., 2005. Subtemporal approach to basilar bifurcation aneurysms: advanced technique and clinical experience. *Acta Neurochir Suppl*, 94, pp.31-38.

Hernesniemi, J., Ishii, K., Niemela, M., Smrcka, M., Kivipelto, L., Fujiki, M., and Shen, H., 2005. Lateral supraorbital approach as an alternative to the classical pterional approach. *Acta Neurochir Suppl*, 94. pp.17-21.

Hernesniemi, J., Vapalahti, M., Niskanen, M., Tapaninaho, A., Kari, A., Luukkonen, M., Puranen, M., Saari, T., and Rajpar, M., 1993. One-year outcome in early aneurysm surgery: a 14 years experience. *Acta Neurochir (Wien)*, 122(1-2), pp.1-10.

Hijdra, A., Braakman, R., van Gijn, J., Vermeulen, M., and van Crevel, H., 1987. Aneurysmal subarachnoid hemorrhage. Complications and outcome in a hospital population. *Stroke*, 18(6), pp.1061-1067.

Hijdra, A., Van Gijn, J., Stefanko, S., Van Dongen, K.J., Vermeulen, M., and Van Crevel, H., 1986. Delayed cerebral ischemia after aneurysmal subarachnoid hemorrhage: clinicoanatomic correlations. *Neurology*, 36(3), pp.329-333.

Hirai, T., Kai, Y., Morioka, M., Yano, S., Kitajima, M., Fukuoka, H., Sasao, A., Murakami, R., Nakayama, Y., Awai, K., Toya, R., Akter, M., Korogi, Y., Kuratsu, J., and Yamashita, Y., 2008. Differentiation between paraclinoid and cavernous sinus aneurysms with contrast-enhanced 3D constructive interference in steady- state MR imaging. *AJNR Am J Neuroradiol*, 29(1), pp.130-133.

Hoeffner, E.G., Case, I., Jain, R., Gujar, S.K., Shah, G.V., Deveikis, J.P., Carlos, R.C., Thompson, B.G., Harrigan, M.R., and Mukherji, S.K., 2004. Cerebral perfusion CT: technique and clinical applications. *Radiology*, 231(3), pp.632-644.

Hoh, B.L., Curry, W.T., Jr., Carter, B.S., and Ogilvy, C.S., 2004. Computed tomographic demonstrated infarcts after surgical and endovascular treatment of aneurysmal subarachnoid hemorrhage. *Acta Neurochir (Wien)*, 146(11), pp.1177-1183.

Hoh, B.L. and Ogilvy, C.S., 2005. Endovascular treatment of cerebral vasospasm: transluminal balloon angioplasty, intra-arterial papaverine, and intra-arterial nicardipine. *Neurosurg Clin N Am*, 16(3), pp.501-516, vi.

Hop, J.W., Rinkel, G.J., Algra, A., and van Gijn, J., 1997. Case-fatality rates and functional outcome after subarachnoid hemorrhage: a systematic review. *Stroke*, 28(3), pp.660-664.

Hop, J.W., Rinkel, G.J., Algra, A., and van Gijn, J., 1998. Quality of life in patients and partners after aneurysmal subarachnoid hemorrhage. *Stroke*, 29(4), pp.798-804.

Hop, J.W., Rinkel, G.J., Algra, A., and van Gijn, J., 1999. Initial loss of consciousness and risk of delayed cerebral ischemia after aneurysmal subarachnoid hemorrhage. *Stroke*, 30(11), pp.2268-2271.

Hop, J.W., Rinkel, G.J., Algra, A., and van Gijn, J., 2001. Changes in functional outcome and quality of life in patients and caregivers after aneurysmal subarachnoid hemorrhage. *J Neurosurg*, 95(6), pp.957-963.

Horn, P., Vajkoczy, P., Bauhuf, C., Munch, E., Poeckler-Schoeniger, C., and Schmiedek, P., 2001. Quantitative regional cerebral blood flow measurement techniques improve noninvasive detection of cerebrovascular vasospasm after aneurysmal subarachnoid hemorrhage. *Cerebrovasc Dis*, 12(3), pp.197-202.

Hunt, W.E., Meagher, J.N., and Hess, R.M., 1966. Intracranial aneurysm. A nine-year study. *Ohio State Med J*, 62(11), pp.1168-1171.

Hutter, B.O. and Gilsbach, J.M., 1993. Which neuropsychological deficits are hidden behind a good outcome (Glasgow = I) after aneurysmal subarachnoid hemorrhage? *Neurosurgery*, 33(6), pp.999-1005; discussion 1005-1006.

Hutter, B.O., Kreitschmann-Andermahr, I., and Gilsbach, J.M., 2001. Health-related quality of life after aneurysmal subarachnoid hemorrhage: impacts of bleeding severity, computerized tomography findings, surgery, vasospasm, and neurological grade. *J Neurosurg*, 94(2), pp.241-251.

Hutter, B.O., Kreitschmann-Andermahr, I., Mayfrank, L., Rohde, V., Spetzger, U., and Gilsbach, J.M., 1999. Functional outcome after aneurysmal subarachnoid hemorrhage. *Acta Neurochir Suppl*, 72, pp.157-174.

Huttunen, T., von und zu Franunberg, M., Frösen, J., Lehecka, M., Tromp, G., Helin, K., Koivisto,T., Rinne, J., Ronkainen, A., Hernesniemi, J., Jääskeläinen, J., 2009. Saccular intracranial aneurysm disease – distribution of site, size and age suggest different etiologies for aneurysm formation and rupture in 316 familial and 1454 sporadic Eastern Finnish patients. *In press*.

Ikeda, K., Iwasaki, Y., Hatanaka, N., and Kinoshita, M., 1998. Causes of perimesencephalic nonaneurysmal subarachnoid hemorrhage. *Neurology*, 50(5), pp.1518.

Imaizumi, T., Chiba, M., Honma, T., and Niwa, J., 2003. Detection of hemosiderin deposition by T2*-weighted MRI after subarachnoid hemorrhage. *Stroke*, 34(7), pp.1693-1698.

Inagawa, T., Tokuda, Y., Ohbayashi, N., Takaya, M., and Moritake, K., 1995. Study of aneurysmal subarachnoid hemorrhage in Izumo City, Japan. *Stroke*, 26(5), pp.761-766.

Insausti, R., Juottonen, K., Soininen, H., Insausti, A.M., Partanen, K., Vainio, P., Laakso, M.P., and Pitkanen, A., 1998. MR volumetric analysis of the human entorhinal, perirhinal, and temporopolar cortices. *AJNR Am J Neuroradiol*, 19(4), pp.659-671.

Investigators, 1998. Unruptured intracranial aneurysms--risk of rupture and risks of surgical intervention. International Study of Unruptured Intracranial Aneurysms Investigators. *N Engl J Med*, 339(24), pp.1725-1733.

Isaksen, J., Egge, A., Waterloo, K., Romner, B., and Ingebrigtsen, T., 2002. Risk factors for aneurysmal subarachnoid haemorrhage: the Tromso study. *J Neurol Neurosurg Psychiatry*, 73(2), pp.185-187.

Jartti, P., Karttunen, A., Isokangas, J.M., Jartti, A., Koskelainen, T., and Tervonen, O., 2008. Chronic hydrocephalus after neurosurgical and endovascular treatment of ruptured intracranial aneurysms. *Acta Radiol*, 49(6), pp.680-686.

Jennett, B. and Bond, M., 1975. Assessment of outcome after severe brain damage. *Lancet*, 1(7905), pp.480-484.

Johnston, S.C., Selvin, S., and Gress, D.R., 1998. The burden, trends, and demographics of mortality from subarachnoid hemorrhage. *Neurology*, 50(5), pp.1413-1418.

Jokinen, H., Kalska, H., Mantyla, R., Pohjasvaara, T., Ylikoski, R., Hietanen, M., Salonen, O., Kaste, M., and Erkinjuntti, T., 2006. Cognitive profile of subcortical ischaemic vascular disease. *J Neurol Neurosurg Psychiatry*, 77(1), pp.28-33.

Juvela, S., Hillbom, M., Numminen, H., and Koskinen, P., 1993. Cigarette smoking and alcohol consumption as risk factors for aneurysmal subarachnoid hemorrhage. *Stroke*, 24(5), pp.639-646.

Juvela, S., Porras, M., and Poussa, K., 2000. Natural history of unruptured intracranial aneurysms: probability of and risk factors for aneurysm rupture. *J Neurosurg*, 93(3), pp.379-387.

Juvela, S. and Siironen, J., 2006. D-dimer as an independent predictor for poor outcome after aneurysmal subarachnoid hemorrhage. *Stroke*, 37(6), pp.1451-1456.

Juvela, S., Siironen, J., Varis, J., Poussa, K., and Porras, M., 2005. Risk factors for ischemic lesions following aneurysmal subarachnoid hemorrhage. *J Neurosurg*, 102(2), pp.194-201.

Kahara, V., 2006. Postprocedural monitoring of cerebral aneurysms. *Acta Radiol*, 47(3), pp.320-327.

Kalviainen, R., Salmenpera, T., Partanen, K., Vainio, P., Riekkinen, P., and Pitkanen, A., 1998. Recurrent seizures may cause hippocampal damage in temporal lobe epilepsy. *Neurology*, 50(5), pp.1377-1382.

Kanal, E. and Shellock, F.G., 1999. Aneurysm clips: effects of long-term and multiple exposures to a 1.5-T MR system. *Radiology*, 210(2), pp.563-565.

Kangasniemi, M., Makela, T., Koskinen, S., Porras, M., Poussa, K., and Hernesniemi, J., 2004. Detection of intracranial aneurysms with two-dimensional and three-dimensional multislice helical computed tomographic angiography. *Neurosurgery*, 54(2), pp.336-340; discussion 340-331.

Kassell, N.F. and Torner, J.C., 1982. The International Cooperative study on timing of aneurysm surgery. *Acta Neurochir (Wien)*, 63(1-4), pp.119-123.

Kassell, N.F. and Torner, J.C., 1983. Aneurysmal rebleeding: a preliminary report from the Cooperative Aneurysm Study. *Neurosurgery*, 13(5), pp.479-481.

Kassell, N.F., Torner, J.C., Haley, E.C., Jr., Jane, J.A., Adams, H.P., and Kongable, G.L., 1990. The International Cooperative Study on the Timing of Aneurysm Surgery. Part 1: Overall management results. *J Neurosurg*, 73(1), pp.18-36.

Kassell, N.F., Torner, J.C., Jane, J.A., Haley, E.C., Jr., and Adams, H.P., 1990. The International Cooperative Study on the Timing of Aneurysm Surgery. Part 2: Surgical results. *J Neurosurg*, 73(1), pp.37-47.

Kawai, N., Nakamura, T., Tamiya, T., and Nagao, S., 2008. Regional cerebral blood flow and oxygen metabolism in aneurysmal subarachnoid hemorrhage: positron emission tomography evaluation of clipping versus coiling. *Acta Neurochir Suppl*, 105), pp.211-215.

Kertesz, A., Black, S.E., Tokar, G., Benke, T., Carr, T., and Nicholson, L., 1988. Periventricular and subcortical hyperintensities on magnetic resonance imaging. 'Rims, caps, and unidentified bright objects'. *Arch Neurol*, 45(4), pp.404-408.

Kistler, J.P., Crowell, R.M., Davis, K.R., Heros, R., Ojemann, R.G., Zervas, T., and Fisher, C.M., 1983. The relation of cerebral vasospasm to the extent and location of subarachnoid blood visualized by CT scan: a prospective study. *Neurology*, 33(4), pp.424-436.

Kivisaari, R.P., Porras, M., Ohman, J., Siironen, J., Ishii, K., and Hernesniemi, J., 2004. Routine cerebral angiography after surgery for saccular aneurysms: is it worth it? *Neurosurgery*, 55(5), pp.1015-1024.

Kivisaari, R.P., Salonen, O., Servo, A., Autti, T., Hernesniemi, J., and Ohman, J., 2001. MR imaging after aneurysmal subarachnoid hemorrhage and surgery: a long-term follow-up study. *AJNR Am J Neuroradiol*, 22(6), pp.1143-1148.

Koebbe, C.J., Veznedaroglu, E., Jabbour, P., and Rosenwasser, R.H., 2006. Endovascular management of intracranial aneurysms: current experience and future advances. *Neurosurgery*, 59(5 Suppl 3), pp.S93-102; discussion S103-113.

Koivisto, T., Vanninen, R., Hurskainen, H., Saari, T., Hernesniemi, J., and Vapalahti, M., 2000. Outcomes of early endovascular versus surgical treatment of ruptured cerebral aneurysms. A prospective randomized study. *Stroke*, 31(10), pp.2369-2377.

Komotar, R.J., Hahn, D.K., Kim, G.H., Starke, R.M., Garrett, M.C., Merkow, M.B., Otten, M.L., Sciacca, R.R., and Connolly, E.S., Jr., 2009. Efficacy of lamina terminalis fenestration in reducing shunt-dependent hydrocephalus following aneurysmal subarachnoid hemorrhage: a systematic review. Clinical article. *J Neurosurg*, 111(1), pp.147-154.

Krayenbuhl, H. and Yasargil, M.G., 1970. Diagnosis and therapy of intracranial aneurysms. *Surg Annu*, 2(0), pp.327-343.

Kreiter, K.T., Copeland, D., Bernardini, G.L., Bates, J.E., Peery, S., Claassen, J., Du, Y.E., Stern, Y., Connolly, E.S., and Mayer, S.A., 2002. Predictors of cognitive dysfunction after subarachnoid hemorrhage. *Stroke*, 33(1), pp.200-208.

Kruyt, N.D., Biessels, G.J., de Haan, R.J., Vermeulen, M., Rinkel, G.J., Coert, B., and Roos, Y.B., 2009. Hyperglycemia and clinical outcome in aneurysmal subarachnoid hemorrhage: a meta-analysis. *Stroke*, 40(6), pp.e424-430.

Kumar, N., 2007. Superficial siderosis: associations and therapeutic implications. *Arch Neurol*, 64(4), pp.491-496.

Kuo, H.K. and Lipsitz, L.A., 2004. Cerebral white matter changes and geriatric syndromes: is there a link? *J Gerontol A Biol Sci Med Sci*, 59(8), pp.818-826.

Kupersmith, M.J., Hurst, R., Berenstein, A., Choi, I.S., Jafar, J., and Ransohoff, J., 1992. The benign course of cavernous carotid artery aneurysms. *J Neurosurg*, 77(5), pp.690-693.

Kusaka, G., Ishikawa, M., Nanda, A., Granger, D.N., and Zhang, J.H., 2004. Signaling pathways for early brain injury after subarachnoid hemorrhage. *J Cereb Blood Flow Metab*, 24(8), pp.916-925.

Laakso, M.P., Soininen, H., Partanen, K., Lehtovirta, M., Hallikainen, M., Hanninen, T., Helkala, E.L., Vainio, P., and Riekkinen, P.J., Sr., 1998. MRI of the hippocampus in Alzheimer's disease: sensitivity, specificity, and analysis of the incorrectly classified subjects. *Neurobiol Aging*, 19(1), pp.23-31.

Lancaster, J.L., Woldorff, M.G., Parsons, L.M., Liotti, M., Freitas, C.S., Rainey, L., Kochunov, P.V., Nickerson, D., Mikiten, S.A., and Fox, P.T., 2000. Automated Talairach atlas labels for functional brain mapping. *Hum Brain Mapp*, 10(3), pp.120-131.

Langmoen, I.A., Ekseth, K., Hauglie-Hanssen, E., and Nornes, H., 1999. Surgical treatment of anterior circulation aneurysms. *Acta Neurochir Suppl*, 72), pp.107-121.

Lawton, M.T., Quinones-Hinojosa, A., Sanai, N., Malek, J.Y., and Dowd, C.F., 2008. Combined microsurgical and endovascular management of complex intracranial aneurysms. *Neurosurgery*, 62(6 Suppl 3), pp.1503-1515.

Leclerc, X., Fichten, A., Gauvrit, J.Y., Riegel, B., Steinling, M., Lejeune, J.P., and Pruvo, J.P., 2002. Symptomatic vasospasm after subarachnoid haemorrhage: assessment of brain damage by diffusion and perfusion-weighted MRI and single-photon emission computed tomography. *Neuroradiology*, 44(7), pp.610-616.

Lezak, M., 1995. *Neuropsychological Assessment.* New York, NY: Oxford University Press.

Lezak MD, H.D., Loring DW, 2004. *Neuropsychological assessment*. New York, NY. 4 edition, ed. Oxford University. Press.

Li, Q., Lv, F., Li, Y., Li, K., Luo, T., and Xie, P., 2009. Subtraction CT angiography for evaluation of intracranial aneurysms: comparison with conventional CT angiography. *Eur Radiol*, 19(9), pp.2261-2267.

Linn, F.H., Rinkel, G.J., Algra, A., and van Gijn, J., 1996. Incidence of subarachnoid hemorrhage: role of region, year, and rate of computed tomography: a meta-analysis. *Stroke*, 27(4), pp.625-629.

Liu, Y., Soppi, V., Mustonen, T., Kononen, M., Koivisto, T., Koskela, A., Rinne, J., and Vanninen, R.L., 2007. Subarachnoid hemorrhage in the subacute stage: elevated apparent diffusion coefficient in normal-appearing brain tissue after treatment. *Radiology*, 242(2), pp.518-525.

Lubicz, B., Leclerc, X., Gauvrit, J.Y., Lejeune, J.P., and Pruvo, J.P., 2005. Three-dimensional packing with complex orbit coils for the endovascular treatment of intracranial aneurysms. *AJNR Am J Neuroradiol*, 26(6), pp.1342-1348.

Lylyk, P., Ferrario, A., Pasbon, B., Miranda, C., and Doroszuk, G., 2005. Buenos Aires experience with the Neuroform self-expanding stent for the treatment of intracranial aneurysms. *J Neurosurg*, 102(2), pp.235-241.

MacDonald, D., Kabani, N., Avis, D., and Evans, A.C., 2000. Automated 3-D extraction of inner and outer surfaces of cerebral cortex from MRI. *Neuroimage*, 12(3), pp.340-356.

Malisch, T.W., Guglielmi, G., Vinuela, F., Duckwiler, G., Gobin, Y.P., Martin, N.A., and Frazee, J.G., 1997. Intracranial aneurysms treated with the Guglielmi detachable coil: midterm clinical results in a consecutive series of 100 patients. *J Neurosurg*, 87(2), pp.176-183.

Martin, J., 1996. *Neuroanatomy text and atlas*. 2nd ed. Stamford: Appleton & Lange.

Masaryk, A.M., Frayne, R., Unal, O., Rappe, A.H., and Strother, C.M., 2000. Utility of CT angiography and MR angiography for the follow-up of experimental aneurysms treated with stents or Guglielmi detachable coils. *AJNR Am J Neuroradiol*, 21(8), pp.1523-1531.

Masaryk, T., Kolonick, R., Painter, T., and Weinreb, D.B., 2008. The economic and clinical benefits of portable head/neck CT imaging in the intensive care unit. *Radiol Manage*, 30(2), pp.50-54.

Mayer, S.A., Kreiter, K.T., Copeland, D., Bernardini, G.L., Bates, J.E., Peery, S., Claassen, J., Du, Y.E., and Connolly, E.S., Jr., 2002. Global and domain-specific cognitive impairment and outcome after subarachnoid hemorrhage. *Neurology*, 59(11), pp.1750-1758.

McCarron, M.O., Flynn, P.A., Owens, C., Wallace, I., Mirakhur, M., Gibson, J.M., and Patterson, V.H., 2003. Superficial siderosis of the central nervous system many years after neurosurgical procedures. *J Neurol Neurosurg Psychiatry*, 74(9), pp.1326-1328.

McKinney, A.M., Palmer, C.S., Truwit, C.L., Karagulle, A., and Teksam, M., 2008. Detection of aneurysms by 64-section multidetector CT angiography in patients acutely suspected of having an intracranial aneurysm and comparison with digital subtraction and 3D rotational angiography. *AJNR Am J Neuroradiol*, 29(3), pp.594-602.

Miley, J.T., Taylor, R.A., Janardhan, V., Tummala, R., Lanzino, G., and Qureshi, A.I., 2008. The value of computed tomography angiography in determining treatment allocation for aneurysmal subarachnoid hemorrhage. *Neurocrit Care*, 9(3), pp.300-306.

Miller, E.K., 2000. The prefrontal cortex and cognitive control. *Nat Rev Neurosci*, 1(1), pp.59-65.

Mitchell, P., Wilkinson, I.D., Hoggard, N., Paley, M.N., Jellinek, D.A., Powell, T., Romanowski, C., Hodgson, T., and Griffiths, P.D., 2001. Detection of subarachnoid haemorrhage with magnetic resonance imaging. *J Neurol Neurosurg Psychiatry*, 70(2), pp.205-211.

Molyneux, A., Kerr, R., Stratton, I., Sandercock, P., Clarke, M., Shrimpton, J., and Holman, R., 2002. International Subarachnoid Aneurysm Trial (ISAT) of neurosurgical clipping versus endovascular coiling in 2143 patients with ruptured intracranial aneurysms: a randomised trial. *Lancet*, 360(9342), pp.1267-1274.

Molyneux, A.J., Cekirge, S., Saatci, I., and Gal, G., 2004. Cerebral Aneurysm Multicenter European Onyx (CAMEO) trial: results of a prospective observational study in 20 European centers. *AJNR Am J Neuroradiol*, 25(1), pp.39-51.

Molyneux, A.J., Kerr, R.S., Birks, J., Ramzi, N., Yarnold, J., Sneade, M., and Rischmiller, J., 2009. Risk of recurrent subarachnoid haemorrhage, death, or dependence and standardised mortality ratios after clipping or coiling of an intracranial aneurysm in the International Subarachnoid Aneurysm Trial (ISAT): long-term follow-up. *Lancet Neurol*, 8(5), pp.427-433.

Molyneux, A.J., Kerr, R.S., Yu, L.M., Clarke, M., Sneade, M., Yarnold, J.A., and Sandercock, P., 2005. International subarachnoid aneurysm trial (ISAT) of neurosurgical clipping versus endovascular coiling in 2143 patients with ruptured intracranial aneurysms: a randomised comparison of effects on survival, dependency, seizures, rebleeding, subgroups, and aneurysm occlusion. *Lancet*, 366(9488), pp.809-817.

Moret, J., Cognard, C., Weill, A., Castaings, L., and Rey, A., 1997. Reconstruction technic in the treatment of wide-neck intracranial aneurysms. Long-term angiographic and clinical results. Apropos of 56 cases. *J Neuroradiol*, 24(1), pp.30-44.

Morita, A., Fujiwara, S., Hashi, K., Ohtsu, H., and Kirino, T., 2005. Risk of rupture associated with intact cerebral aneurysms in the Japanese population: a systematic review of the literature from Japan. *J Neurosurg*, 102(4), pp.601-606.

Muench, E., Meinhardt, J., Schaeffer, M., Schneider, U.C., Czabanka, M., Luecke, T., Schmiedek, P., and Vajkoczy, P., 2007. The use of the excimer laser-assisted anastomosis technique alleviates neuroanesthesia during cerebral high-flow revascularization. *J Neurosurg Anesthesiol*, 19(4), pp.273-279.

Murphy, M., Bell, D., Worth, R.D., Jehle, K.S., Critchley, G.R., and Norris, J.S., 2005. Angiography postclipping and coiling of cerebral aneurysms. *Br J Neurosurg*, 19(3), pp.225-228.

Naderi, S., Ozguven, M.A., Bayhan, H., Gokalp, H., Erdogan, A., and Egemen, N., 1994. Evaluation of cerebral vasospasm in patients with subarachnoid hemorrhage using single photon emission computed tomography. *Neurosurg Rev*, 17(4), pp.261-265.

Naidech, A.M., Bendok, B.R., Bassin, S.L., Bernstein, R.A., Batjer, H.H., and Bleck, T.P., 2009. Classification of cerebral infarction after subarachnoid hemorrhage impacts outcome. *Neurosurgery*, 64(6), pp.1052-1057; discussion 1057-1058.

Naidech, A.M., Drescher, J., Tamul, P., Shaibani, A., Batjer, H.H., and Alberts, M.J., 2006. Acute physiological derangement is associated with early radiographic cerebral infarction after subarachnoid haemorrhage. *J Neurol Neurosurg Psychiatry*, 77(12), pp.1340-1344.

Nieuwkamp, D.J., Setz, L.E., Algra, A., Linn, F.H., de Rooij, N.K., and Rinkel, G.J., 2009. Changes in case fatality of aneurysmal subarachnoid haemorrhage over time, according to age, sex, and region: a meta-analysis. *Lancet Neurol*, 8(7), pp.635-642.

Nijjar, S., Patel, B., McGinn, G., and West, M., 2007. Computed tomographic angiography as the primary diagnostic study in spontaneous subarachnoid hemorrhage. *J Neuroimaging*, 17(4), pp.295-299.

Norman G, S.D., 1994. *Biostatistics The bare essentials*. St. Louis.

Ogden, J.A., Utley, T., and Mee, E.W., 1997. Neurological and psychosocial outcome 4 to 7 years after subarachnoid hemorrhage. *Neurosurgery*, 41(1), pp.25-34.

Ogilvy, C.S., Hoh, B.L., Singer, R.J., and Putman, C.M., 2002. Clinical and radiographic outcome in the management of posterior circulation aneurysms by use of direct surgical or endovascular techniques. *Neurosurgery*, 51(1), pp.14-21; discussion 21-12.

Okahara, M., Kiyosue, H., Hori, Y., Yamashita, M., Nagatomi, H., and Mori, H., 2004. Three-dimensional time-of-flight MR angiography for evaluation of intracranial aneurysms after endosaccular packing with Guglielmi detachable coils: comparison with 3D digital subtraction angiography. *Eur Radiol*, 14(7), pp.1162-1168.

Okahara, M., Kiyosue, H., Yamashita, M., Nagatomi, H., Hata, H., Saginoya, T., Sagara, Y., and Mori, H., 2002. Diagnostic accuracy of magnetic resonance angiography for cerebral aneurysms in correlation with 3D-digital subtraction angiographic images: a study of 133 aneurysms. *Stroke*, 33(7), pp.1803-1808.

Okazaki, H., 1989. *Malformative vascular lesions. in Fundamentals of Neuropathology*. 2. edition, Igaku-Schoin.

Orakcioglu, B., Schuknecht, B., Otani, N., Khan, N., Imhof, H.G., and Yonekawa, Y., 2005. Distal posterior inferior cerebellar artery aneurysms: clinical characteristics and surgical management. *Acta Neurochir (Wien)*, 147(11), pp.1131-1139; discussion 1139.

Orbo, M., Waterloo, K., Egge, A., Isaksen, J., Ingebrigtsen, T., and Romner, B., 2008. Predictors for cognitive impairment one year after surgery for aneurysmal subarachnoid hemorrhage. *J Neurol*, 255(11), pp.1770-1776.

Osborn, A.G., 1994. *Normal Vascular Anatomy. In Osborn AG. Diagnostic Neuroradiology*. St Louis: Mosby.

Osborn, A.G., 1999. *Diagnostic Cerebral Angiography*. Vol. Second edition: Lippincott Williams&Wilkins.

Pakarinen, S., 1967. Incidence, aetiology, and prognosis of primary subarachnoid haemorrhage. A study based on 589 cases diagnosed in a defined urban population during a defined period. *Acta Neurol Scand*, 43, pp.Suppl 29:21-28.

Pantoni, L. and Garcia, J.H., 1995. The significance of cerebral white matter abnormalities 100 years after Binswanger's report. A review. *Stroke*, 26(7), pp.1293-1301.

Papke, K., Kuhl, C.K., Fruth, M., Haupt, C., Schlunz-Hendann, M., Sauner, D., Fiebich, M., Bani, A., and Brassel, F., 2007. Intracranial aneurysms: role of multidetector CT angiography in diagnosis and endovascular therapy planning. *Radiology*, 244(2), pp.532-540.

Park, S., Yamaguchi, M., Zhou, C., Calvert, J.W., Tang, J., and Zhang, J.H., 2004. Neurovascular protection reduces early brain injury after subarachnoid hemorrhage. *Stroke*, 35(10), pp.2412-2417.

Pechlivanis, I., Schmieder, K., Scholz, M., Konig, M., Heuser, L., and Harders, A., 2005. 3-Dimensional computed tomographic angiography for use of surgery planning in patients with intracranial aneurysms. *Acta Neurochir (Wien)*, 147(10), pp.1045-1053; discussion 1053.

Pennanen, C., Kivipelto, M., Tuomainen, S., Hartikainen, P., Hanninen, T., Laakso, M.P., Hallikainen, M., Vanhanen, M., Nissinen, A., Helkala, E.L., Vainio, P., Vanninen, R., Partanen, K., and Soininen, H., 2004. Hippocampus and entorhinal cortex in mild cognitive impairment and early AD. *Neurobiol Aging*, 25(3), pp.303-310.

Poca, M.A., Sahuquillo, J., Mataro, M., Benejam, B., Arikan, F., and Baguena, M., 2005. Ventricular enlargement after moderate or severe head injury: a frequent and neglected problem. *J Neurotrauma*, 22(11), pp.1303-1310.

Powell, J., Kitchen, N., Heslin, J., and Greenwood, R., 2002. Psychosocial outcomes at three and nine months after good neurological recovery from aneurysmal subarachnoid haemorrhage: predictors and prognosis. *J Neurol Neurosurg Psychiatry*, 72(6), pp.772-781.

Powers, W.J., Grubb, R.L., Jr., Baker, R.P., Mintun, M.A., and Raichle, M.E., 1985. Regional cerebral blood flow and metabolism in reversible ischemia due to vasospasm. Determination by positron emission tomography. *J Neurosurg*, 62(4), pp.539-546.

Proust, F., Debono, B., Hannequin, D., Gerardin, E., Clavier, E., Langlois, O., and Freger, P., 2003. Treatment of anterior communicating artery aneurysms: complementary aspects of microsurgical and endovascular procedures. *J Neurosurg*, 99(1), pp.3-14.

Proust, F., Martinaud, O., Gerardin, E., Derrey, S., Leveque, S., Bioux, S., Tollard, E., Clavier, E., Langlois, O., Godefroy, O., Hannequin, D., and Freger, P., 2009. Quoality of life and brain damage after microsurgical clip occlusion or endovascular coil embolization for ruptured anterior communicating artery aneurysms: neuropsychological assessment. *J Neurosurg*, 110 (1), pp.19-29.

Rabinstein, A.A., Friedman, J.A., Nichols, D.A., Pichelmann, M.A., McClelland, R.L., Manno, E.M., Atkinson, J.L., and Wijdicks, E.F., 2004. Predictors of outcome after endovascular treatment of cerebral vasospasm. *AJNR Am J Neuroradiol*, 25(10), pp.1778-1782.

Rabinstein, A.A., Friedman, J.A., Weigand, S.D., McClelland, R.L., Fulgham, J.R., Manno, E.M., Atkinson, J.L., and Wijdicks, E.F., 2004. Predictors of cerebral infarction in aneurysmal subarachnoid hemorrhage. *Stroke*, 35(8), pp.1862-1866.

Rabinstein, A.A., Weigand, S., Atkinson, J.L., and Wijdicks, E.F., 2005. Patterns of cerebral infarction in aneurysmal subarachnoid hemorrhage. *Stroke*, 36(5), pp.992-997.

Raftopoulos, C., 2005. Is surgical clipping becoming underused? *Acta Neurochir (Wien)*, 147(2), pp.117-123; discussion 123-114.

Rankin, J., 1957. Cerebral vascular accidents in patients over the age of 60. I. General considerations. *Scott Med J*, 2(4), pp.127-136.

Reitan, R., 1958. Validity of the Trail making Tests as an indicator of organic brain damage. *Percept mot Skills.*, 8, pp.271-276.

Renowden, S.A., Benes, V., Bradley, M., and Molyneux, A.J., 2009. Detachable coil embolisation of ruptured intracranial aneurysms: a single center study, a decade experience. *Clin Neurol Neurosurg*, 111(2), pp.179-188.

Report of World Federation of Neurological Surgeons Committee on a Universal Subarachnoid Hemorrhage Grading Scale. 1988. Journal of Neurosurgery (June, 68(6)), pp.985-986.

Rinkel, G.J., 2008. Natural history, epidemiology and screening of unruptured intracranial aneurysms. *J Neuroradiol*, 35(2), pp.99-103.

Rinkel, G.J., Djibuti, M., Algra, A., and van Gijn, J., 1998. Prevalence and risk of rupture of intracranial aneurysms: a systematic review. *Stroke*, 29(1), pp.251-256.

Rinne, J., Hernesniemi, J., Niskanen, M., and Vapalahti, M., 1996. Analysis of 561 patients with 690 middle cerebral artery aneurysms: anatomic and clinical features as correlated to management outcome. *Neurosurgery*, 38(1), pp.2-11.

Rinne, J., Hernesniemi, J., Puranen, M., and Saari, T., 1994. Multiple intracranial aneurysms in a defined population: prospective angiographic and clinical study. *Neurosurgery*, 35(5), pp.803-808.

Romner, B., Olsson, M., Ljunggren, B., Holtas, S., Saveland, H., Brandt, L., and Persson, B., 1989. Magnetic resonance imaging and aneurysm clips. Magnetic properties and image artifacts. *J Neurosurg*, 70(3), pp.426-431.

Romner, B., Sonesson, B., Ljunggren, B., Brandt, L., Saveland, H., and Holtas, S., 1989. Late magnetic resonance imaging related to neurobehavioral functioning after aneurysmal subarachnoid hemorrhage. *Neurosurgery*, 25(3), pp.390-396; discussion 396-397.

Ronkainen, A., Hernesniemi, J., Puranen, M., Niemitukia, L., Vanninen, R., Ryynanen, M., Kuivaniemi, H., and Tromp, G., 1997. Familial intracranial aneurysms. *Lancet*, 349(9049), pp.380-384.

Rooij, W.J.v. and Sluzewski, M., 2009. Opinion: Imaging Follow-Up after Coiling of Intracranial Aneurysms. *AJNR Am J Neuroradiol*, 30(9), pp.1646-1648.

Rosengart, A.J., Schultheiss, K.E., Tolentino, J., and Macdonald, R.L., 2007. Prognostic factors for outcome in patients with aneurysmal subarachnoid hemorrhage. *Stroke*, 38(8), pp.2315-2321.

Sadowski, E.A., Bennett, L.K., Chan, M.R., Wentland, A.L., Garrett, A.L., Garrett, R.W., and Djamali, A., 2007. Nephrogenic systemic fibrosis: risk factors and incidence estimation. *Radiology*, 243(1), pp.148-157.

Sakamoto, S., Kiura, Y., Shibukawa, M., Ohba, S., Arita, K., and Kurisu, K., 2006. Subtracted 3D CT angiography for evaluation of internal carotid artery aneurysms: comparison with conventional digital subtraction angiography. *AJNR Am J Neuroradiol*, 27(6), pp.1332-1337.

Salary, M., Quigley, M.R., and Wilberger, J.E., Jr., 2007. Relation among aneurysm size, amount of subarachnoid blood, and clinical outcome. *J Neurosurg*, 107(1), pp.13-17.

Sandvei, M.S., Romundstad, P.R., Muller, T.B., Vatten, L., and Vik, A., 2009. Risk factors for aneurysmal subarachnoid hemorrhage in a prospective population study: the HUNT study in Norway. *Stroke*, 40(6), pp.1958-1962.

Sarti, C., Tuomilehto, J., Salomaa, V., Sivenius, J., Kaarsalo, E., Narva, E.V., Salmi, K., and Torppa, J., 1991. Epidemiology of subarachnoid hemorrhage in Finland from 1983 to 1985. *Stroke*, 22(7), pp.848-853.

Saveland, H., Hillman, J., Brandt, L., Edner, G., Jakobsson, K.E., and Algers, G., 1992. Overall outcome in aneurysmal subarachnoid hemorrhage. A prospective study from neurosurgical units in Sweden during a 1-year period. *J Neurosurg*, 76(5), pp.729-734.

Schievink, W.I., 1997. Genetics of intracranial aneurysms. *Neurosurgery*, 40(4), pp.651-662; discussion 662-653.

Schievink, W.I., Riedinger, M., and Maya, M.M., 2005. Frequency of incidental intracranial aneurysms in neurofibromatosis type 1. *Am J Med Genet A*, 134A(1), pp.45-48.

Schievink, W.I., Wijdicks, E.F., Piepgras, D.G., Chu, C.P., O'Fallon, W.M., and Whisnant, J.P., 1995. The poor prognosis of ruptured intracranial aneurysms of the posterior circulation. *J Neurosurg*, 82(5), pp.791-795.

Schmidt, R., Fazekas, F., Kapeller, P., Schmidt, H., and Hartung, H.P., 1999. MRI white matter hyperintensities: three-year follow-up of the Austrian Stroke Prevention Study. *Neurology*, 53(1), pp.132-139.

Schmidt, R., Fazekas, F., Kleinert, G., Offenbacher, H., Gindl, K., Payer, F., Freidl, W., Niederkorn, K., and Lechner, H., 1992. Magnetic resonance imaging signal hyperintensities in the deep and subcortical white matter. A comparative study between stroke patients and normal volunteers. *Arch Neurol*, 49(8), pp.825-827.

Schuknecht, B., Fandino, J., Yuksel, C., Yonekawa, Y., and Valavanis, A., 1999. Endovascular treatment of cerebral vasospasm: assessment of treatment effect by cerebral angiography and transcranial colour Doppler sonography. *Neuroradiology*, 41(6), pp.453-462.

Sethi, H., Moore, A., Dervin, J., Clifton, A., and MacSweeney, J.E., 2000. Hydrocephalus: comparison of clipping and embolization in aneurysm treatment. *J Neurosurg*, 92(6), pp.991-994.

Shellock, F.G. and Curtis, J.S., 1991. MR imaging and biomedical implants, materials, and devices: an updated review. *Radiology*, 180(2), pp.541-550.

Shellock, F.G., Detrick, M.S., and Brant-Zawadski, M.N., 1997. MR compatibility of Guglielmi detachable coils. *Radiology*, 203(2), pp.568-570.

Shigeno, T., Fritschka, E., Brock, M., Schramm, J., Shigeno, S., and Cervos-Navarro, J., 1982. Cerebral edema following experimental subarachnoid hemorrhage. *Stroke*, 13(3), pp.368-379.

Shimoda, M., Takeuchi, M., Tominaga, J., Oda, S., Kumasaka, A., and Tsugane, R., 2001. Asymptomatic versus symptomatic infarcts from vasospasm in patients with subarachnoid hemorrhage: serial magnetic resonance imaging. *Neurosurgery*, 49(6), pp.1341-1348; discussion 1348-1350.

Silvennoinen, H.M., Hamberg, L.M., Valanne, L., and Hunter, G.J., 2007. Increasing contrast agent concentration improves enhancement in first-pass CT perfusion. *AJNR Am J Neuroradiol*, 28(7), pp.1299-1303.

Slob, M.J., van Rooij, W.J., and Sluzewski, M., 2005. Coil thickness and packing of cerebral aneurysms: a comparative study of two types of coils. *AJNR Am J Neuroradiol*, 26(4), pp.901-903.

Soininen, H.S., Partanen, K., Pitkanen, A., Vainio, P., Hanninen, T., Hallikainen, M., Koivisto, K., and Riekkinen, P.J., Sr., 1994. Volumetric MRI analysis of the amygdala and the hippocampus in subjects with age-associated memory impairment: correlation to visual and verbal memory. *Neurology*, 44(9), pp.1660-1668.

Solomon, R.A., 2001. Anterior communicating artery aneurysms. *Neurosurgery*, 48(1), pp.119-123.

Squire, L.R., Stark, C.E., and Clark, R.E., 2004. The medial temporal lobe. *Annu Rev Neurosci*, 27, pp.279-306.

Strother, C.M., Graves, V.B., and Rappe, A., 1992. Aneurysm hemodynamics: an experimental study. *AJNR Am J Neuroradiol*, 13(4), pp.1089-1095.

Suzuki, J., Komatsu, S., Sato, T., and Sakurai, Y., 1980. Correlation between CT findings and subsequent development of cerebral infarction due to vasospasm in subarachnoid haemorrhage. *Acta Neurochir (Wien)*, 55(1-2), pp.63-70.

Sviri, G.E., Britz, G.W., Lewis, D.H., Newell, D.W., Zaaroor, M., and Cohen, W., 2006. Dynamic perfusion computed tomography in the diagnosis of cerebral vasospasm. *Neurosurgery*, 59(2), pp.319-325; discussion 319-325.

Sviri, G.E., Mesiwala, A.H., Lewis, D.H., Britz, G.W., Nemecek, A., Newell, D.W., Lam, A., and Cohen, W., 2006. Dynamic perfusion computerized tomography in cerebral vasospasm following aneurysmal subarachnoid hemorrhage: a comparison with technetium-99m-labeled ethyl cysteinate dimer-single-photon emission computerized tomography. *J Neurosurg*, 104(3), pp.404-410.

Tahtinen, O.I., Vanninen, R.L., Manninen, H.I., Rautio, R., Haapanen, A., Niskakangas, T., Rinne, J., and Keski-Nisula, L., 2009. Wide-necked intracranial aneurysms: treatment with stent-assisted coil embolization during acute (<72 hours) subarachnoid hemorrhage--experience in 61 consecutive patients. *Radiology*, 253(1), pp.199-208.

Tamraz, J.C., Comair, Y.G, 2006. *Atlas of Regional Anatomy of the Brain Using MRI With Functional Correlations*: Springer-Verlag Berlin Heidelberg New York.

Tanoue, S., Kiyosue, H., Kenai, H., Nakamura, T., Yamashita, M., and Mori, H., 2000. Three-dimensional reconstructed images after rotational angiography in the evaluation of intracranial aneurysms: surgical correlation. *Neurosurgery*, 47(4), pp.866-871.

Tapaninaho, A., Hernesniemi, J., Vapalahti, M., Niskanen, M., Kari, A., Luukkonen, M., and Puranen, M., 1993. Shunt-dependent hydrocephalus after subarachnoid haemorrhage and aneurysm surgery: timing of surgery is not a risk factor. *Acta Neurochir (Wien)*, 123(3-4), pp.118-124.

Tatu, L., Moulin, T., Bogousslavsky, J., and Duvernoy, H., 1996. Arterial territories of human brain: brainstem and cerebellum. *Neurology*, 47(5), pp.1125-1135.

Tatu, L., Moulin, T., Bogousslavsky, J., and Duvernoy, H., 1998. Arterial territories of the human brain: cerebral hemispheres. *Neurology*, 50(6), pp.1699-1708.

Teasdale, G. and Jennett, B., 1976. Assessment and prognosis of coma after head injury. *Acta Neurochir (Wien)*, 34(1-4), pp.45-55.

Teipel, S.J., Meindl, T., Grinberg, L., Heinsen, H., and Hampel, H., 2008. Novel MRI techniques in the assessment of dementia. *Eur J Nucl Med Mol Imaging*, 35 Suppl 1, pp.S58-69.

Tejada, J.G., Taylor, R.A., Ugurel, M.S., Hayakawa, M., Lee, S.K., and Chaloupka, J.C., 2007. Safety and feasibility of intra-arterial nicardipine for the treatment of subarachnoid hemorrhage-associated vasospasm: initial clinical experience with high-dose infusions. *AJNR Am J Neuroradiol*, 28(5), pp.844-848.

Thielen, K.R., Nichols, D.A., Fulgham, J.R., and Piepgras, D.G., 1997. Endovascular treatment of cerebral aneurysms following incomplete clipping. *J Neurosurg*, 87(2), pp.184-189.

Thomas, B., Somasundaram, S., Thamburaj, K., Kesavadas, C., Gupta, A.K., Bodhey, N.K., and Kapilamoorthy, T.R., 2008. Clinical applications of susceptibility weighted MR imaging of the brain - a pictorial review. *Neuroradiology*, 50(2), pp.105-116.

Thomsen, H.S., 2007. Current evidence on prevention and management of contrast-induced nephropathy. *Eur Radiol*, 17 Suppl 6, pp.F33-37.

Thornton, J., Bashir, Q., Aletich, V.A., Debrun, G.M., Ausman, J.I., and Charbel, F.T., 2000. What percentage of surgically clipped intracranial aneurysms have residual necks? *Neurosurgery*, 46(6), pp.1294-1298; discussion 1298-1300.

Todd, M.M., Hindman, B.J., Clarke, W.R., and Torner, J.C., 2005. Mild intraoperative hypothermia during surgery for intracranial aneurysm. *N Engl J Med*, 352(2), pp.135-145.

Tokuda, Y., Inagawa, T., Katoh, Y., Kumano, K., Ohbayashi, N., and Yoshioka, H., 1995. Intracerebral hematoma in patients with ruptured cerebral aneurysms. *Surg Neurol*, 43(3), pp.272-277.

Tsuboi, T., Tokunaga, K., Shingo, T., Itoh, T., Mandai, S., Kinugasa, K., and Date, I., 2007. Differentiation between intradural and extradural locations of juxta-dural ring aneurysms by using contrast-enhanced 3-dimensional time-of-flight magnetic resonance angiography. *Surg Neurol*, 67(4), pp.381-387.

Uysal, E., Ozel, A., Erturk, S.M., Kirdar, O., and Basak, M., 2009. Comparison of multislice computed tomography angiography and digital subtraction angiography in the detection of residual or recurrent aneurysm after surgical clipping with titanium clips. *Acta Neurochir (Wien)*, 151(2), pp.131-135.

Walker, M.T., Tsai, J., Parish, T., Tzung, B., Shaibani, A., Krupinski, E., and Russell, E.J., 2005. MR angiographic evaluation of platinum coil packs at 1.5T and 3T: an in vitro assessment of artifact production: technical note. *AJNR Am J Neuroradiol*, 26(4), pp.848-853.

van der Jagt, M., Hasan, D., Bijvoet, H.W., Pieterman, H., Dippel, D.W., Vermeij, F.H., and Avezaat, C.J., 1999. Validity of prediction of the site of ruptured intracranial aneurysms with CT. *Neurology*, 52(1), pp.34-39.

van der Schaaf, I., Algra, A., Wermer, M., Molyneux, A., Clarke, M., van Gijn, J., and Rinkel, G., 2005. Endovascular coiling versus neurosurgical clipping for patients with aneurysmal subarachnoid haemorrhage. *Cochrane Database Syst Rev*, (4), pp.CD003085.

van der Schaaf, I., Wermer, M.J., van der Graaf, Y., Velthuis, B.K., van de Kraats, C.I., and Rinkel, G.J., 2006. Prognostic value of cerebral perfusion-computed tomography in the acute stage after subarachnoid hemorrhage for the development of delayed cerebral ischemia. *Stroke*, 37(2), pp.409-413.

van Gijn, J., Kerr, R.S., and Rinkel, G.J., 2007. Subarachnoid haemorrhage. *Lancet*, 369(9558), pp.306-318.

van Gijn, J. and Rinkel, G.J., 2001. Subarachnoid haemorrhage: diagnosis, causes and management. *Brain*, 124(Pt 2), pp.249-278.

van Gijn, J. and van Dongen, K.J., 1980. Computerized tomography in subarachnoid hemorrhage: difference between patients with and without an aneurysm on angiography. *Neurology*, 30(5), pp.538-539.

van Gijn, J. and van Dongen, K.J., 1982. The time course of aneurysmal haemorrhage on computed tomograms. *Neuroradiology*, 23(3), pp.153-156.

van Munster, C.E., von und zu Fraunberg, M., Rinkel, G.J., Rinne, J., Koivisto, T., and Ronkainen, A., 2008. Differences in aneurysm and patient characteristics between cohorts of Finnish and Dutch patients with subarachnoid hemorrhage: time trends between 1986 and 2005. *Stroke*, 39(12), pp.3166-3171.

van Rooij, W.J., Peluso, J.P., Sluzewski, M., and Beute, G.N., 2008. Additional value of 3D rotational angiography in angiographically negative aneurysmal subarachnoid hemorrhage: how negative is negative? *AJNR Am J Neuroradiol*, 29(5), pp.962-966.

van Rooij, W.J., Sprengers, M.E., de Gast, A.N., Peluso, J.P., and Sluzewski, M., 2008. 3D rotational angiography: the new gold standard in the detection of additional intracranial aneurysms. *AJNR Am J Neuroradiol*, 29(5), pp.976-979.

Vanninen, R., Koivisto, T., Saari, T., Hernesniemi, J., and Vapalahti, M., 1999. Ruptured intracranial aneurysms: acute endovascular treatment with electrolytically detachable coils--a prospective randomized study. *Radiology*, 211(2), pp.325-336.

Vapalahti, M., Ljunggren, B., Saveland, H., Hernesniemi, J., Brandt, L., and Tapaninaho, A., 1984. Early aneurysm operation and outcome in two remote Scandinavian populations. *J Neurosurg*, 60(6), pp.1160-1162.

Watson, C., Andermann, F., Gloor, P., Jones-Gotman, M., Peters, T., Evans, A., Olivier, A., Melanson, D., and Leroux, G., 1992. Anatomic basis of amygdaloid and hippocampal volume measurement by magnetic resonance imaging. *Neurology*, 42(9), pp.1743-1750.

Waugh, J.R. and Sacharias, N., 1992. Arteriographic complications in the DSA era. *Radiology*, 182(1), pp.243-246.

Wechsler, D., 1974. *Wechsler Memory Scale Manual*. San Antonio: The Psychological Corporation.

Wechsler, D., 1981. *Wechsler Adult Intelligence Scale-Revised*. New York: The psychological corporation.

Weidauer, S., Lanfermann, H., Raabe, A., Zanella, F., Seifert, V., and Beck, J., 2007. Impairment of cerebral perfusion and infarct patterns attributable to vasospasm after aneurysmal subarachnoid hemorrhage: a prospective MRI and DSA study. *Stroke*, 38(6), pp.1831-1836.

Weidauer, S., Vatter, H., Beck, J., Raabe, A., Lanfermann, H., Seifert, V., and Zanella, F., 2008. Focal laminar cortical infarcts following aneurysmal subarachnoid haemorrhage. *Neuroradiology*, 50(1), pp.1-8.

Vergouwen, M.D., Vermeulen, M., Coert, B.A., Stroes, E.S., and Roos, Y.B., 2008. Microthrombosis after aneurysmal subarachnoid hemorrhage: an additional explanation for delayed cerebral ischemia. *J Cereb Blood Flow Metab*, 28(11), pp.1761-1770.

Wermer, M.J., Kool, H., Albrecht, K.W., and Rinkel, G.J., 2007. Subarachnoid hemorrhage treated with clipping: long-term effects on employment, relationships, personality, and mood. *Neurosurgery*, 60(1), pp.91-97; discussion 97-98.

Westerlaan, H.E., Gravendeel, J., Fiore, D., Metzemaekers, J.D., Groen, R.J., Mooij, J.J., and Oudkerk, M., 2007. Multislice CT angiography in the selection of patients with ruptured intracranial aneurysms suitable for clipping or coiling. *Neuroradiology*, 49(12), pp.997-1007.

Westerlaan, H.E., van der Vliet, A.M., Hew, J.M., Meiners, L.C., Metzemaekers, J.D., Mooij, J.J., and Oudkerk, M., 2005. Time-of-flight magnetic resonance angiography in the follow-up of intracranial aneurysms treated with Guglielmi detachable coils. *Neuroradiology*, 47(8), pp.622-629.

White, P.M., Teasdale, E.M., Wardlaw, J.M., and Easton, V., 2001. Intracranial aneurysms: CT angiography and MR angiography for detection prospective blinded comparison in a large patient cohort. *Radiology*, 219(3), pp.739-749.

Wiebers, D.O., Whisnant, J.P., Huston, J., 3rd, Meissner, I., Brown, R.D., Jr., Piepgras, D.G., Forbes, G.S., Thielen, K., Nichols, D., O'Fallon, W.M., Peacock, J., Jaeger, L., Kassell, N.F., Kongable-Beckman, G.L., and Torner, J.C., 2003. Unruptured intracranial aneurysms: natural history, clinical outcome, and risks of surgical and endovascular treatment. *Lancet*, 362(9378), pp.103-110.

Wijdicks, E.F., Vermeulen, M., ten Haaf, J.A., Hijdra, A., Bakker, W.H., and van Gijn, J., 1985. Volume depletion and natriuresis in patients with a ruptured intracranial aneurysm. *Ann Neurol*, 18(2), pp.211-216.

Vilkki, J., Holst, P., Ohman, J., Servo, A., and Heiskanen, O., 1989. Cognitive deficits related to computed tomographic findings after surgery for a ruptured intracranial aneurysm. *Neurosurgery*, 25(2), pp.166-172.

Vilkki, J.S., Juvela, S., Siironen, J., Ilvonen, T., Varis, J., and Porras, M., 2004. Relationship of local infarctions to cognitive and psychosocial impairments after aneurysmal subarachnoid hemorrhage. *Neurosurgery*, 55(4), pp.790-802; discussion 802-793.

Villarreal, G., Hamilton, D.A., Petropoulos, H., Driscoll, I., Rowland, L.M., Griego, J.A., Kodituwakku, P.W., Hart, B.L., Escalona, R., and Brooks, W.M., 2002. Reduced hippocampal volume and total white matter volume in posttraumatic stress disorder. *Biol Psychiatry*, 52(2), pp.119-125.

Wills, S., Ronkainen, A., van der Voet, M., Kuivaniemi, H., Helin, K., Leinonen, E., Frosen, J., Niemela, M., Jaaskelainen, J., Hernesniemi, J., and Tromp, G., 2003. Familial intracranial aneurysms: an analysis of 346 multiplex Finnish families. *Stroke*, 34(6), pp.1370-1374.

Vinuela, F., Duckwiler, G., and Mawad, M., 1997. Guglielmi detachable coil embolization of acute intracranial aneurysm: perioperative anatomical and clinical outcome in 403 patients. *J Neurosurg*, 86(3), pp.475-482.

Wu, O., Ostergaard, L., and Sorensen, A.G., 2005. Technical aspects of perfusion-weighted imaging. *Neuroimaging Clin N Am*, 15(3), pp.623-637, xi.

Vymazal, J., Urgosik, D., and Bulte, J.W., 2000. Differentiation between hemosiderin- and ferritin-bound brain iron using nuclear magnetic resonance and magnetic resonance imaging. *Cell Mol Biol (Noisy-le-grand)*, 46(4), pp.835-842.

Yasargil, M.G. and Fox, J.L., 1975. The microsurgical approach to intracranial aneurysms. *Surg Neurol*, 3(1), pp.7-14.

Yeh, H. and Tew, J.M., Jr., 1985. Anterior interhemispheric approach to aneurysms of the anterior communicating artery. *Surg Neurol*, 23(2), pp.98-100.

Yonas, H., Sekhar, L., Johnson, D.W., and Gur, D., 1989. Determination of irreversible ischemia by xenon-enhanced computed tomographic monitoring of cerebral blood flow in patients with symptomatic vasospasm. *Neurosurgery*, 24(3), pp.368-372.

Yoon, D.Y., Choi, C.S., Kim, K.H., and Cho, B.M., 2006. Multidetector-row CT angiography of cerebral vasospasm after aneurysmal subarachnoid hemorrhage: comparison of volume-rendered images and digital subtraction angiography. *AJNR Am J Neuroradiol*, 27(2), pp.370-377.

Zabramski, J.M., Kiris, T., Sankhla, S.K., Cabiol, J., and Spetzler, R.F., 1998. Orbitozygomatic craniotomy. Technical note. *J Neurosurg*, 89(2), pp.336-341.

Zhang, Y., Londos, E., Minthon, L., Wattmo, C., Liu, H., Aspelin, P., and Wahlund, L.O., 2008. Usefulness of computed tomography linear measurements in diagnosing Alzheimer's disease. *Acta Radiol*, 49(1), pp.91-97.

Zyed, A., Hayman, L.A., and Bryan, R.N., 1991. MR imaging of intracerebral blood: diversity in the temporal pattern at 0.5 and 1.0 T. *AJNR Am J Neuroradiol*, 12(3), pp.469-474.

Kuopio University Publications D. Medical Sciences

D 434. Hassinen, Maija. Predictors and consequences of the metabolic syndrome: population-based studies in aging men and women.
2008. Acad. Diss.

D 435. Saltevo, Juha. Low-grade inflammation and adiponectin in the metabolic syndrome.
2008. 109 p. Acad. Diss.

D 436. Ervasti, Mari. Evaluation of Iron Status Using Methods Based on the Features of Red Blood Cells and Reticulocytes.
2008. 104 p. Acad. Diss.

D 437. Muukka, Eija. Luomun tie päiväkotiin: luomuruokailun toteutettavuus ja ravitsemuksellinen merkitys päiväkotilapsille.
2008. 168 p. Acad. Diss.

D 438. Sörensen, Lars. Work ability and health-related quality of life in middle-aged men: the role of physical activity and fitness.
2008. 83 p. Acad. Diss.

D 439. Maaranen, Päivi. Dissociation in the finnish general population.
2008. 97 p. Acad. Diss.

D 440. Hyvönen, Juha. Suomen psykiatrinen hoitojärjestelmä 1990-luvulla historian jatkumon näkökulmasta. 2008. 279 p. Acad. Diss.

D 441. Mäkinen, Heidi. Disease activity and remission in rheumatoid arthritis: comparison of available disease activity measures and development of a novel disease sctivity indes: the mean overall index for rheumatoid arthritis (MOI-RA).
2008. 129 p. Acad. Diss.

D 442. Kousa, Anne. The regional association of the hardness in well waters and the incidence of acute myocardial infarction in rural Finland.
2008. 92 p. Acad. Diss.

D 443. Olkku, Anu. Glucocorticoid-induced changes in osteoblastic cells: cross-talk with wnt and glutamate signalling pathways.
2009. 118 p. Acad. Diss.

D 444. Mattila, Riikka. Effectiveness of a multidisciplinary lifestyle intervention on hypertension, cardiovascular risk factors and musculoskeletal symptoms.
2009. 92 p. Acad. Diss.

D 445. Hartmann-Petersen, Susanna. Hyaluronan and CD44 in epidermis with special reference to growth factors and malignant transformation.
2009. 103 p. Acad. Diss.

D 446. Tolppanen, Anna-Maija. Genetic association of the tenomodulin gene (TNMD) with obesity- and inflammation-related phenotypes.
2009. 111 p. Acad. Diss.

D 447. Lehto, Soili Marianne. Biological findings in major depressive disorder with special reference to the atypical features subtype.
2009. 115 p. Acad. Diss.

D 448. Nieminen, Jyrki. Effect of functional loading on remodelling in canine, and normal and collagen type II transgenic murine bone.
2009. 107 p. Acad. Diss.

D 449. Torpström, Jaana. Yliopistokoulutus ravitsemusasiantuntijuuden kehittäjänä.
2009. 164 p. Acad. Diss.